Exploring Selectivity in Nonenzymatic and Enzymatic DNA-Templated Ligation Reactions

By

Eiman Abd Elrahman Osman

A thesis submitted in partial fulfillment of the requirements for the degree of

Doctor of Philosophy

Department of Chemistry

University of Alberta

Abstract

DNA-templated reactions have been utilized in many applications from the detection of a nucleic acid target to applications in nanotechnology. This thesis explores developing bioanalytical strategies based on DNA-templated ligation reactions for sensitive, rapid single nucleotide polymorphism (SNP) detection, specifically single-basepair mismatches and methylated sites. Finding a good assay that can discriminate single-base differences in a biomarker sequence is important for point-of-care diagnostics aimed at the early detection of cancer. Chemical ligation strategies have some advantages in point-of-care diagnostics compared to enzymatic ligation as they are less expensive and do not require freezer for storage. Thus, we investigated the DNA-templated Cu(I) catalyzed azide-alkyne cycloaddition (CuAAC) using 5'-azide ODN and 3'-O-propargyl ODN. Under our newly optimized conditions, the reaction is as rapid as enzymatic ligation using the highest commercially available concentration of T4 DNA ligase with k_{obs} value of 1.1 min^{-1}. The DNA-templated CuAAC reaction is also more selective to single nucleotide mismatches compared to the enzymatic ligation at a temperature that affords the best discrimination of T4 DNA ligase: a temperature below the thermal dissociation temperature, or melting temperature (T_m), of the matched nicked duplex and above that of the mismatched nicked duplexes.

Our next aim involved improving the selectivity of T4 DNA ligase for single basepair mismatches as it is the most commonly used ligase in molecular biology and bioanalytical labs despite its low selectivity for single basepair mismatches at the site of ligation. We decided to explore the selectivity of T4 DNA ligase over a temperature range that extended far above the dissociation temperature of the nicked duplex of the perfectly matched template. Surprisingly, with the use of low concentration of T4 DNA ligase, the assay can be quite selective resulting in

100% ligation of the matched target and <2% ligation of the mismatched target when the temperature is 6-12 degrees higher than the T_m. This temperature range of high selectivity can be increased to 12-18 degrees higher than the T_m if a high concentration of enzyme is used. Finally, the assay can also work at around the T_m of the nicked duplex when we introduce an abasic group to the 5'-phosphate terminus of one of the ligating probes.

Finally, I will discuss our efforts to detect methylated nucleobases as the ability to sequence such methylated groups on the KRAS gene can help in the early detection of cancer. The KRAS gene is a key controller for the expression of an epidermal growth factor receptor that is overly expressed in many types of cancer. We are able to amplify a target 18-mer sequence from the KRAS gene that contains an O^6-methylated G at the codon 12 and 13 position using the isothermal amplification method that was developed in our group (lesion-induced DNA amplification, LIDA). The amplification of the methylated template resulted in a net amplification factor of 650 in a comparison of LIDA reactions initiated with 1.4 nM methylated target and 1.4 nM non-methylated target.

Preface

The DNA-templated Cu(I) catalyzed azide-alkyne cycloaddition kinetic and selectivity study was conceived by J. M. Gibbs, T. Gadzikwa and myself. Preliminary kinetic studies and turnover experiments were performed by T. Gadzikwa and myself. Dr. Gadzikwa also taught me how to perform the solid-phase synthesis of the 5'-azide strands that required Schlenk techniques. However, all of the experiments in chapter 2 were done by me. Portions of chapter 2 have been published as Osman, E. A., Gadzikwa, T., and Gibbs, J. M., Quick Click: The DNA-Templated Ligation of 3'-*O*-Propargyl and 5'-Azide Modified Strands is As Rapid and More Selective Than Ligase, *ChemBioChem* 2018, 219, 2081–2087 with a cover feature. Dr. Gadzikwa helped developed the strategy of the paper. The corresponding author is J. M. Gibbs and she supervised the project, provided helpful discussions and suggestions and composed the manuscript in collaboration with me. All experiments, data analysis and manuscript edits were done by me.

The project of chapter 3 was conceived by J. M. Gibbs and represented a collaboration with S. Alladin-Mustan, a graduate student in the Gibbs lab, and S. Hale and G. Matharu, undergraduate students in the Gibbs lab. All of strands were synthesized by me except for the 3'-fluorescein-5'-phosphate abasic strand which was synthesized by S. Alladin-Mustan and S. Hale. I did a majority of the DNA-templated ligation experiments using the typical 5'-fluorescein-3'-hydroxy probes, but some of these experiments were conducted by S. Alldin-Mustan, S. Hale, and G. Matharu. The AMP study and the melting temperature experiments for the chemical and enzymatic system with the abasic-containing nicked duplexes were done by S. Hales. Portions of this chapter were modified from a manuscript in preparation. J. M. Gibbs supervised the project, provided helpful discussions and suggestions and composed a draft of this manuscript. A portion

of this chapter has been published as Kausar, A.; Osman, E. A.; Gadzikwa, T.; Gibbs-Davis, J. M., The presence of a 5′-abasic lesion enhances discrimination of single nucleotide polymorphisms while inducing an isothermal ligase chain reaction. *Analyst* 2016, 141 (14), 4272-4277.

Chapter 4 is a collaboration with the lab of Prof. Shana Sturla at ETH in the Department of Health Science and Technology. The ExBIM probes were synthesized by N. Arman in the Sturla group. The 3'-fluorescein-5'-phosphate di-abasic strand was made by A. Ubeda, a graduate student in the Gibbs lab. All the other strands were synthesized by me. All the experiments were done by me except the single cycle experiments, which were performed by A. Ubeda. J. M. Gibbs supervised the project, provided helpful discussions and suggestions.

Appendix I was partly collaboration with R. Grotsch in J. Boekhoven's group to develop fuel driven turnover in a DNA hybridization/dehybridization cycle. Part of the work was done during my ATUMS research visit in Germany from May-July 2017. The project was conceived by J. M. Gibbs, J. Boekhoven and me. J. M. Gibbs and J. Boekhoven supervised the project, provided helpful discussions and suggestions.

Dedication

To my parents, sisters, and brothers

Acknowledgements

My deepest gratitude and appreciation to my supervisor Dr. Julianne M. Gibbs for all her help and support throughout my PhD program. She has been providing helpful suggestions and advices that help not only to pursue a PhD but also to help after the degree. I would like to thank her for always being there to discuss the projects or any issue that might come up. I am so grateful to all the help that she offered me during my program and also special thanks for her help and time with editing my thesis.

Special thanks to my supervisory committee members, Dr. Christopher Cairo and Dr. Chris. Le for helpful discussions and observing the progress of projects.

I am glad being part of the Gibbs group as we have a nice and supportive group that always supports each other. And I would like to thank all the current and former Gibbs group students.

Special thanks to Gareth Lambkin, Biological services for the trainigs in the biological lab and support with useful advices.

Special thanks to Dr. Anna Jordan for her help with editing the appendix and early version of chapter 4.

My thanks are extending to Wayne Moffat, Analytical & Instrumentation Laboratory for the training on the fluorometer.

My thanks are extending to Jing Zheng and Randy Whittal, Mass Spectrometry Facility for the help with MALDI training and related questions on MS.

I would like to thank my family and friends who have been always there for me with their constant support.

Finally, I would like to thank ATUMS for funding my German exchange trip at TUM University and for all the professional development and training.

Table of Contents

List of Tables

List of Figures and Schemes

List of Symbols/ Abbreviations

ADP	Adenosine diphosphate
AMP	Adenosine monophosphate
ATP	Adenosine triphosphate
AZT	Azidothymidine
$(BimC_4A)_3$	5,5′,5″-[2,2′,2″-nitrilotris(methylene)tris(1H-benzimidazole-2,1-diyl)]tripentano-ate hydrate
CEU	Cohesive end units
CGE-LIF	Capillary gel electrophoresis with laser-induced fluorescence detection
CuAAC	Cu(I) catalyzed azide-alkyne cycloaddition
DIBO	Dibenzocyclooctyne
EDC	1-Ethyl-3-(3-dimethylaminopropyl)carbodiimide
Ellman's reagent	5,5'-dithiobis-(2-nitrobenzoic acid)
ExBenzi	1′-β-[1-naphtho[2,3-d]imidazol-2(3H)-one)]-2′-deoxy-D-ribofuranose
ExBIM	1′-β-[1-naphtho[2,3-d]-imidazole]-2′-deoxy-D-ribofuranose
FRET	Fluorescence resonance energy transfer
LIDA	Lesion induced DNA amplification
MALDI	Matrix-assisted laser desorption/ionization
NSCO	Non-substituted cyclooctyne
Nt	Nucleotide

ODN	Oligodeoxynucleotide
PAGE	Polyacrylamide gel electrophoresis
Per	Perimidinone-derived nucleoside
PNA	Peptide-nucleic acid
QUAL	Quenched auto ligation
SNP	Single nucleotide polymorphisms
SPAAC	Strain promoted alkyne-azide cycloaddition
TAMRA	Carboxytetramethylrhodamine
THPTA	Tris(3-hydroxypropyltriazolylmethyl)amine
T_m	Melting temperature
UPLC-MS	Ultra-high performance liquid chromatography mass spectrometr

Chapter One

General Introduction

1.1 Nucleic Acids-Templated Reactions: Overview and Motivation

Nucleic acid-templated reactions have been utilized to detect the presence of nucleic acid targets,[1-8] drug release,[9] and can be applied in nanotechnology.[10-11] In this thesis we will focus on one category of such templated reactions, DNA-templated ligations. In these reactions, the DNA template brings two complementary DNA pieces (probes) into close proximity and the groups on the 3' and 5' position can ligate together enzymatically, with the help of enzymes such as T4 DNA ligase to form a phosphodiester bond, or chemically, where the groups on the 3' and 5' termini typically contain an unnatural modification that can undergo a chemical reaction to form a covalent bond.[3, 12-18]

One interesting example of nucleic acid-templated ligations involves the development of self-replicating systems. The motivations for such a self-replicating system are that it could be applied in point-of-care-diagnostics as a simple means of nucleic acid amplification and detection as well as in nanotechnology. Indeed, DNA self-replication based on templated chemical ligation reactions has been explored in two strategies: by auto-catalysis[19] and cross-catalysis.[20] In autocatalytic replication the product sequence from the DNA-templated ligation is identical to the template sequence, so a palindromic sequence is required. In cross-catalysis the product sequence of the first templated cycle is the template for the second cycle. Similarly, the product of the second ligation cycle is the template for the first cycle. Because of the intrinsic feedback between these two cycles, exponential amplification of the original DNA template sequence is possible. Consequently, cross-catalysis is a more general way to amplify nucleic acid sequences as it does not require a palindromic sequence like auto-catalysis and is therefore of greater interest for biodiagnostics. The ideal cross-catalysis reaction should produce sigmoidal amplification of both the original target and the complementary sequence; specifically the system

initiated by sub-stoichiometric amounts of the template replicates exponentially until it begins to level off as the limiting reagent probe is consumed (Figure 1.1). However, such sigmoidal reaction progress is often not observed as we will see in the coming example.

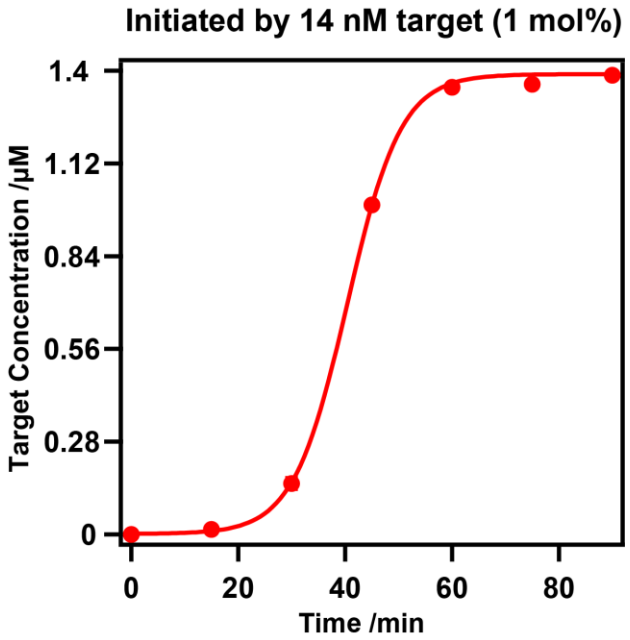

Figure 1.1 The sigmoidal graph of an ideal cross-catalysis reaction initiated with sub-stoichiometric amount of target. Self-replication of the target proceeds exponentially at first until the limiting probe is consumed and the production of target levels off.

1.1.1 Isothermal DNA Self-Replication

1.1.1.1 Non-enzymatic DNA Self-Replication

The earliest example of DNA self-replication by cross-catalysis using chemical ligation was presented by von Kiedrowski and co-workers.[20] They used a hexamer DNA as the target to self-replicate (Scheme 1.1A). To a small amount of this target they added four pieces of DNA: two pieces complementary to the target and two that were identical in sequence to different halves of the target. Each of these pieces was terminated with either a 5'-amine or a 3'-phosphate so that in the presence of 1-ethyl-3-(3-dimethylaminopropyl)carbodiimide (EDC) a phosphoramidate linkage would form (Scheme 1.1B). In order for the system to self-replicate,

the template needed to dissociate spontaneously from the product in each cycle. In Scheme 1.1C, the formation of different products versus time is shown in a reaction initiated with a sub-stoichiometric amount of BpB template, which should lead to greater formation of both its complement ApA and itself. However, the greatest amount of product was the ApA indicating that the product duplex did not readily dissociate to allow the ApA to initiate the formation of more BpB. The inability of the product to dissociate to initiate the second cycle is referred to as product inhibition. This is the fundamental problem in nucleic acid self-replicating systems that researchers have been trying to solve.[21] Another problem with this self-replicating system is illustrated by the amount of mixed products formed in the reaction (ApB and BpA) as these occurred from non-templated processes, which could then self-replicate. In this system, the high background (non-templated reactions) was likely due to the use of high concentrations of reactants, which were in the mM concentration range.

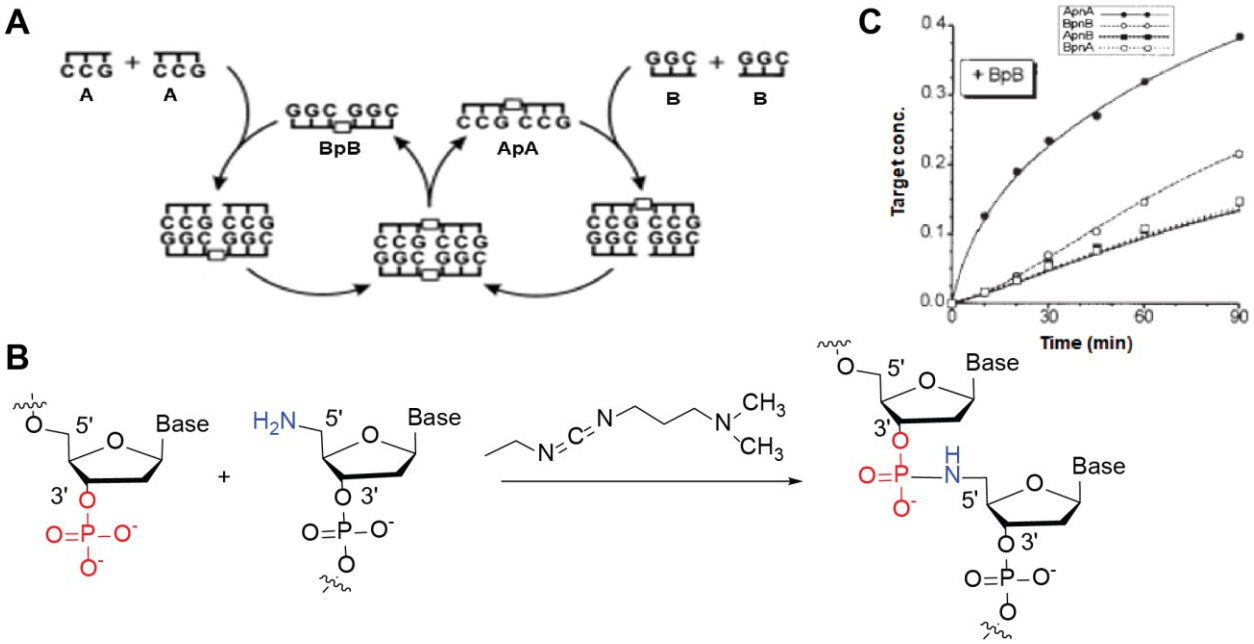

Scheme 1.1 Self-replication of DNA hexamers by templated ligation of 3'-phosphorothioate and 5'-amine probes. A) Cross-catalysis scheme for the template and the four trimer probes. B) Phosphoramidate linkage formation between 5'-amine and 3'-phosphate in the presence of EDC. C) The formation of different products versus time is shown in a reaction initiated with a sub-stoichiometric amount of BpB template in the presence of the four trimer probes. Image A regenerated with permission from ref. 21, Copyright © 2008, John Wiley and Sons. Image B repdrawn with permission from ref. 21, Copyright © 2008, John Wiley and Sons. Image C regenerated with permission from ref. 20, Copyright © 1994, Springer Nature.

1.1.1.2 Enzymatic DNA Self-Replication

One way to overcome the product inhibition issue in cross-catalytic replication was reported by our group with the introduction of an abasic lesion in one of the probes in an enzymatic ligation chain reaction called lesion induced DNA amplification (LIDA).[22-23] The key idea in LIDA is to incorporate a destabilizing abasic lesion (which is a nucleotide with a hydrogen in the 1' position of the deoxyribose ring instead of the nucleobase) into one of four DNA pieces or probes that undergo cross-catalytic self-replication. As a result of this destabilizing group, product inhibition that usually prevents turnover in cross-catalysis can be avoided. Using this approach our group demonstrated that an 18 base DNA sequence can be amplified exponentially (sigmoidally) with no need for temperature cycling (Scheme 1.2). As

LIDA proceeds isothermally at,[24] or near room temperature,[22-23] it has promise in point-of-care diagnostics as a method to amplify nucleic acid biomarker sequences without heating. One of the limitations for our system, however, is a non-templated background reaction that occurs in the absence of any target by a pseudo-blunt end ligation of the probe strands. This slow non-templated reaction makes the target template, which can then self-replicate rapidly.

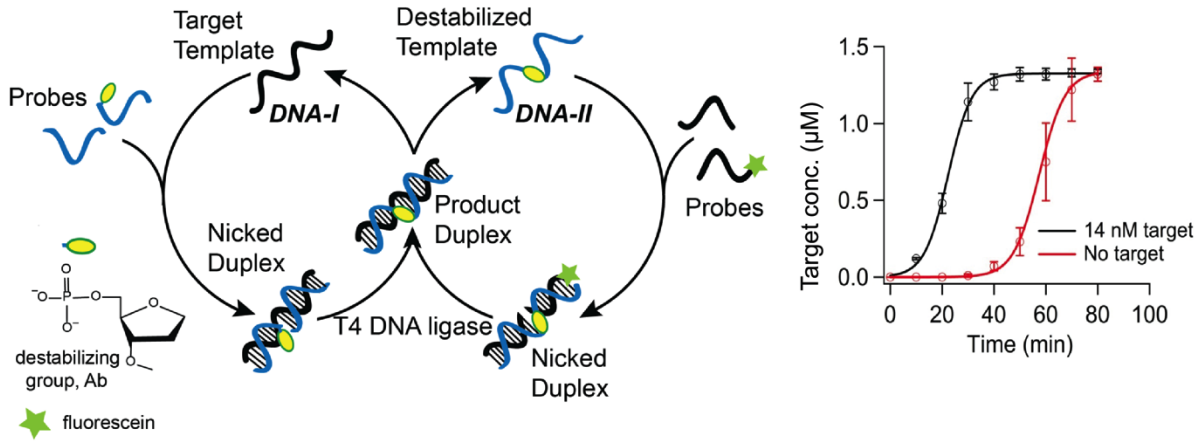

Scheme 1.2 Left: an illustrative scheme of lesion induced DNA amplification. Right: Sigmoidal amplification of a templated and non-templated cross-catalysis initiated with 14 nM and 0 M target, respectively.

The ultimate goal motivating the work in this thesis was to generate a version of LIDA that utilized chemical rather than enzymatic ligation. We were motivated by problems associated with employing enzymes in point-of-care diagnostics. Specifically using an enzyme has disadvantages such as its high cost and the need for storage in a -20 °C freezer. As such, replacing the enzymatic ligation by a chemical ligation reaction would be advantageous for the application of LIDA in point-of-care diagnostics.

1.2 Isothermal Turnover in Single Cycle Nucleic Acid-Templated Chemical Ligations

Although, we were the first to use a destabilizing group in an isothermal ligation chain reaction, previous work had explored generating turnover in single nucleic acid-templated

ligation cycles using destabilizing groups.[25] Just as in cross-catalysis, such turnover requires the spontaneous dissociation of the product duplex and thus results in many copies of the product from sub-stoichiometric amounts of the initial target template. Prior to our work, Kool's group utilized a destabilizing group to generate turnover isothermally in DNA-templated reactions using a flexible linker as a destabilizing group, albeit not in a cross-catalytic platform.[25] They incorporated this destabilizing approach into the ligation method that was developed in their lab called the quenched auto ligation (QUAL) procedure.[3] QUAL is a chemical ligation system with one of the probes terminated by a 3'-phosphorothioate and the other with a 5'-dabsylate adjacent to a fluorescein modification on the probe sequence. The dabsylate quenches the fluorescence of the fluorescein; however upon the templated ligation between the phosphorthioate and the alkyl dabsylate, the dabsylate anion leaves and the fluorescence appears. In the destabilizing version of QUAL, the presence of a flexible alkyl linker was added between the dabsylate and the probe sequence (with n = 0 or 1) which helped in the spontaneous dissociation of the product duplex. The butyl flexible linker led to 92 turnovers in 24 hours when the template was 0.01 mol% with respect to the probes (Scheme 1.3). The turnover number is determined from the amount of the complementary product formed divided by the amount of the initial target. Using this approach, the authors also detected mRNA in vivo suggesting that destabilization was a useful strategy for signal amplification.[25] Yet, this approach was not extended to generating a self-replicating system. However, very recently Kool and co-workers reported a cross-catalytic system using destabilizing QUAL for one cycle and a chain transfer reaction for the other cycle.[26] This greatly enhanced the signal amplification although it did not yield exponential replication of any target or complement.

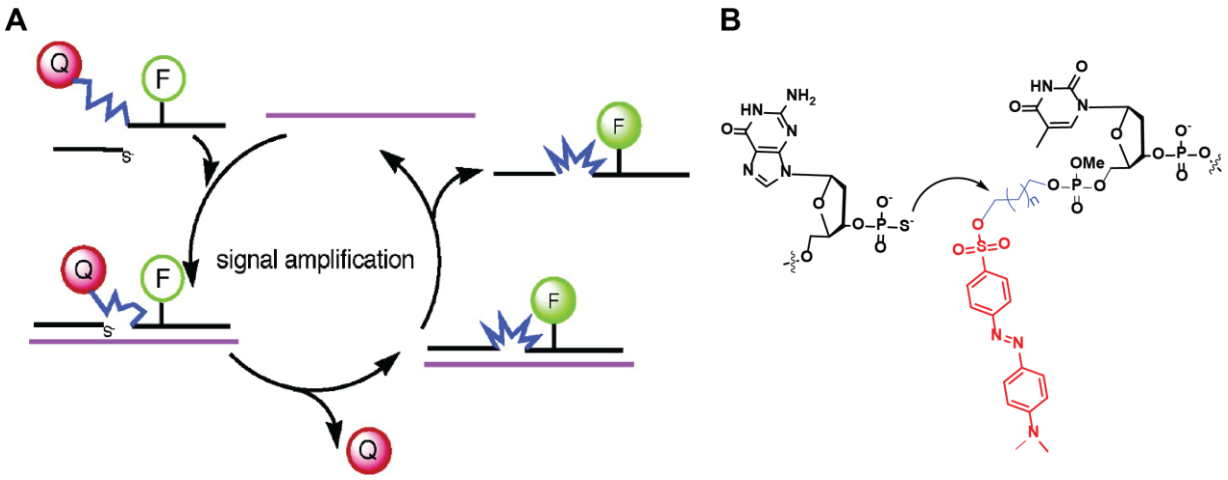

Scheme 1.3 Quenched auto ligation of phosphorothioate and alkyl dabsylate probes. A) The amplification scheme using QUAL. B) The structure of the ligating probes. Image A regenerated with permission from ref. 25. Image B modified from the same ref. Copyright © 2004, American Chemical Society.

Lynn and co-workers also reported one of the earliest examples of DNA-templated chemical ligation that led to isothermal turnover based on the reductive amination of 5'-amine DNA probe and 3'-aldehyde DNA probe.[27-29] The ligation reaction produced an imine product, which was then reduced to an amine by $NaBH_3CN$ (Scheme 1.4). The alkylamine linkage in the amine product had greater flexibility which resulted in substantial decrease in stability 10^6 fold less compared to the imine product, allowing for spontaneous dissociation isothermally. The authors achieved 13 turnovers per min with a total of 50 turnovers upon using 0.01 mol equivalents of the template at 25 °C.[28] When comparing to similar equivalents of initial template, it is the highest rate of turnover in an isothermal DNA-templated chemical ligation system to date.[13, 25, 30]

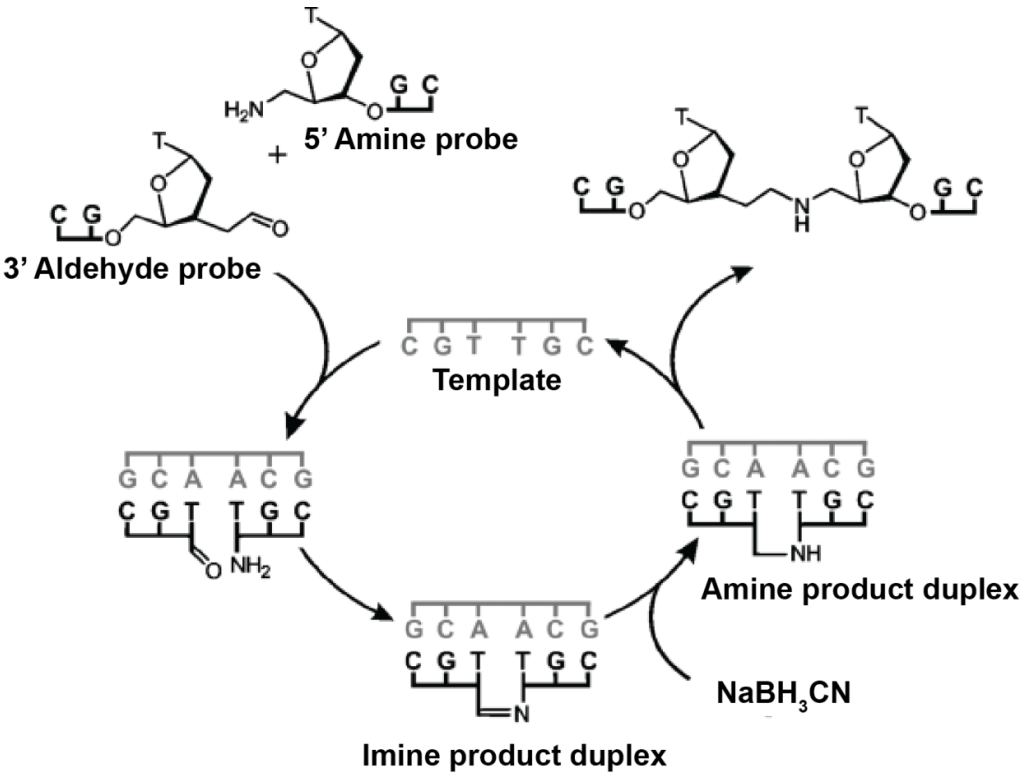

Scheme 1.4 DNA-templated reductive amination of 3'-aldehyde and 5'-amine DNA probes. Image regenerated with permission from ref. 21, Copyright © 2008, John Wiley and Sons.

The von Kiedrowski group, which was the first to explore DNA self-replication non-enzymatically, has also reported a rapid DNA-templated reaction based on disulfide bond formation between two 9-mer thiol DNA probes.[13] One of the thiols on the 3' or 5' end was activated using 5,5'-dithiobis-(2-nitrobenzoic acid) (Ellman's reagent) coupled to a dabcyl group as a quencher. This modification allowed the reaction to be monitored with fluorescence resonance energy transfer (FRET) as the quencher will leave upon ligation and a fluorescence signal can be detected (Scheme 1.5). The templated reaction (1 equivalent) with the activation on the 5'-thiol DNA probe was very rapid, completing in 5 min with no ligation product for the non-templated reaction at 25 °C and 35 °C.[13] The authors achieved 6 turnovers in 100 min upon using 0.01 equivalent template which is better than 9 turnovers and 10 turnovers in 24 h achieved by

Kool's[25] and Seitz's[30] group respectively with using 0.01 equivalent. However, it is not as good as Lynn's[28] system which yielded 13 turnovers per min.

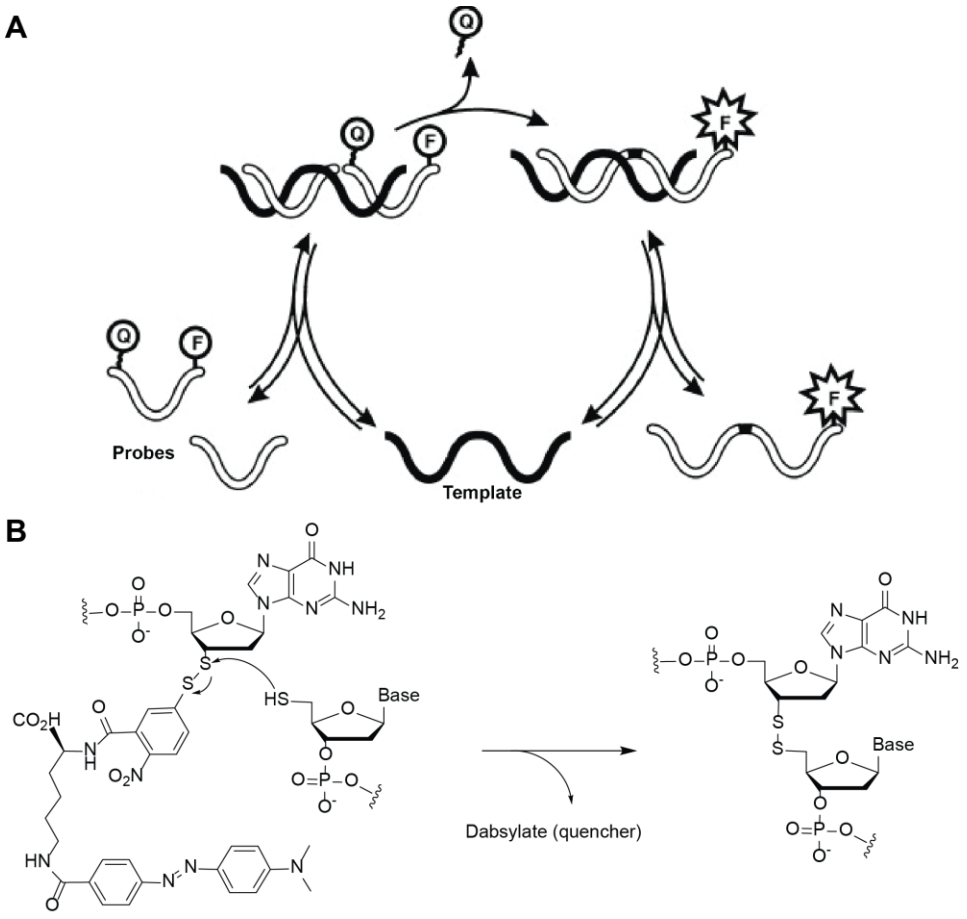

Scheme 1.5 DNA-templated disulfide bond formation. A) The reaction scheme of the disulfide bond formation. B) The chemical structures of the reactants and product. Image A regenerated with permission from ref. 13, Image B modified from the same ref. Copyright © 2014, John Wiley and Sons.

1.3 Reaction Rates and Selectivity in Chemical Ligations Based on Modified DNA

1.3.1 Examples of Rapid Chemical Ligation Methods

We have seen in the previous section some examples where researchers generated turnover isothermally. To achieve a higher turnover frequency, the ideal DNA-templated ligation reaction is rapid. In this section we will review the literature for some examples of rapid DNA-

templated chemical ligation. One of the fastest DNA-templated chemical ligation reactions is an inverse electron-demand Diels-Alder cycloaddition between tetrazine as a diene and strained dienophiles such as cyclooctyne and trans-cyclooctene. This reaction represents a good candidate for biorthogonal applications owing to its selectivity and functional group tolerance.[31-35] Using this strategy, Devaraj and co-workers have shown a rapid DNA-templated fluorogenic ligation between a 13-mer 5'-tetrazine DNA probe with a fluorescein and a 13-mer 3'-cyclopropene DNA probe.[15] Tetrazine, besides acting as a diene for this reaction, is also a quencher; therefore, the fluorescence signal will turn on upon the ligation with the cyclopropene as the diazole product is not a quencher. As such this ligation allows for easy monitoring of the product by fluorescence detection (Scheme 1.6). The reaction was so rapid in the presence of a template with one or two extra nucleotides (nt) across from the ligation site, yielding 100% ligation product in less than a minute. The reaction was also fast with a 27-mer RNA template.

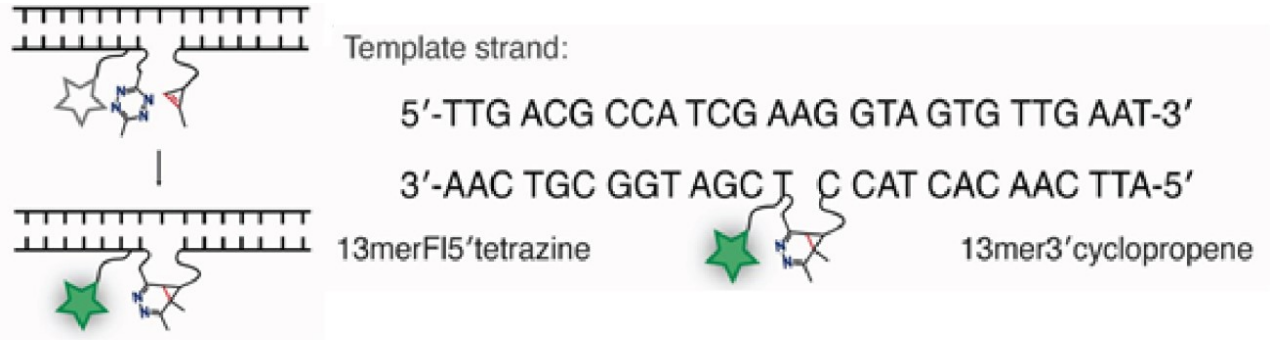

Scheme 1.6 DNA-templated fluorogenic ligation of tetrazine and cyclopropene. Image regenerated with permission from ref. 15, Copyright © 2013, Oxford University Press.

Another example of a rapid DNA-templated ligation is a DNA-templated Diels-Alder reaction that was reported by Brown's group.[36] Here, the authors prepared two different Diels-Alder probes, one with 5'-maleimide and the other with 3'-furan modifications (Type I) the other with 5'-furan and 3'-maleimide modifications (Type II). The two types were monitored

separately for the DNA-templated Diels-Alder ligation. In the presence of a complementary template, and type I Diels-Alder probes a ligation occurred between the two reacting groups (Scheme 1.7). The reaction was rapid with almost 100% conversion in 1 min and a much slower non-templated reaction. The DNA-templated type II Diels-Alder probes was as rapid as type I Diels-Alder probes despite the difference in the linkage orientation between the two products. The reaction was also efficient in ligating three DNA probes with ligation points of furan and maleimide simultaneously in the presence of a complementary template.

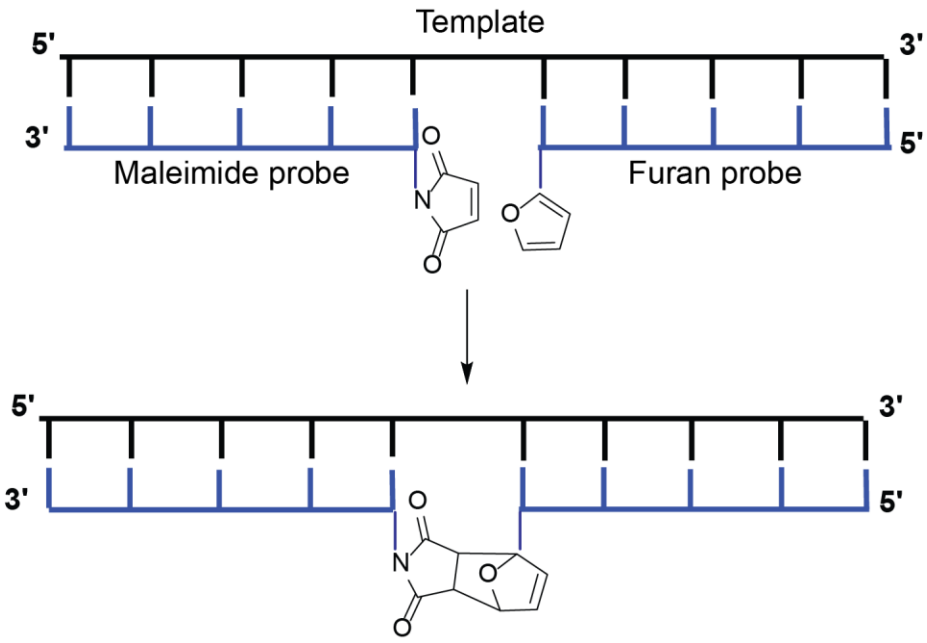

Scheme 1.7 DNA-templated Diels-Alder reaction of furan and maleimide DNA probes. The scheme was modified from ref. 36

Another example of a rapid chemical DNA ligation developed by the Brown lab is a Cu(I) catalyzed azide-alkyne cycloaddition pioneered by the Sharpless[37] and Meldal[38] groups. The reaction requires an azide group and an alkyne group that can undergo a cycloaddition reaction in the presence of Cu(I) catalyst to produce a triazole product. This reaction has been used widely for different applications such as templated synthesis,[39] nanotechnology,[40] self-

assembly of polymers,[41] attaching DNA to surfaces,[42] etc. The Brown group showed the compatibility of the triazole linkage with PCR,[43-44] gene synthesis,[45] and in *E. coli*.[14] An early report by the Brown group showed the first example of synthesis of a triazole linkage coupled with PCR amplification.[43] In this first report, the authors designed the linkage from an ODN with a 3′-azidothymidine (AZT) unit and a 5′-propargylamido on a T terminated ODN to form a triazole methylene amide linkage which acted as a PCR template (Scheme 1.8). However, the T-triazole methylene amide-T linkage read through by polymerase formed only a single T in the amplicon indicating that the other base beside the linkage was not copied.[43] In a later report by the group they attributed that to the rigidity of the amide bond on the linkage which does not allow the T to hybridize with the forming strand by the polymerase.[44] Thus, they designed a new triazole linkage more similar in size to a phosphodiester linkage from a 5'-azide nucleotide and a 3'-*O*-propargyl probe.[44] The PCR template (300 base pairs) with the triazole linkage (T-triazole-T) was read through by the DNA polymerase and in two steps of PCR forms (T-phosphodiester bond-T), indicating that DNA polymerase was able to read through the two bases on either side of the linkage. Moreover, such a template functioned well in *E. coli*.[44] Another report by the same group showed the biocompatibility of an assembled plasmid that had two triazole linkages in *E. coli*.[14]

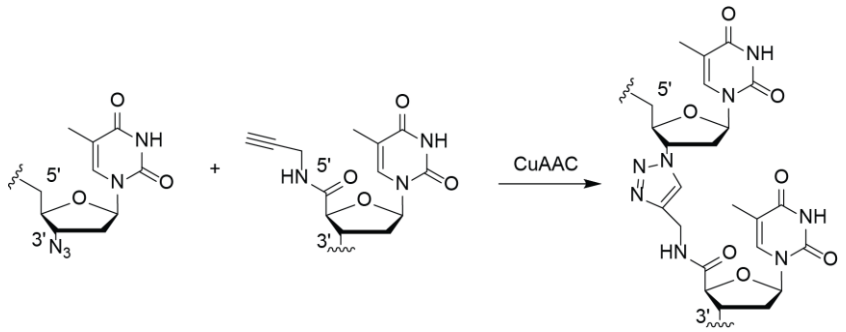

Scheme 1.8 DNA-templated CuAAC DNA ligation between 3′-azidothymidine and 5′-propargylamido DNA probes. Modified from ref. 43

Another example of a rapid DNA-templated chemical ligation is Cu-free alkyne-azide cycloaddition or strain-promoted alkyne-azide cycloaddition (SPAAC) also reported by the Brown group.[46] The SPAAC reaction was developed by the Bertozzi lab for in vivo imaging.[47] In this reaction, the alkyne is internal rather than terminal and located in a large ring, like dibenzocyclooctyne (DIBO) (Scheme 1.9). This ring is a strained molecule that releases its strain by undergoing cycloaddition with an azide. The authors synthesized two 3'-cyclooctyne DNA probes, one was non-substituted cyclooctyne (NSCO) and the other one was dibenzocyclooctyne (DIBO), and a 5'-azide-fluorescein DNA probe. The templated reaction was faster with the DIBO (as it is more strained compared to NSCO compound) yielding 100% ligation product in 1 min at room temperature.

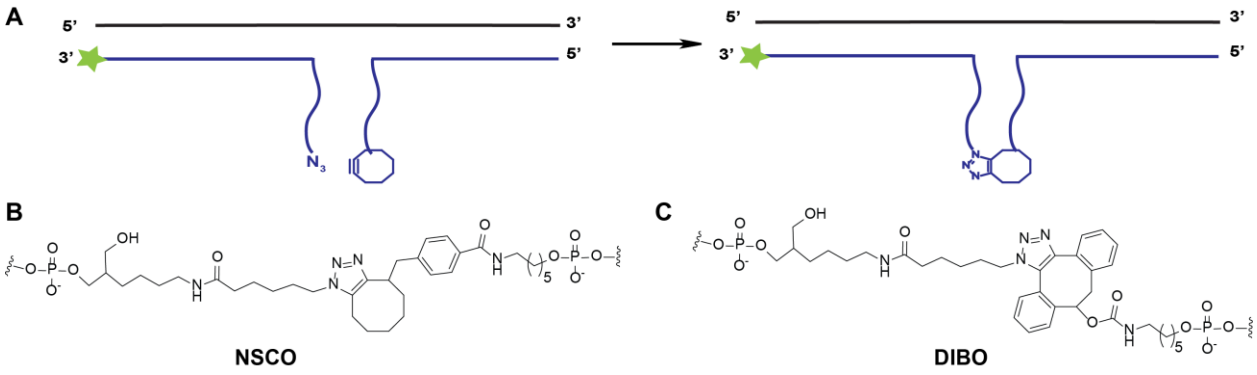

Scheme 1.9 A) DNA-templated SPAAC DNA ligation between 5' azide-fluorescein and 3'-cyclooctyne-based probes. Chemical structures of the ligation product from the 3'probes containing: (B) NSCO and (C) DIBO. Modified from ref. 46

Having a rapid DNA-templated chemical ligation could also be helpful in achieving turnover by temperature cycling, the reason for that is, it will reduce the amount of time required at the ligation temperature in each cycle. This approach was utilized by Ito and co-workers based on the chemical ligation between a 3'-phosphorothioate and a 5'-amide-linked methyl iodide (Scheme 1.10).[48] In the presence of the template and the complementary 8-mer 5'-iodide terminated DNA probe, and 7-mer 3'-phosphorothioate DNA probe, the reaction resulted in 20%

ligation after 15 seconds while a 6-mer phosphorothioate yielded 24 % after the same amount of time. After 60 seconds, the reaction levelled off at 40% conversion. Using this method, the authors cycled the temperature from a low temperature (25 °C) to allow for ligation to a higher temperature of 60 °C to initiate the dissociation of the product. This led to 60 turnovers in around 2 hours.

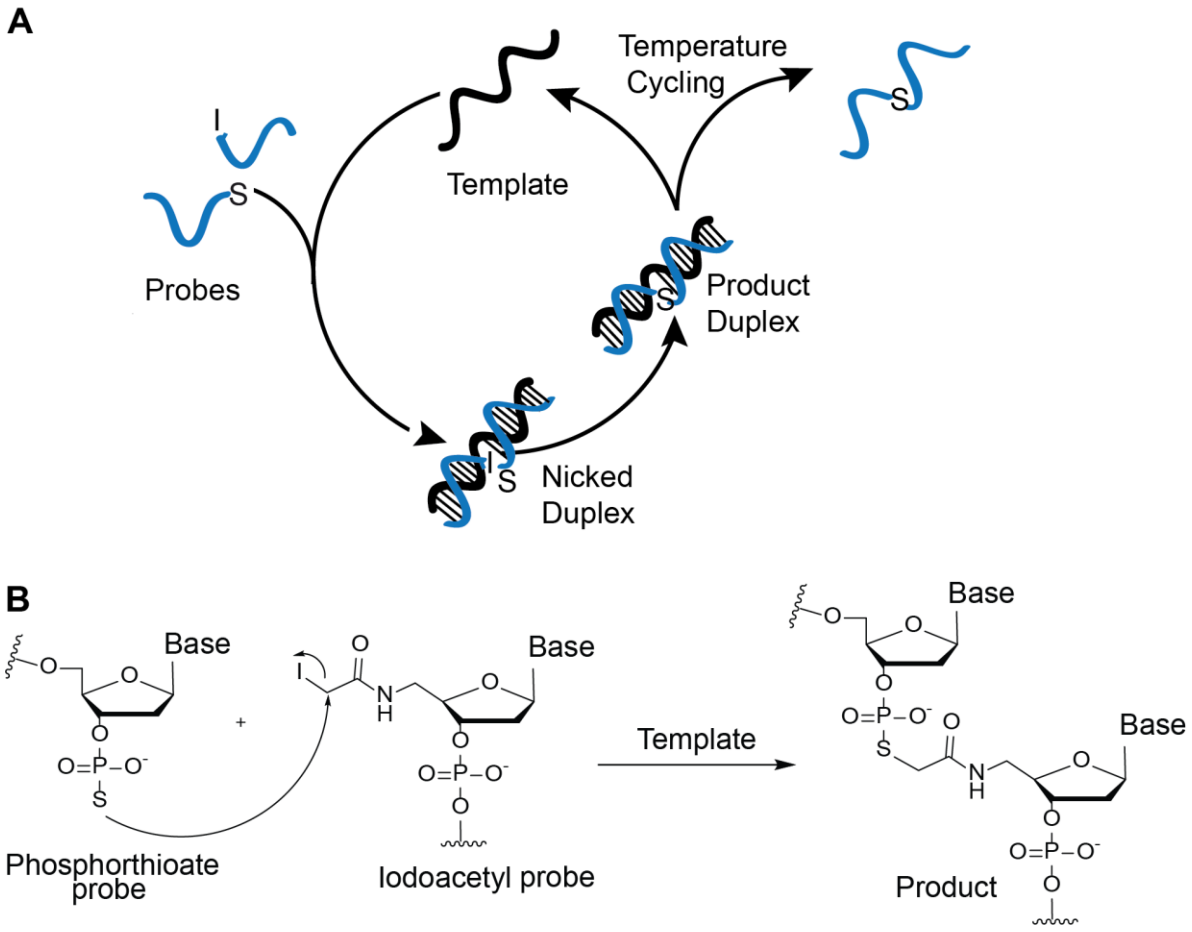

Scheme 1.10 A) General temperature cycling scheme for the templated ligation reaction of iodoacetyl probe and phosphorothioate B) The templated reaction between the iodoacetyl probe and phosphorothioate probe. Modified from ref. 48

1.3.2 Selectivity in DNA-Based Templated Chemical Ligations

DNA-templated reactions are often utilized to identify single nucleotide polymorphisms (SNP) like basepair mismatches, gaps, and deletions. In enzymatic systems, the motivation to use

ligation as a means to detect such SNPs arises from the enhanced selectivity of most ligase enzymes compared with polymerase.[49-50] Chemical ligation methods have also been successful at identifying SNPs based on the sensitivity of the ligation reaction to the presence of a mismatch.[51] To aid in the comparison of the following examples, I calculated the selectivity factors if it was not reported, based on the ratio of the % yield of the matched template to the mismatched template at a specific time.

Zhang and co-workers recently reported the use of DNA-templated CuAAC in SNP detection based on capillary gel electrophoresis using a 3'-azide probe (across from the mismatch) and 5'-alkyne probe.[52] The selectivity factors were determined by me from the ratio of the product peak areas for the matched and mismatched templates after 30 minutes at 30 °C. For the C:A and C:T mismatches, which were three bases from the ligation site of the azide probe, the selectivity factors were 4 and 6, respectively, which we will see in Chapter 2 are in line with our observations for the 5'-azide and 3'-propargyl system developed by Brown. The authors fixed the ratio of the 3'-azide probe (the mutated probe) to 1 while increasing the ratio of the 5'-alkyne probe, they found with a ratio of 1:10 (3'-azide probe: 5'-alkyne probe), they achieved the greatest selectivity between the perfect matched and mismatched. They attributed that to the azide probe, because the alkyne probe will be equally hybridized with the two templates but the azide probe will not be as well hybridized to the mismatched template compared to the matched template at 30 °C.

Another report of selectivity of DNA-templated CuAAC was reported by Peng and co-workers in a fluorogenic assay.[51] A DNA-templated ligation between a 12-mer 5'-azide DNA probe and a 12-mer 3'-coumarin alkyne DNA probe resulted in a fluorogenic CuAAC ligation

assay. The system was selective to mismatches with 80% conversion for the perfect match (C:G) and 5% for the single mismatch (C:A) at 45 °C, resulting in a selectivity factor of 16.

In the Deveraj's system of tetrazine-cyclopropene ligation described above, the selectivity for SNPs was assessed.[15] A 27-mer DNA-template with a 13-mer 5'-tetrazine probe and a 13-mer 3'-cyclopropene probe yielded 100% ligation product in ~ 3 min with the perfect matched template while no ligation product was detected in the presence of a single mismatch on the third position from the ligation site of the cyclopropene probe. This reaction has the greatest selectivity among the reaction discussed in this chapter. They have found that the selectivity is highly dependent on the cyclopropene probe length; the reaction with 7-mer 3'-cyclopropene probe had less selectivity compared to the use of 13-mer 3'-cyclopropene probe. To test the versatility of the reaction, the authors performed a SNP reaction with a 27-mer RNA template, and it was as selective as the 27-mer DNA template.

Finally, the SNP selectivity was assessed in the quenched auto ligation (QUAL) procedure developed by Kool and co-workers using a 3'-phosphorothioate probe and a 5'-alkyl dabsylate probe adjacent to a fluorescein modification.[25] In the presence of a single mismatch (C:A) on the template, the ligation rate was slower by 9 and 12.3 fold upon using propyl dabsylate probe and butyl dabsylate probe respectively indicating its selectivity to mismatches. I calculated the selectivity factors based on the relative fluorescence intensity of the matched template to the mismatched template to be 40 after 2 h.

1.4 Reaction Rates and Selectivity in Chemical Ligations Based on Peptide Nucleic Acid (PNA) Probes

1.4.1 Examples of Rapid PNA-Based Chemical Ligation Systems

Peptide-nucleic acids (PNA) are DNA analogs in a non-ionic form.[17] They consist of aminoethylglycine monomers that are connected to the nucleobases via carboxymethylene linkages.[17] Seitz and co-workers are the pioneers in native chemical ligation (NCL) of PNA.[7, 30, 53-54] The C-terminus of the ligation site is modified with a glycine thioester and a cysteine residue is located at the N-terminus; in the presence of a DNA template, native chemical ligation occurs between these two PNA probes (Scheme 1.11).

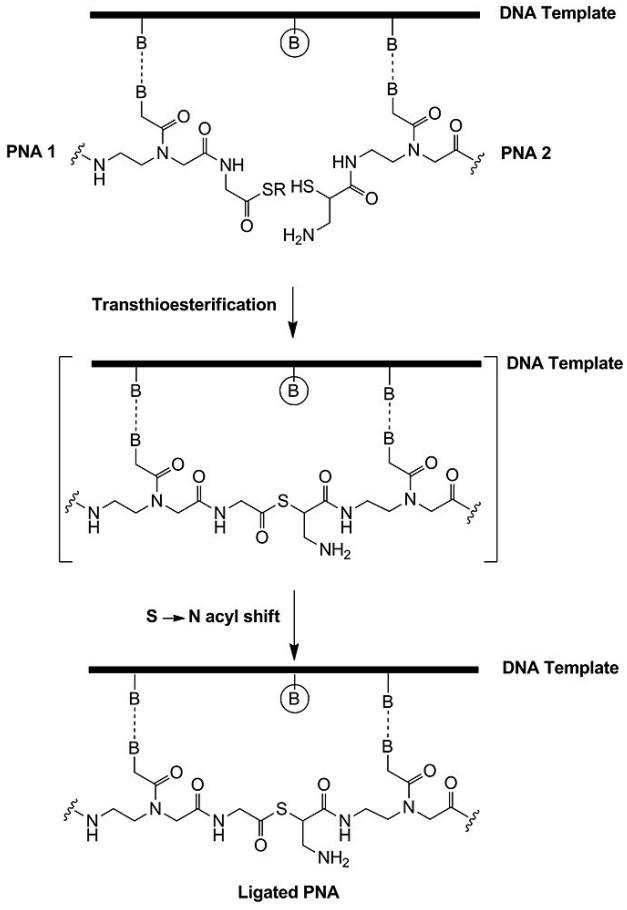

Scheme 1.11 Native chemical PNA ligation. Image regenerated with permission from ref. 17 Copyright © 2014, John Wiley and Sons.

To achieve isothermal turnover in a nucleic acid-templated ligation, Seitz and co-workers used destabilization in their PNA (peptide-nucleic acid) native chemical ligation system.[30] In this system, one of their probes was terminated with an iso-cysteine amino acid and the other one by a glycine thioester. The thiol on the iso-cysteine attacked the carbonyl of the thioester glycine to form a thioester bond with thioate as a leaving group (Scheme 1.12). This intermediate rearranged to the amide introducing an extra methylene group in the PNA backbone, which led to destabilization of the product and caused turnover.[30] Using this approach, they achieved 226 turnovers in 24 hours when the template was 0.01 mol% with respect to the probes.

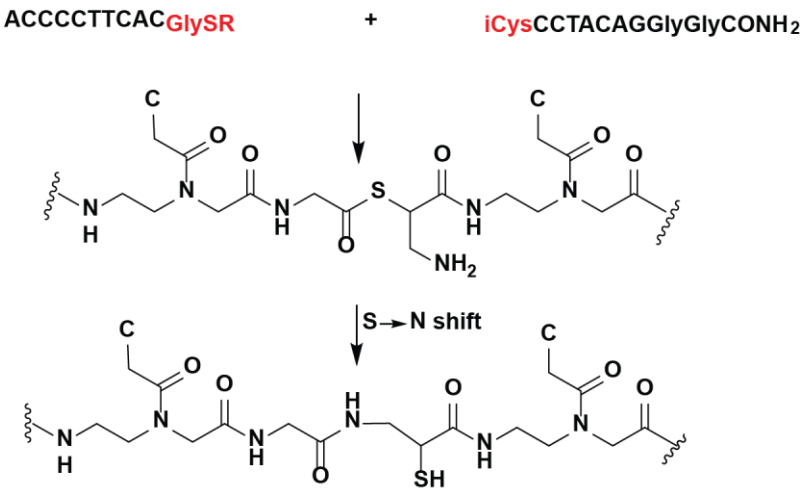

Scheme 1.12 Peptide-nucleic acid native chemical ligation of cysteine resulting in an S → N shift and destabilization. Modified from ref. 30

1.4.2 Examples of Selectivity in Templated Peptide-Nucleic Acid Ligations

Seitz and co-workers also developed a selective templated PNA ligation for SNP detection of a ras gene, which was as fast as enzymatic ligation.[7] The authors introduced an abasic ligation site by removing a PNA monomer from the ligation site.[54] The PNA ligation yielded 80% in 60 min in the presence of a perfectly matched template (rasTG), while less than 0.2% was detected for a singly mismatched template (rasGG) with selectivity factors of 400,

which is the most selective PNA example we discussed here. They also looked at the ratio of the pseudo first-order rate constants for the matched to be 206 Ms^{-1} $\times 10^{-11}$ while the mismatched were less than 0.06, they calculated the selectivity factors based on the ratio of the rate constants between the matched and mismatched to be >1:3450.

Seidman and co-workers designed a CuAAC version of PNA-DNA ligation.[55] The authors synthesized a 5'-azide DNA probe and a PNA probe with a propargylglycine on the N-terminus. In the presence of a complementary template and Cu(I) catalyst, a DNA-PNA CuAAC ligation occurred between the azide oligonucleotide and the propargyl PNA yielded 90% in 30 min. The assay was efficient in the detection of SNPs as well, four templates with single mismatches were prepared, and the templated ligation reactions were assessed (Scheme 1.13). The perfect match (C:G) yielded 92% while less than 2% ligation product was detected for the mismatched templates (C:C), (C:A), and (C:T) in one hour resulting in a selectivity factor of 46, which is quite selective.

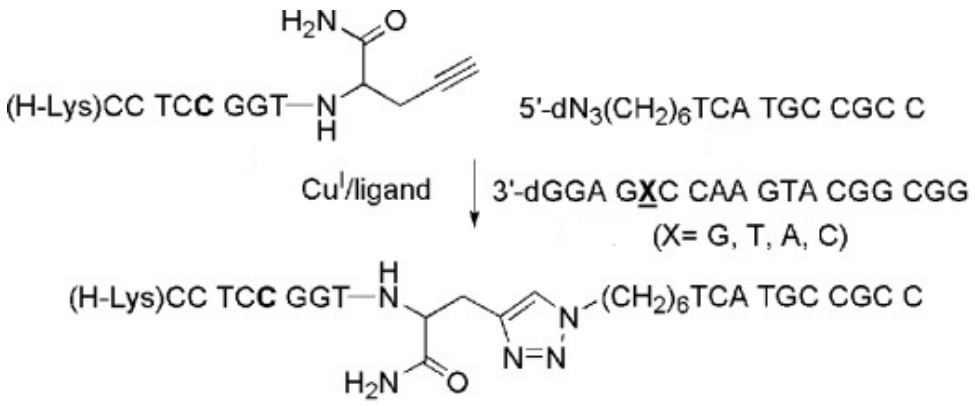

Scheme 1.13 Templated CuAAC PNA-DNA ligation of a perfect matched and mismatched templates. Image regenerated with permission from ref. 55, Copyright © 2010, John Wiley and Sons.

1.5 Motivating Observations

The initial goal of my PhD work was to develop a non-enzymatic version of LIDA. To begin, we focused on understanding the kinetics of different steps in the cross-catalytic cycle that had made LIDA so successful. For example, one thing that we noticed about our enzymatic LIDA is that it required a high concentration of enzyme. Using 6.5 Weiss units of enzyme, the cross-catalysis reaction initiated with 1% target led to 100 fold amplification in approximately 45 minutes (Figure 1.2 A, red circles). In contrast, when 1 Weiss unit was used only 9 fold amplification was observed after 2 hours and the reaction leveled at an amplification factor of 11 (Figure 1.2 A, black squares). This enzyme dependence surprised us, as it suggested the enzyme could influence the rate determining step in cross-catalysis, which had been thought to be product dissociation (see Chapter 1.1.1.2). Instead it appeared that the rate of ligation could also influence the kinetics of self-replication.

To confirm that the enzyme concentration influenced the rate of the ligation step, we ran a single cycle experiment at lower temperature where the nicked duplex formed between the target and two complementary probes should be stable. The experiment involved one equivalent of template, one equivalent of the 3'-hydroxy complementary probe and two equivalents of the 5'-abasic phosphate complementary probe in the presence of two different concentrations of T4 DNA ligase (1 Weiss unit and 6.5 Weiss units). The stoichiometric reaction representing cycle 1 in cross-catalysis was much faster using the higher concentration of enzyme (Figure 1.2B, red circles) compared to the use of 1 unit enzyme (Figure 1.2B, black squares). This experiment supported that the rate of the ligation step was important for the success of self-replicating nucleic acid systems. Thus, one goal of my thesis was to find a fast templated chemical ligation reaction, which could potentially lead to exponential amplification in cross-catalysis.

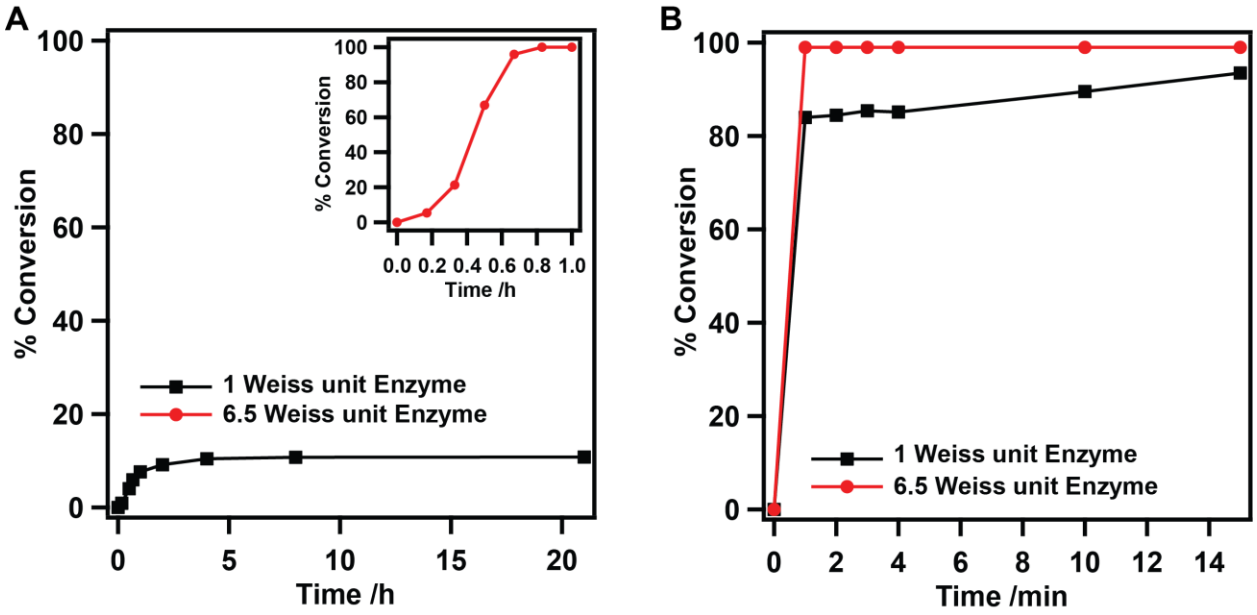

Figure 1.2 The effect of enzyme concentration on the DNA-templated ligation of an 18-mer. A) Cross-catalysis at 30 ºC. B) Single cycle stoichiometric reaction at 16 ºC. *Experimental conditions* for A*:* Template (14 nM), 5'phosphate-abasic probe (2.8 µM), 3'-hydroxy probe (2.8 µM), 3'-hydroxy-5' fluorescein probe (1.4 µM), 5' phosphate probe (2.8 µM). *Experimental conditions* for B*:* Template (1.4 µM), 5'phosphate-abasic probe (2.8 µM), and 3' hydroxy-5' fluorescein probe (1.4 µM), T4 DNA ligase (1 or 6.5 Weiss unit per 15 µL), 0.01 M $MgCl_2$.

1.6 Thesis Objectives

The original goal for this thesis was to develop an enzyme-free self-replicating system for point-of-care diagnostics. Although we did not achieve this goal, the work herein will help inform the design of a non-enzymatic DNA replicator. For example, one of the most important steps that we realized in order to develop such system is the ligation step. The ligation step has to be rapid in the presence of the template and no reaction should occur when no template is present. In chapter two, I will show how we investigated the kinetics and selectivity of the DNA-templated CuAAC ligation first developed by Brown and co-workers. This ligation was as rapid as enzymatic ligation using a high concentration of T4 DNA ligase enzyme. The selectivity of CuAAC was superior to the enzymatic system at temperatures between the dissociation temperatures of the perfect match and mismatched nicked duplexes.

In chapter three, I will discuss our efforts to develop a single nucleotide polymorphism assay to improve the selectivity of DNA-templated ligation using T4 DNA ligase, which is known to have low fidelity in discriminating between mismatches. Most of the previous reports on T4 DNA ligase employed temperatures that were less than the melting temperature (T_m) of the nicked duplex and higher than the T_m of the mismatched nicked duplex. We first studied the influence of raising the temperature far above the T_m of the nicked duplex on SNP selectivity in DNA-templated ligation using high and low concentration of T4 DNA ligase. We found that the SNP assay was selective with increasing the temperature far from the T_m of the nicked duplex of the perfect matched template. The effect of the abasic group on the SNP assay as a function of temperature was studied and the abasic makes the enzymatic reaction selective at around the T_m of the nicked duplex of the perfect match. To understand the lower ligation yield for the mismatched ligation, we studied the effect of the adenylating step on the kinetics of the ligation.

We observed an increase of the adenylating product in the presence of the mismatched compared to the matched template suggesting that the mismatched templates ligation stopped at this step.

In chapter four, I will discuss how we investigated the amplification of 6-*O*-methyl guanine modification in the KRAS gene using lesion induced DNA amplification (LIDA). Mutations in the KRAS gene, especially in codon 12 and 13, have a negative impact on cell proliferation and could lead to tumor cell resistance to epidermal growth factor receptor therapies. Finding a way to easily amplify the methylated template would be helpful. The KRAS sequence is rich in GC content, thus we introduced another abasic group in the abasic LIDA system. The amplification was studied using a modified nucleoside complementary to the O^6-methyl G developed by the Sturla lab at ETH. We have also studied the amplification of the methylated template when the modified base was not present in the system. However, we only observed facile amplification of methylated target using a C nucleotide rather than the modified base in our probe strand across from the O^6-methyl G substitutions.

In chapter five, I will provide a conclusion for all the results and the future work for these projects.

In appendix I, I will discuss different strategies for controlling the hybridization and dehybridization of DNA for a potential application in nanoswitch devices or for turnover amplification. First, we studied a strategy of using EDC as a fuel to induce DNA hybridization and dehybridization. Another strategy of using magnesium salt to drive DNA hybridization and dehybridization will also be discussed that resulted in many cycles of association and dissociation of the duplex. This project is an ATUMS collaboration travel exchange with the Boekhoven group at TUM.

In appendix II, I have the supporting information for chapter two.

Chapter Two

Quick Click: The DNA-Templated Ligation of 3′-*O*-Propargyl and 5′-Azide Modified Strands is as Rapid and More Selective than Ligase

2.1 Introduction

The copper-catalyzed version of the Huisgen azide-alkyne cycloaddition reaction pioneered by Sharpless[56] and Meldal[57] has been enormously impactful in the field of bioconjugation owing to its simplicity, bioorthogonality,[58] and click-like[59] properties (lack of by-products, rapid kinetics, and high chemoselectivity). As such, it is no surprise that this reaction has been incorporated into nucleic acid research in a myriad of ways,[60-62] from introducing unnatural appendages off of the nucleobase[63-67] to incorporating terminal modifications into the strand.[68-71] Such modification strategies allow nucleic acids to be interfaced with other materials[72] or confer to the oligonucleotide useful characteristics such as electrochemical[73] properties.

Another class of nucleic-acid based reactions that has utilized copper-catalyzed (or mediated) azide-alkyne cycloaddition (CuAAC) are templated ligations, which take advantage of the significant change in effective concentration of azide and alkyne functionalities that can result from localization by an oligonucleotide (ODN) or small molecule template. Indeed, despite the large rate constants for CuAAC,[74] low micromolar concentrations of azide and alkyne reactant ODNs make the reaction incredibly slow without the addition of a template. Consequently, reactions using small molecules or ODN templates to localize the azide and alkyne ODN and enhance the rate of CuAAC have been employed in a variety of applications such as in the recognition of small molecules through split aptamer systems,[75] in single nucleotide polymorphism (SNP) detection based on a fluorogenic scheme[51] or capillary gel electrophoresis with laser-induced fluorescence detection (CGE-LIF),[52] and in the preparation of surface immobilized strands.[76]

One particularly exciting example of CuAAC templated nucleic acid reactions was developed by Brown and co-workers using 3'-*O*-propargyl 5-methyldeoxycytidine at the 3'-terminus of an ODN strand and a 5'-azide on any deoxyribonucleotide at the 5' strand terminus (Scheme 2.1).[14] Upon templated CuAAC, a triazole linkage results that is similar in length to a natural phosphate-sugar linkage,[77] which is tolerated by many different enzymes such as DNA and RNA polymerases.[44, 78] Thus, DNA strands with these terminal groups can be used to construct genes that are subsequently translated and transcribed in *E.* coli.[14, 79] Moreover, using this CuAAC approach epigenetic modifications can be incorporated into the gene to determine the influence of such modifications.[79] This work indicates that CuAAC of 5'-azido and 3'-*O*-propargyl modifications might emerge as a non-enzymatic tool for ligation that could complement or replace ligase systems once strategies for labelling biosynthesized nucleic acids become available.[14]

One of the hallmarks of ligase enzymes is that they are simple to work with, are selective against base pair mismatches at the ligation site, and can be very rapid; this is of particular use in the construction of plasmids. Despite numerous reports in this area, most nucleic acid-templated reactions using the 3'-*O*-propargyl and 5'-azido modifications wait a pre-set amount of time, such as two hours, before isolating the ligation product.[14] To determine the viability of this ligation strategy as an alternative to T4 DNA ligase, here we monitored the kinetics of the DNA-templated CuAAC reaction using the 3'-*O*-propargyl and 5'-azido modifications[14] under aerobic conditions. Firstly, we found that ligand choice is important for accelerating the reaction and stabilizing Cu (I).[74, 80-82] With a newly optimized system using a benzimidazole ligand rather than the typical triazole ligand, we observed rapid ligation with rate constants that are comparable to those of T4 DNA ligase at the high concentrations used in *Quick Ligase* kits,[83]

and on par with the rapid DNA-templated tetrazine-methylcyclopropene system developed by Devaraj and co-workers.[15] Once more, these experiments were done in the presence of air making them as simple to set-up as a typical enzymatic ligation reaction. Finally, CuAAC of these modified ODN was able to discriminate certain single mismatches at the ligation site better than T4 DNA ligase at temperatures between the T_m of the perfect and mismatched nicked duplexes, suggesting that this CuAAC strategy is not just comparable but superior to the most commonly used ligation enzyme. The commercial availability of the 3'-propargyl modification and the simple solid-phase chemistry required for introducing the 5'-azido modification indicate that this templated reaction can be widely used for rapid ligation applications.

2.2 CuAAC Templated Ligation using a Triazole Derivative Ligand

In the Brown lab's original work the authors utilized tris(3-hydroxypropyltriazolylmethyl)amine (THPTA), the most common ligand choice in CuAAC strategies with nucleic acids.[14] Therefore, we first explored the reaction kinetics under similar conditions, which involved using excess copper complex compared with the nucleic acid probes (accordingly this would be an example of copper-mediated rather than copper-catalyzed azide-alkyne cycloaddition). For simplicity, we decided to work in the presence of air although argon is often used to prevent re-oxidation of the Cu(I) complex by ambient conditions.[84] We synthesized a 9-mer 5'-azide DNA probe (5' N_3 –TCT ATA CAA- 3'), a 9-mer 3'-propargyl DNA probe (5' T_F- ATC AAT TAC-alkyne- 3') and their 18-mer complementary target (5' TTG TAT AGA GTA ATT GAT 3'). The 5' azide DNA probe was synthesized using solid-phase synthesis following a previous report.[25] To assess the rate of ligation, we modified the 5'-terminus of the probe strand that contained the 3'-propargyl group with a fluorescein-modified thymidine as this is commercially available and allows for simple monitoring of the ligation

reaction by fluorescent imaging coupled with polyacrylamide gel electrophoresis (PAGE). Upon ligation, the distance travelled by the fluorescent ODN in the PAGE gel was significantly reduced allowing for easy quantification of the reaction.

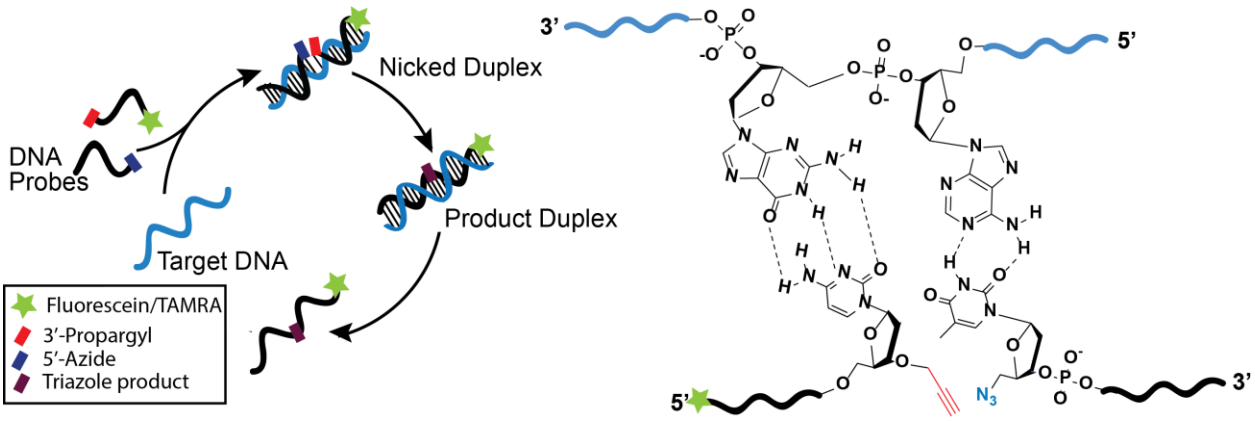

Scheme 2.1 DNA-templated Cu(I) catalyzed azide-alkyne cycloaddition, the template brings the azide and the alkyne group into close proximity.

The stoichiometric reaction was run in the presence and absence of an 18-mer DNA template with 100 μM $CuSO_4$, 1 mM sodium ascorbate and 700 μM of THPTA. The reaction was very fast as it yielded 81% of the triazole product in 10 minutes (Figure 2.1, + lanes, top band). However, one drawback that was the presence of a band near the product band in the absence of any template. Although this band had a very similar position to the triazole product, we postulated it was due to dimerization of the alkyne probe, which would also lead to an 18-mer product. One of the most common side-reactions in CuAAC is the Glaser coupling[85] of two alkyne groups in the presence of Cu(I) and air[86] which results in a di-yne product.

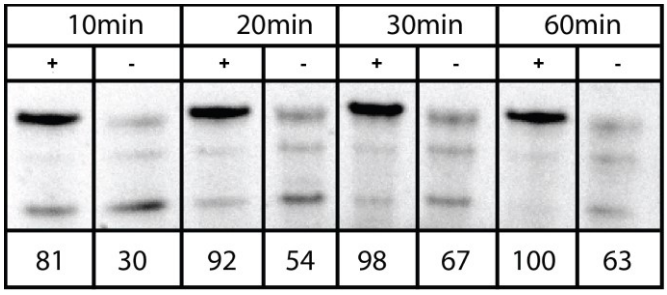

Figure 2.1 Polyacrylamide gel electrophoresis image of templated ligation reaction using CuAAC and a fluorescein-labeled alkyne strand. (+): template present. (-): no template. *Experimental conditions:* 1 μM template, 1 μM 5'-azide probe and 1 μM 3'-alkyne-5' fluorescein. 100 μM $CuSO_4$, 1 mM sodium ascorbate and 700 μM of THPTA, 27 ºC.

2.2.1 CuAAC Templated Ligation using a Longer 3'-Propargyl DNA Probe

To determine whether that band in the control lacking the template was the non-templated click reaction or alkyne dimerization, we synthesized a longer labeled alkyne 12-mer (5' T_F- ATA ATC AAT TAC-alkyne- 3'), so that the click product should be 21 bases but the homo-coupling of the alkyne should result in a product of 24 bases. We also changed the fluorophore to 5-carboxytetramethylrhodamine (TAMRA) as we had noticed fluorescein fading overtime (Figure 2.2). The figure showed that the by-product band was slightly higher than the product band indicating that non-templated reaction was not CuAAC but potentially a Glaser coupling of the alkyne. The identity of the extra band between the triazole product and the alkyne reactant remains unknown, but we confirmed that it occurred even in the absence of the azide probe suggesting it also originated from the alkyne probe.

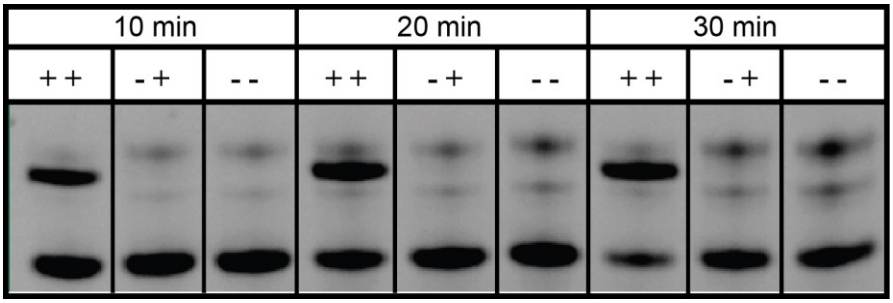

Figure 2.2 Templated CuAAC using a longer 3'-propargyl labeled with 5' TAMRA. (+ +): both template and azide probe present. (- +): no template but azide probe present, (- -) neither template nor azide probe present. *Experimental conditions:* 1 μM template, 1μM 5'-azide probe and 1μM 3'-alkyne-5' fluorescein 100 μM $CuSO_4$; 700 μM THPTA; 11 mM NaAsc, 27 ºC.

2.2.2 CuAAC Templated Ligation with a Labeled 5'-Azide DNA Probe

To ensure that the extra bands in the control reaction (non-templated reaction) were from the alkyne ODN, we decided to attach the fluorophore to the azide probe instead of the alkyne. Consequently, we synthesized new strands with the fluorophore at the 3'-terminus of the 5'-azido modified ODN. The stoichiometric reaction of CuAAC was run using the 5'-azide-3' fluorescein DNA probe, 3'-propargyl DNA probe and the complementry template. As anticipated, we observed a cleaner PAGE gel confirming that the main side reaction came from the alkyne-terminated strands (Figure 2.3). Rather than switching to use the azide as our limiting reagent, we decided to explore another ligand system to see if we could minimize side reactions involving the alkyne probe.

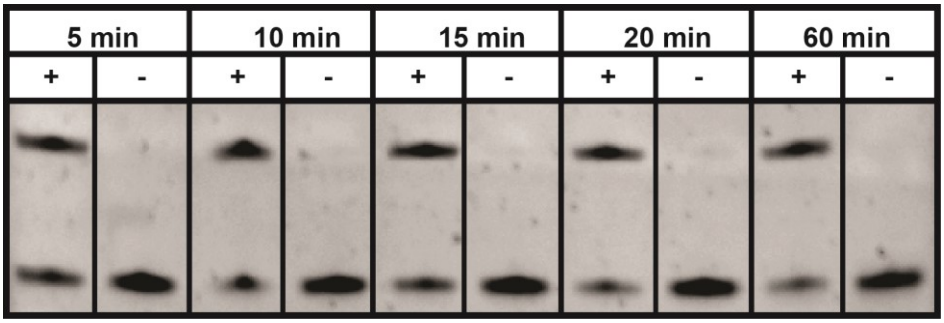

Figure 2.3 PAGE image of CuAAC templated chemical ligation. (+): template present. (-): no template. *Experimental conditions*: 1 μM template, 1 μM 5'-azide probe and 3'-alkyne- 5' fluorescein probe, 1000 μM THPTA, 200 μM $CuSO_4$, 11 mM Na ascorbate, 0.2 M NaCl, 27 °C.

2.3 CuAAC Templated Ligation using a Benzimidazole Derivative Ligand

The presence of the side reaction draws attention to one disadvantage of CuAAC: the Cu(II)/sodium ascorbate mixture can generate reactive oxygen species that react indiscriminately.[87-88] One way to tune the reactivity of the catalyst so that it is optimized for the reaction of interest and minimizes such side reactions is by judicious choice of ligand.[74, 80, 82] Consequently, we decided to explore CuAAC of the DNA using a benzimidazole-based ligand with a higher affinity for copper rather than a triazole-based ligand. Finn and co-workers have shown that the benzimidazole ligands are ideal for the rapid synthesis of triazoles.[74, 80] Additionally, they found that a lower ligand/catalyst ratio in comparison to that used for triazole-based ligands is often beneficial to the reaction rate, a result attributed to the stronger Cu affinity of the benzimidazole ligand.[80]

To optimize the DNA-templated CuAAC using this new ligand system 5,5′,5″-[2,2′,2″-nitrilotris(methylene)tris(1H-benzimidazole-2,1-diyl)]tripentano-ate hydrate ($(BimC_4A)_3$), we next varied the copper concentration while maintaining a 1:1 ratio of Ligand:Cu (Figure 2.4A). We observed that increasing the copper concentration from 200 μM to 600 μM greatly increased the ligation yield. Next we explored optimizing the ligand-to-copper ratio using this higher

copper concentration. Consistent with the previous work by Finn and co-workers,[80] we observed a non-monotonic effect of the ratio on the ligation yield assessed at 5 minutes. Specifically, the optimal ligand/copper ratio was 1.5; at higher ligand ratios the activity of the system decreased notably (Figure 2.4B).

With these newly optimized conditions in hand, we explored the reaction kinetics using target sequences that were completely complementary to the azide and alkyne ODN as well as target sequences that contained a mismatch at the ligation site (across from the 5-methylcytosine on the 3'-propargyl terminus).

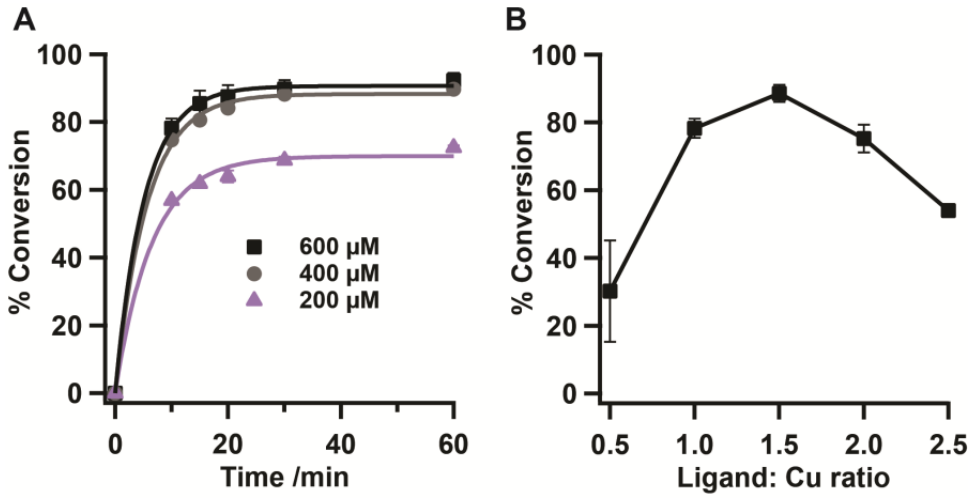

Figure 2.4 Optimization of CuAAC reaction using the $(BimC_4A)_3$ ligand. A) Cu^{+2} concentration variation (with [ligand]:[Cu] = 1). (B) Ligand/Cu ratio optimization (with 600 µM $CuSO_4$). *Experimental Conditions:* 11 mM sodium ascorbate, 1 µM template, 1 µM 5'-azide ODN and 1 µM 3'-alkyne-5' fluorescein ODN, 17 °C.

2.4 Comparison of CuAAC Templated Ligation with Enzymatic Templated Ligation

As a point of reference, we monitored the rate of ligation of the same sequences using 3'-hydroxyl and 5'-phosphate ODN that could be ligated by T4 DNA ligase. We utilized the highest commercially available concentration of T4 DNA ligase (2,000 cohesive end units per microliter), which is the concentration used in "quick" ligation kits for rapid sticky-end or blunt-

end ligations often used to construct plasmids for gene transfection.[83] We were pleased to see that the CuAAC system was very rapid at 23 °C, with quantitative conversion of the 3'-propargyl ODN after just 5 minutes for the perfectly complementary target (Figure 2.5C). Interestingly, the presence of mismatches still led to rapid ligation but reduced the absolute ligation conversion to between 20 and 30% after 10 minutes. The same experiments performed with T4 DNA ligase also revealed that the mismatched targets exhibited levelling off at 10 minutes at the same reaction temperature indicating that CuAAC exhibited similar reaction rates as this rapid enzymatic system (Figure 2.5D). Yet, the selectivity was much worse for the ligase than for CuAAC as several mismatches resulted in high % conversions for the former within 10 minutes. To see how elevated temperatures affected the kinetics and selectivity, we next performed the same experiment at 29 °C. For the CuAAC system the matched and mismatched templates resulted in ~ 88% and between 10-20% conversion, respectively (Figure 2.5E). For the enzymatic ligation at this higher temperature, the matched template resulted in nearly quantitative conversion, while significant conversions were also observed for the C:A and C:T mismatches (Figure 2.5F).

2.5 Selectivity of CuAAC Templated Ligation

To quantify the selectivity of the reaction, we calculated a selectivity factor from the ratio of % conversion (%con) with matched-to-mismatched template evaluated at 15 minutes. This selectivity factor was significantly better for CuAAC than for enzymatic ligation at both 23 and 29 °C (Table 2.1). Specifically, at 29 °C the CuAAC system yielded selectivity factors of 16, 6 and 11 while the enzymatic system was 24, 2 and 1.5 for the C:C, C:T, and C:A mismatches, respectively.

To determine how CuAAC imparted additional selectivity over the enzyme, we monitored the dissociation temperatures of the nicked duplexes formed between the ODN fragments to be ligated and the various templates at the salt concentrations that corresponded to their respective ligation conditions (0.2 M NaCl, 0.01 M $MgCl_2$ for CuAAC and 0.01 M $MgCl_2$ for enzymatic ligation).

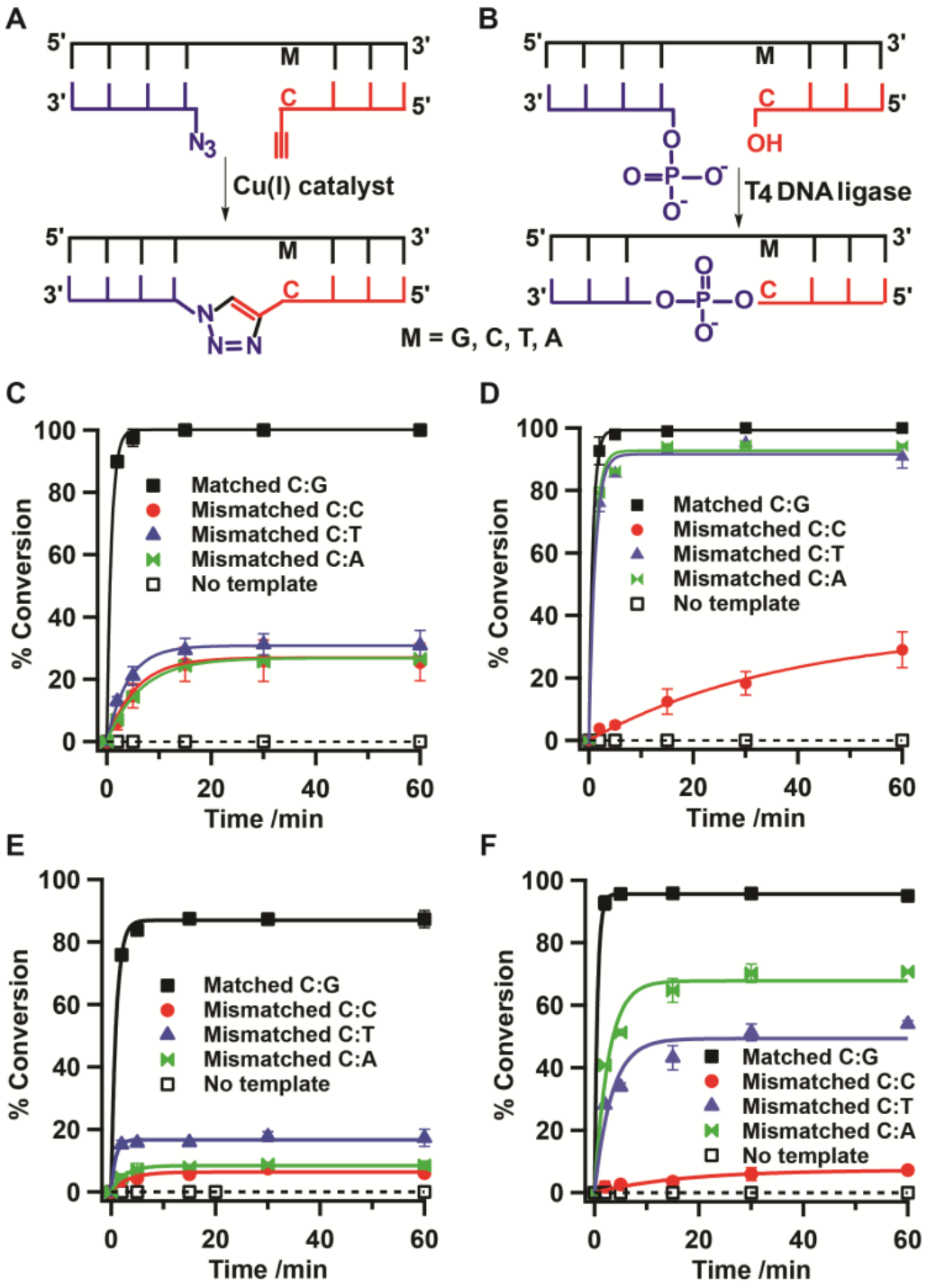

Figure 2.5 A) CuAAC templated ligation scheme. B) Enzymatic templated ligation scheme. Reaction profile of CuAAC with matched or mismatched template. at: C) 23 °C E) 29 °C. Reaction profile of enzymatic ligation at D) 23 °C F) 29 °C. CuAAC *Experimental Conditions:* 1 μM template, 2 μM 5'-azide ODN, 1 μM 3'-alkyne ODN; 0.2 M NaCl; 0.010 M $MgCl_2$. *Enzymatic Experimental Conditions:* 1.4 μM template, 2.8 μM 5'-phosphate ODN, 1.4 μM 3'-OH ODN in ligase buffer (0.010 M $MgCl_2$, 50 mM Tris-HCl, pH 7.5).

2.6 The Dissociation Temperature and its Effect on CuAAC and Enzymatic Templated Ligation

The dissociation temperature, or T_m, corresponds to the temperature where half the nicked duplex had dissociated allowing us to quantify the change in thermal stability upon introduction of the mismatches. For both systems, 29 °C lay near or above the T_m for the matched nicked duplex and well above the T_m values for nicked duplexes formed with the various mismatched templates (Table 4.1 and 4.2). These thermal stability data explain why at 29 °C the selectivity factors were better for both the CuAAC and enzymatic ligations in comparison to the selectivity factors at 23 °C. Generally, the trend in T_m values was consistent for the observed trend in selectivity factors. However, for the enzymatic system the magnitude of the T_m differences was not similar to the differences in selectivity factors. For example the T_m of the matched system was 31 °C, while that of the C:C and C:A mismatched systems were ~20 °C. Yet the selectivity ratios for these two mismatches were 24 and 1.5, respectively at 29 °C. We suspect that the enzyme stabilized the C:A mismatch better than the C:C mismatch as the former represents a pyrimidine: purine base pair suggesting a shape preference in the binding interaction between the enzyme and the nicked duplex.

We infer from these results that the difference in dissociation temperature can be used as a clear indicator of the selectivity factor for the CuAAC reaction as the click reaction captures the amount of nicked duplex present without affecting the duplex stability. In contrast, T4 DNA ligase stabilizes the nicked duplex thereby affecting its dissociation temperature.[89] Additionally, in the presence of the enzyme the extent of stabilization depends not only on the intrinsic stability of the nicked duplex but also on the mismatch geometry.[90] As such the selectivity of the enzymatic ligation reaction cannot be predicted from the dissociation temperatures of the nicked

duplexes. Moreover, temperature optimization also becomes less intuitive as the T_m values for the nicked duplexes have a weaker correlation with the amount of nicked duplex present in the ligation mixture owing to the varying extent of stabilization or reactivity of the ligase with the nicked duplex.

Table 2.1 Kinetic, Thermodynamic and Selectivity Parameters for the CuAAC System

	C:G	**C:C**	**C:T**	**C:A**
k_{obs} (min^{-1}), 23 °C	1.141 ± 0.008	0.18 ± 0.01	0.25 ± 0.02	0.154 ± 0.003
k_{obs} (min^{-1}), 29 °C	1.02 ± 0.07	0.3 ± 0.1	1.2 ± 0.3	0.39 ± 0.04
%con, 23 °C, 15 min	quant.	25 ± 5	30 ± 4	24 ± 4
%con, 29 °C, 15 min	88.5 ± 0.4	5.7 ± 0.4	15.9 ± 0.1	7.9 ± 0.3
T_m (°C)	31	17	18	20
Selectivity factor, 23 °C	1	4	3	4
Selectivity factor, 29 °C	1	16	6	11

Table 2.2 Kinetic, Thermodynamic and Selectivity Parameters for the Enzymatic System

	C:G	**C:C**	**C:T**	**C:A**
k_{obs} (min^{-1}), 23 °C	1.35 ± 0.07	0.026 ± 0.006	0.9 ± 0.1	0.9 ± 0.1
k_{obs} (min^{-1}), 29 °C	1.77 ± 0.07	0.06 ± 0.02	0.31 ± 0.08	0.38 ± 0.06
%con, 23 °C, 15 min	99 ± 1	12 ± 4	93 ± 1	94.1 ± 0.7

%con, 29 °C, 15 min	95.8 ± 0.1	4 ± 1	43 ± 4	65 ± 4
T_m (°C)	31	19	23	20
Selectivity factor, 23 °C	1	8	1	1
Selectivity factor, 29 °C	1	24	2	1.5

2.7 Comparison of Reactivity of CuAAC and Enzymatic Templated Ligation

Finally, to quantify the intrinsic reactivity of both systems as manifested in the observed pseudo-first order rate constant (k_{obs}), we fit the reaction profiles to: $f(t)= \%con_{max}(1-\exp(-k_{obs}t)$. The k_{obs} fit parameters and the reported standard deviation from the fit are shown in Table 2.1. These k_{obs} for the matched templates were similar for the CuAAC and T4 DNA ligase systems at 23 °C (1.1 and 1.4 min^{-1}, respectively, Table 2.1 and 2.2). Furthermore, to quantify the selectivity based on the rate constants, which is another method that has been used to report SNP discrimination,[7] the ratios of k_{obs} between the matched and mismatched templated reaction were determined. For CuAAC, this k_{obs} ratio was greatest at 23 °C: 6 for C:C, 4 for C:T and 7 for C:A. This optimal temperature might result from the difficulty in capturing early % conversion values at 29 °C for the matched and mismatched nicked duplexes owing to the rapidity of CuAAC at this temperature. For the enzymatic ligation the reaction did not level off as quickly at 29 °C, so the greatest values were observed at that temperature yielding k_{obs} ratios of 30, 6 and 5 for C:C, C:T and C:A mismatches respectively. These k_{obs} ratios indicate that even by this metric, the CuAAC is better at discriminating the C:A mismatch than enzymatic ligation by T4 DNA ligase. Using this approach to quantify SNP discrimination, however, does not provide any advantage in CuAAC compared with taking the ratio of the percent conversion, which is simpler than trying to

capture the rapid kinetics at early time points with high precision (likely involving stopped-flow kinetic experiments not amenable for simple detection applications).

Although this is the first kinetic study of CuAAC using 5'-azide and 3'-propargyl ether modified ODN strands, other templated alkyne-azide cycloadditions involving modified ODN have been explored. For example, a templated ligation using azide and alkyne ODN but without copper was developed and evaluated by Brown, El-Sagheer and co-workers in a strain promoted system using a 3'-cyclooctyne modification and a 5'-azide.[16] The authors found that the reaction yielded almost 100% ligation product within 1 min using dibenzocyclooctynol (DIBO). The Brown group has also reported a rapid interstrand cross-linking system via CuAAC.[84] In this example, the authors synthesized 5-alkyne or azide modified deoxyuridine with the reactive group off the nucleobase rather than the phosphate sugar backbone. Cross-linking upon duplex formation was rapid with almost complete conversion in 5 min. Finally, Peng's group developed a fluorogenic CuAAC system with an alkyne modified coumarin at the 5' position and a 3'-azide ODN. In the presence of a template and THPTA-Cu (I) complex, ligation readily occurred between the two DNA strands forming a triazole product.[51] For this system, the authors measured a k_{obs} of $1.1x10^{-3}$ s^{-1} and a half-life of 10.5 min, which is more than an order of magnitude slower than our measured value for the 3'-propargyl ether 5'-azide system ($t_{1/2}$= 0.63 min at 23 °C). We reason that the size of the 3'-*O*-propargyl group is more optimal for ligation leading to the great rate constant. Additionally, we note that they observed a similar selectivity for the C:A mismatch consistent with our hypothesis that CuAAC maintains the intrinsic selectivity of DNA hybridization. More recently, Zhang and co-workers reported the use of DNA-templated CuAAC in SNP detection based on capillary gel electrophoresis using 3'-azide and 5' alkyne ODN (the authors did not provide information of the exact structure of these

modified strands nor the resulting triazole linkage).[52] The selectivity factors based on their ligation yields after 30 minutes for C:A and C:T mismatches are in line with our observations at 23 °C, providing more evidence that CuAAC does not bias selectivity. However, the rate constant of CuAAC using these modified strands was not assessed.

2.8 Exploring Turnover with DNA-Templated Ligation by CuAAC

After achieving a fast and clean templated CuAAC reaction with no background reaction in the absence of template, we wanted to test whether we could observe turnover in the reaction. A substoichiometric amount of the template (1 and 10 mol%) was used in the presence of 2 μM of 5'-azide and 1 μM of 3'-alkyne- 5'-fluorescein at temperature range between 17 and 31 ºC. The results were not conclusive. Figure 2.21, is representative of one of the previous temperatures studied with 10 mol% template at 21 ºC. The reaction yielded 13, 16 and 20 % after 1, 2 and 4 hours, respectively. Indicating the maximum turnover number was only 2. This number is somewhat impressive given the large amount of template and the correlation between lower turnover number with higher relative amount of template.[25, 30] Thus, the reaction initiated with 1 mol% template should result in a higher turnover compared to 10 mol%, however we did not get turnover (the product was <1.5%). The reason for not getting turnover with 1 mol% is not clear but probably the fluorescein is fading after a long interaction period with Cu (I) catalyst which makes it hard to detect the product on PAGE.

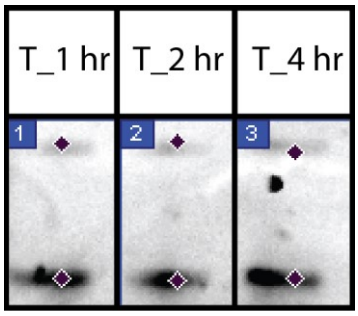

Figure 2.6 Turnover experiment of CuAAC using 10 mol% of the template, 2 μM azide probe, 1 μM 3'-alkyne-5' fluorescein 600 μM $CuSO_4$, 900 μM $(BimC_4A)_3$; 11 mM NaAsc, 21 °C.

2.9 Conclusions

In summary, we have assessed the reaction rate of Cu(I) mediated alkyne azide cycloaddition using 3'-propargyl ether and 5'-azide modifications under aerobic conditions as these modification result in the most biocompatible triazole linkage to date. The k_{obs} for the optimized reaction at 23 °C was 1.1 min^{-1} similar to that of the reaction catalyzed by T4 DNA ligase at high enzyme concentration and on par with one of the most rapid DNA based ligation systems to date: the reaction of 5'-tetrazine and 3'-cyclopropene ODN reported by the Devaraj group.[15] Moreover, in the presence of single basepair mismatches, CuAAC was able to discriminate most mismatches better than T4 DNA ligase at both 23 °C and 29 °C. We reason that CuAAC selectivity depends on the amount of nicked duplex present at a given temperature, which can be predicted by the thermal dissociation temperature of the nicked duplexes. In contrast, the temperature dependence of the enzymatic ligation depends not only on the intrinsic stability of the nicked duplex but also the stabilizing effect of the enzyme on the duplex. Additionally, the rate of ligation is also sequence specific suggesting a strong shape preference of the enzyme for the nicked site leading to indiscriminate ligation of C:A mismatches. These results indicate that CuAAC of the 5'-azide and 3'-propargyl modifications leads to enzyme-like rates and superior selectivities with negligible side reactions. Given the ability of the resulting triazole linkage to be tolerated in biological processes and the simplicity with which these functional groups can be introduced, we anticipate that this system will complement and even replace enzymes in advanced ligation applications.

Unfortunately, however, CuAAC does not appear to be the ideal chemical ligation strategy for developing a non-enzymatic version of LIDA. We reason that the failure of CuAAC is due to the short time of the Cu (I) catalyst activity (~ 1 h) compared to the long time needed to

perform cross-catalysis (hours). Even when we attempted to use argon to stabilize the catalyst for longer, we did not exhibit improves in turnover (data not shown).

2.10 Experimental Section

2.10.1 General

All the DNA synthesis reagents were purchased from Glen Research. Copper sulphate, sodium ascorbate, $(BimC_4A)_3$, THPTA, and ammonium persulfate were purchased from Sigma-Aldrich. Tris base, boric acid, EDTA, and tetramethylethylenediamine (cat. #T9281) were purchased from Fisher. 40% Acrylamide/bisacrylamide solution, 19:1 (cat. #1610144) was purchased from Bio-Rad. T4 DNA ligase enzyme (2,000,000 cohesive end units/mL, cat. #M0202T) and ligase buffer were purchased from New England Biolabs.

Table 2.3 DNA sequences used in this study

Name	**Sequence**
Template	5' TTG TAT AGA XTA ATT GAT 3' X = G, C, T, A
5'-Azide ODN	5' N_3 –TCT ATA CAA- 3'
3'-Propargyl, Fluorescein ODN	5' T_F- ATC AAT TAC-alkyne- 3'
3'-Propargyl, TAMRA ODN	5' TAMRA- ATC AAT TAC -alkyne- 3'
5'-Phosphate ODN	5' P –TCT ATA CAA- 3'
3'-Hydroxyl- 5' Fluorescein ODN	5' T_F- ATC AAT TAC 3'

2.10.2 Enzymatic Ligation Method

The matched or mismatched template, 5' phosphate ODN and 3'-hydroxy ODN- 5' fluorescein were added to an Eppendorf tube and diluted 10 μL MQ H_2O. The mixture was allowed to incubate in a covered thermal incubator at the specific temperature of 23 or 29 °C. A master mix (5 μL) with T4 DNA ligase (2000 cohesive end units, New England Biolabs) and the provided buffer (1.5 μL) was added to the previous mixture and timing started. The final volume was 15 μL and the DNA concentrations were: 1.4 μM matched or mismatched template, 2.8 μM 5' phosphate ODN and 1.4 μM 3'-hydroxy ODN-5' fluorescein. At different times of the reaction, aliquots (2 μL) were taken from the reaction mixture and put in an eppendorf tube containing a running dye (0.25% w/v bromophenol blue with 80% w/v sucrose in 0.5 M EDTA (aq) (2 μL). Samples were analyzed by 15% denaturing PAGE as described previously.[22]

2.10.3 CuAAC Templated Ligation Method

The matched or mismatched templates, 5'-azide ODN and 3'-alkyne -5' fluorescein ODN were combined in an eppendorf tube that contained a salt solution of 0.2 M NaCl and 0.01 M $MgCl_2$ (a total volume of 26.5 μL). This mixture was allowed to incubate in a covered thermal incubator at the specific temperature of 23 or 29 °C for 15 min. During this time copper sulfate (18 mM, 5 μL) and $(BimC_4A)_3$ (18 mM, 7.5 μL) were mixed together and left to stand for 5 min, then sodium ascorbate (33 mM, 5 μL) was added to this pre-mix and the mixture left to stand for another 5 min. Next, the Cu (I) complex pre-mix (3.5 μL) was added to the incubated ODNs and timing started. The total volume was 30 μL and the final concentrations were: 1 μM matched or mismatched template, 2 μM 5'-azide ODN, 1 μM 3'-alkyne -5' fluorescein-ODN, 600 μM $CuSO_4$, 900 μM $(BimC_4A)_3$ and 11 mM Na ascorbate. For the ligand type and ligand and copper concentration variation experiments the pre-mix composition changed accordingly. For the

kinetic experiments, aliquots (4 µL) were removed from the bulk ligation mixture at various reaction times and placed in an Eppendorf tube containing running dye (2 µL, 0.5 M) and urea (2 µL, 8 M). Samples were analyzed by 15% denaturing PAGE in a similar manner as the enzymatic ligation system.

2.10.4 T_m Measurements

1.3 nmol of each DNA strand (template and ligating ODN) were diluted in a 1 ml of salt solution (0.2 M NaCl, 0.01 M $MgCl_2$) for the 5‘ azide- 3’ alkyne system or in 1 ml of 0.01 M $MgCl_2$ for the 5’ phosphate- 3’-hydroxy system. The sample was hybridized in the fridge for around 1 hour. UV melting curves were measured using an HP 8453 diode-array spectrophotometer with an HP 89090A Peltier temperature controller instrument at 260 nm with a heating range of 12- 50 °C with 1 °C intervals, and 100 rpm stirring.

2.10.5 DNA Synthesis and Purification

The synthesis of the DNA strands were done using Glen Research reagents on an ABI solid-phase synthesizer, Model 392. Strands were purified following DMT-On GlenPak purification protocol using GlenPak DNA cartridges (cat. 60-5200-01). Standard DNA phosphoramidite, CPG’s and the following modifications: chemical phosphorylation reagent II (cat. 10-1901-90)], fluorescein-dT phosphoramidite (cat.10-1056-95)] and 3'-propargyl-5-Me-dC CPG (cat. 20-2982-41) were used (Figure 2.7). The 5’-azide strands were synthesized according to the literature[14] and purified using a Glen-Pak DNA purification cartridge. The azide modified strands eluted in the water wash and the subsequent elution step with 50% ACN eluent following a standard Glen-Pak DMT on purification with the omission of the TFA step. Note: standard DMT-on purification results in elution of the DNA in the 50% ACN step, not in the water wash.

We reason that the azide is not very hydrophobic, which is why it begins eluting in the water wash. However, as failure strands are eluted in the previous step, which is a saline wash, the azide strands are still well purified using these purification cartridges.

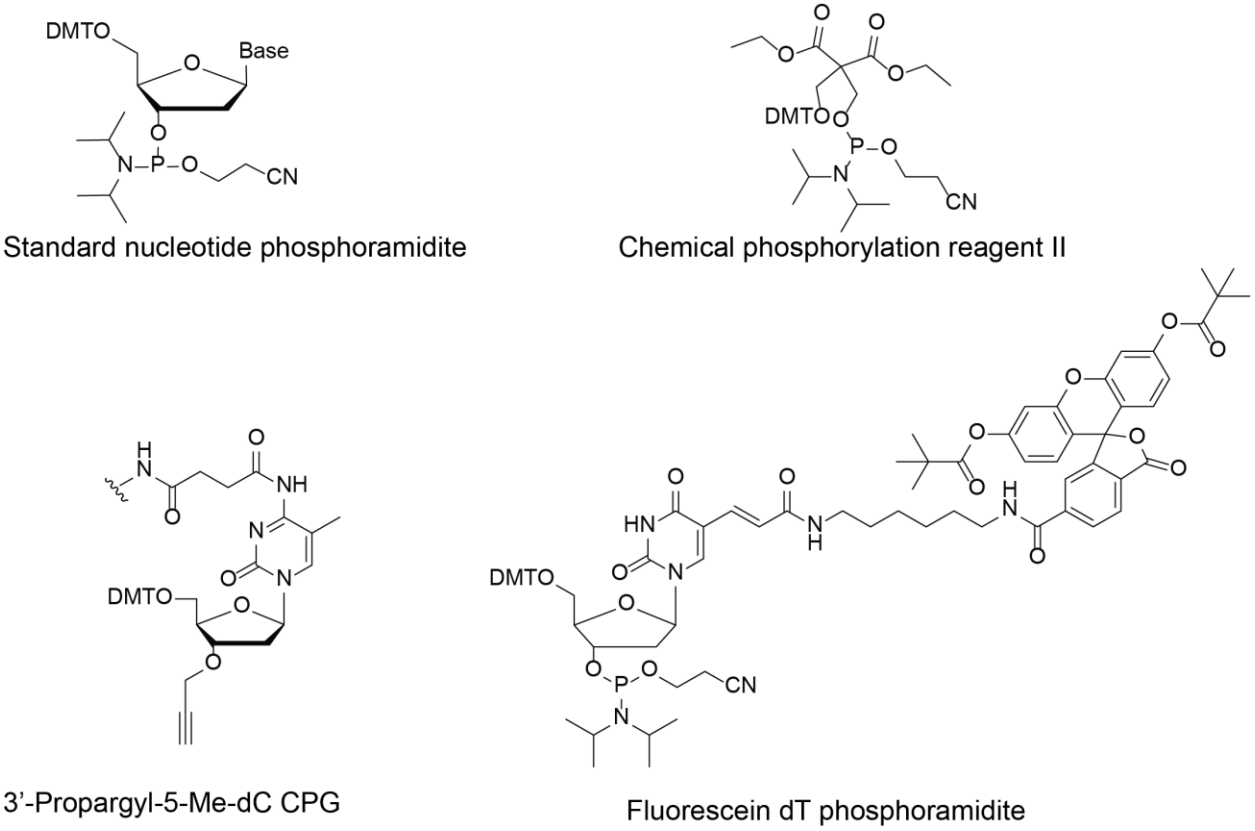

Figure 2.7 The chemical structures of the phosphoramidites and CPG used in this study. Dmt is dimethoxytrityl.

2.10.6 MALDI-TOF Characterization

Synthesised DNA strands were analyzed by MALDI-TOF. First a matrix solution of 3-hydroxypicolinic acid in 1:1 acetonitrile:water was prepared (25 mg/mL) as well as an ammonium citrate solution in water (25 mg/mL). These two solutions were mixed in a 9:1 ratio to yield the final matrix mixture. The synthesized DNA (5 nmol) was desalted using ZipTip

(ZTC18S096) purchased from Millipore Sigma and was mixed in a 1:1 ratio with the matrix mixture. The measurements were carried out on a Voyager Elite (Applied BioSystems, Foster City, CA, USA) time of flight-mass spectrometer.

2.10.7 Denaturing Polyacrylamide Gel Electrophoresis

A denaturing 15% polyacrylamide gel was prepared by dissolving urea (4.8 g) in 40% Acrylamide/Bis Solution 19:1 (3.75 mL) (Bio-Rad Cat.161-0144) and 5 x TBE buffer (1 mL), then diluted to 10 mL with MQ water. Tetramethylethylenediamine (10.7 µL, TEMED) and aqueous ammonium persulfate (80 µL) were added after urea was dissolved to induce polymerization. A portion of the aliquot and running dye mixture (3 µL) was loaded into a denaturing 15% polyacrylamide gel (8 M urea in 0.5 X TBE, 37.5 vol% of 40% acrylamide/bisacrylamide solution, 0.75 mm thick, 10 wells). PAGE was run at 150 V for 80 min. A fluorescent image was taken of the gel using a fluorescent imager with trans-UV illumination using an ImageQuant RT ECL instrument from GE Healthcare Life Science. Quantification of the fluorescence emitted by each band was analysed by using ImageQuant TL analysis software. The %con was determined based on the ratio of the fluorescence intensity of the product band over the sum of the fluorescence intensity of the product and reactant bands multiplied by 100%.[22]

The equation is as follow:

$$\%\ Yield = \frac{I_{\text{Product Band}}}{I_{\text{Product Band}} + I_{\text{Reactant Band}}} \times 100\%$$

2.10.8 Testing the Purity of the Synthesized DNA Probes by Stains-All

The DNA strands were loaded into 15% denaturing PAGE then stained with Stains-All (Aldrich cat # E9379). The Stains-All solution was prepared by dissolving Stains-All (25 mg) in 50 mL mixture of 1:1 (MilliQ H2O: Formamide). The PAGE is placed in a container contained the Stains-All solution, covered with foil and placed in a shaker for 15 min. The presence of one band only for each strand is an indication of the purity of the DNA strand.

Chapter Three

Enhanced Mismatch Selectivity of T4 DNA Ligase Far Above the Nicked Duplex Dissociation Temperature

3.1 Introduction

The most commonly utilized ligase in bioanalytical and molecular biology laboratories is T4 DNA ligase as it is available from a variety of suppliers and can be acquired at different concentrations and formulations depending on the application.[91] One reason why T4 DNA ligase has proven so useful is that it can be utilized not just in sticky-end ligations but also to ligate blunt ends that contain no complementary interactions.[92] Yet one problem with T4 DNA ligase is that it will ligate certain basepair mismatches fairly efficiently, even when they are located at the 3'-terminus of the ligation site.[93-99] Consequently, this lack of selectivity makes T4 DNA ligase less applied in one key area of bioanalytical chemistry: ligase-mediated discrimination of single nucleotide polymorphisms. Indeed, T4 DNA ligase is often used as a reference of low fidelity when evaluating the fidelity of different ligase enzymes.[100-101]

As such, recent efforts have been made to increase the selectivity of T4 DNA ligase. One strategy reported by Jang et al utilized modified bases at the 5'-phosphate end of a ligating probe strand to greatly enhance the selectivity of T4 DNA ligase.[102] Based on the authors' observations and supporting MD simulations, they proposed that a bulky non-hydrogen bonding modified nucleobase improved selectivity by increasing the distance between the template and the ligating strands. A similar approach has also been pursued in the biotechnology industry.[103] To determine whether an abasic lesion, which by definition lacks any steric bulk at the nucleobase position, enhanced the ability of the ligase to discriminate mismatches, we compared the kinetics of DNA templated ligation of wild type and mismatched targets and probes with either an abasic or complementary thymidine at the 5′ phosphorylated end of the ligation site. In the absence of the abasic lesion (where the 5′ end of the ligation site contains an A : T basepair), we found that all but one mismatched target had templated the formation of product, though the mismatched

targets had done so at a slower rate: after 1 hour the matched target had resulted in quantitative yield of the ligation product, whereas the A : X mismatch that resulted from the mismatched targets, where X is C and A, yielded 24 ± 0.4% and 20 ± 3% of ligation product, respectively (Fig. 3.1B).[104] In contrast, when the same experiment was performed with the probe bearing the abasic lesion at the 5′ end of the ligation site, much greater discrimination was observed: in 1 hour the complementary target had again resulted in quantitative yield of the destabilizing template product, whereas no product was observed for any of the mismatched targets (X), where X = A, C or G; Fig. 3.1C). These results indicated that the abasic lesion greatly enhanced the selectivity of T4 DNA ligase, which, to the best of our knowledge, has not been previously reported. Moreover, it indicates that steric bulk is not required for hindering mismatch ligation but instead a modification with significant destabilizing effects, such as the abasic lesion, can facilitate discrimination.[104]

In addition to containing the 5'-phosphate abasic modification, these above experiments were performed under ideal conditions for the isothermal ligase chain reaction method developed in our lab: lesion-induced DNA amplification (LIDA).[22-23] Specifically, we performed DNA-templated ligation with a high concentration of enzyme at 30 °C, a temperature significantly greater than the nicked duplex dissociation temperature (T_m = 16 °C) as this temperature led to the most facile DNA amplification by LIDA.

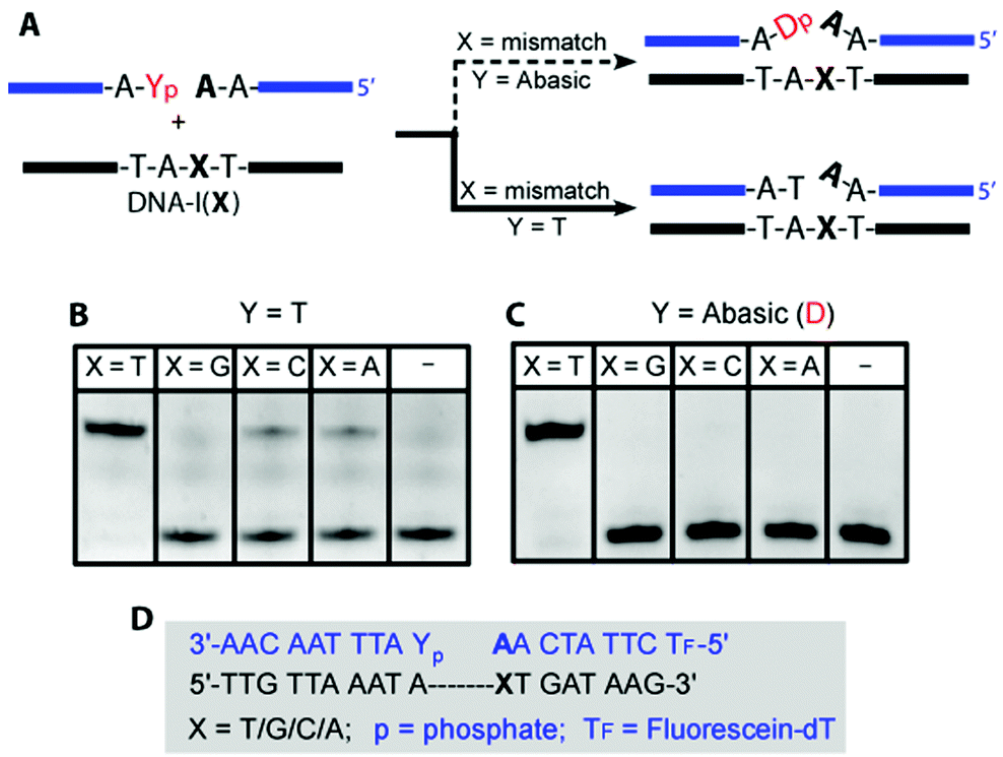

Scheme 3.1 The presence of an abasic group enhanced the selectivity of T4 DNA ligase to single mismatch. A) Schematic diagram for the system. B) PAGE image for the enzymatic ligation in the absence of a 5' abasic group. C) PAGE image for the enzymatic ligation in the presence of a 5' abasic group. D) DNA sequences used. *Experimental conditions*: 1.4 μM matched or mismatched template, 2.8 μM 5'-phosphate or 5'-abasic phosphate ODN, 1.4 μM 3'-hydroxy-5' fluorescein ODN, T4 DNA ligase (2000 cohesive end units, New England Biolabs) in ligase buffer (0.010 M $MgCl_2$, 50 mM Tris-HCl, pH 7.5), 30 °C.

Although it is well known that increasing the temperature improves ligase selectivity, not only for T4 DNA ligase but other ligases as well.[100] The only temperature recommendation that we found in the literature that lay above the T_m of the nicked duplex was for *Thermus thermophilus* ligase. The authors recommended that the T_m be 0-5 °C above the T_m of the ligating probes, with the two probe T_m values ideally being similar to one another.[100] However, as previously mentioned we had observed excellent selectivity when we performed DNA-templated ligation with T4 DNA ligase at a temperature >10 °C above the dissociation temperature of the perfect nicked duplex using a 5'-phosphate abasic terminus at the nick site.[104]

This selectivity was in stark contrast to the poor selectivity observed at the same temperature for the probe terminated with the complementary 5'-phosphate thymidine nucleotide rather than the abasic group.[104] We attributed the improved selectivity to the presence of the abasic group at the 5'-terminus as Jang et al. had shown that modifications at the 5'-end improved the selectivity of T4 DNA ligase.[102]

However, one aspect that we did not consider was the influence of temperature (relative to the T_m of the nicked duplex) and enzyme concentration on the selectivity of DNA-templated ligation using T4 DNA ligase. In this chapter we explore both parameters as well as determining the temperature-dependent selectivity in the presence of the 5'-phosphate abasic group.

3.2 Comparing Ligation Selectivity as a Function of Enzyme Concentration in the Temperature Window Between the T_m of the Matched and Mismatched Nicked Duplexes

Previous work exploring the SNP selectivity of T4 DNA ligase proposed that the ideal temperature that maintained greatest selectivity was a temperature below the dissociation temperature of the perfect matched nicked duplex and above that of the mismatched duplexes.[105] However, even in this temperature window some basepair mismatches at the 3'-terminus of the ligation site resulted in ligation. In contrast, *Thermus thermophilus* DNA ligase exhibited very little ligation of such mismatches suggesting that T4 DNA ligase has low fidelity compared with other ligase.[106]

We wanted to examine a temperature range much greater than the nicked duplex dissociation temperature as well as in the recommended temperature window. Therefore we measured the melting temperature of the matched and mismatched nicked duplexes templates for an 18-mer sequence shown in Figure 3.1. Based on the 18-mer sequence we selected, this temperature window between the perfect and mismatched duplexes was 19-29 °C.

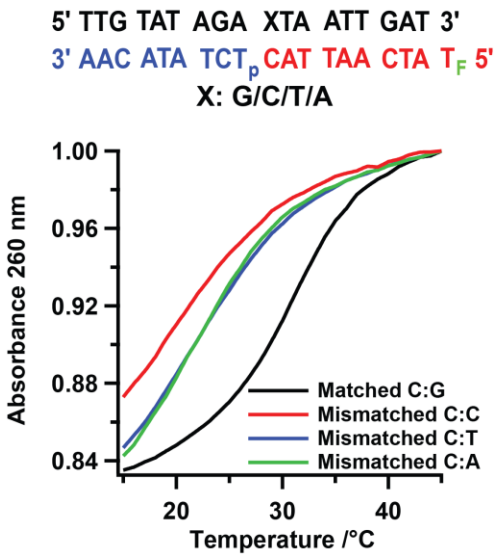

Figure 3.1 Thermal dissociation curves for nicked duplexes formed with the matched and mismatched templates. The absorbance was normalized. *Experimental conditions*: 1.3 nmol from each DNA (template, 5' phosphate-abasic probe or 5'-phosphate probe and 3'-hydroxy- 5' fluorescein probe), 10 mM $MgCl_2$, 10 mM PBS.

To assess SNP selectivity in DNA-templated ligations catalyzed by T4 DNA ligase, we utilized denaturing polyacrylamide gel electrophoresis coupled with fluorescent imaging. We prepared a 9-mer strand that made up the 3'-hydroxy terminus of the ligation site and included a fluorescein-modified thymidine using standard solid-phase synthesis. Upon ligation with the 5'-phosphate terminated strand (also a 9-mer), the mobility of the strand greatly decreased in the polyacrylamide gel electrophoresis experiment (Figure 3.2, top band). By comparing the intensity of this top band to the fluorescent intensity of both, the top and bottom (reactant) bands, the ligation conversion was quantified.

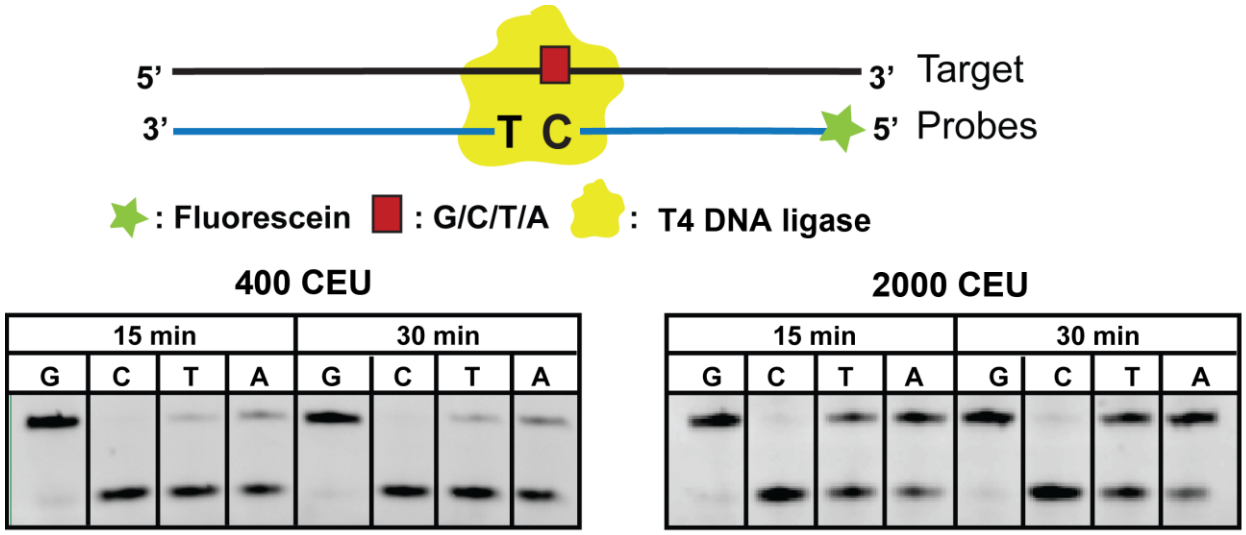

Figure 3.2 Polyacrylamide gel electrophoresis images from aliquots of the reaction using two concentrations of the enzyme. Experimental: 1.4 µM matched or mismatched template, 2.8 µM 5'-phosphate ODN, 1.4 µM 3'-hydroxy-5' fluorescein ODN in ligase buffer (0.010 M $MgCl_2$, 50 mM Tris-HCl, pH 7.5), T4 DNA ligase (400 and 2000 cohesive end units, New England Biolabs), 29 °C.

We began our investigation using low concentration enzyme at 29 °C, which lay in this temperature window between the matched and mismatched nicked duplexes for our probe sequences. The resulting fluorescent gel image for the ligation reactions with the perfect C:G match at the 3'-hydroxy position of the nicked site in comparison to the C:A, C:T and C:C mismatches are shown in Figure 3.2. Consistent with many reports on the low fidelity of T4 DNA ligase, we observed significant ligation of the C:T and C:A mismatches, 7% and 23% respectively after 15 min, under these conditions.[107-109] Increasing the enzyme concentration from 400 cohesive end units (CEU) to 2,000 CEU per 15 µL reaction made matters worse, 39% and 61% for C:T and C:A mismatches after 15 min (Figure 3.2), which is also consistent with previous reports that found that selectivity decreased with increasing ligase concentration.[110]

3.3 SNP Selectivity as a Function of Temperature

3.3.1 SNP Selectivity Using Low Concentration of T4 DNA Ligase

Next, we varied the temperature and performed the same type of analysis using the low concentration of T4 DNA ligase of 400 CEU as this is the more typical concentration used in SNP assays (the selectivity of lower concentrations has also been reported but those preparations are not commercially available).[100] Interestingly, the selectivity improved greatly upon increasing the temperature from 17-47 °C. Specifically, at 17 and 23 °C, the selectivity was poor which is expected as it is in the temperature window of the perfect match and mismatched nicked duplexes. The perfect matched yielded 100% in 2 min while the C:A and C:T are both above 80% and 70% after 15 min at 17 and 23 °C, respectively (Figure 3.3). In contrast, the experiments at 35 and 41 °C yielded excellent results with the perfect match resulting in >90% conversion after 15 minutes and the mismatched templates resulting in negligible amount at the same time point (Figure 3.3). This highest temperature lay 13 °C above the T_m of the perfect probe:template duplex revealing the excellent selectivity observed in our initial results using high temperatures, high enzyme concentration, and the 5'-phosphate abasic terminus were at least in part due to the enhanced selectivity of T4 DNA ligase at temperatures far above the dissociation temperature of the nicked duplex. In other words, these results indicated that even without the abasic modification or the high enzyme concentration, high selectivities could be achieved using temperatures far above the T_m of the nicked duplex of the perfect matched template.

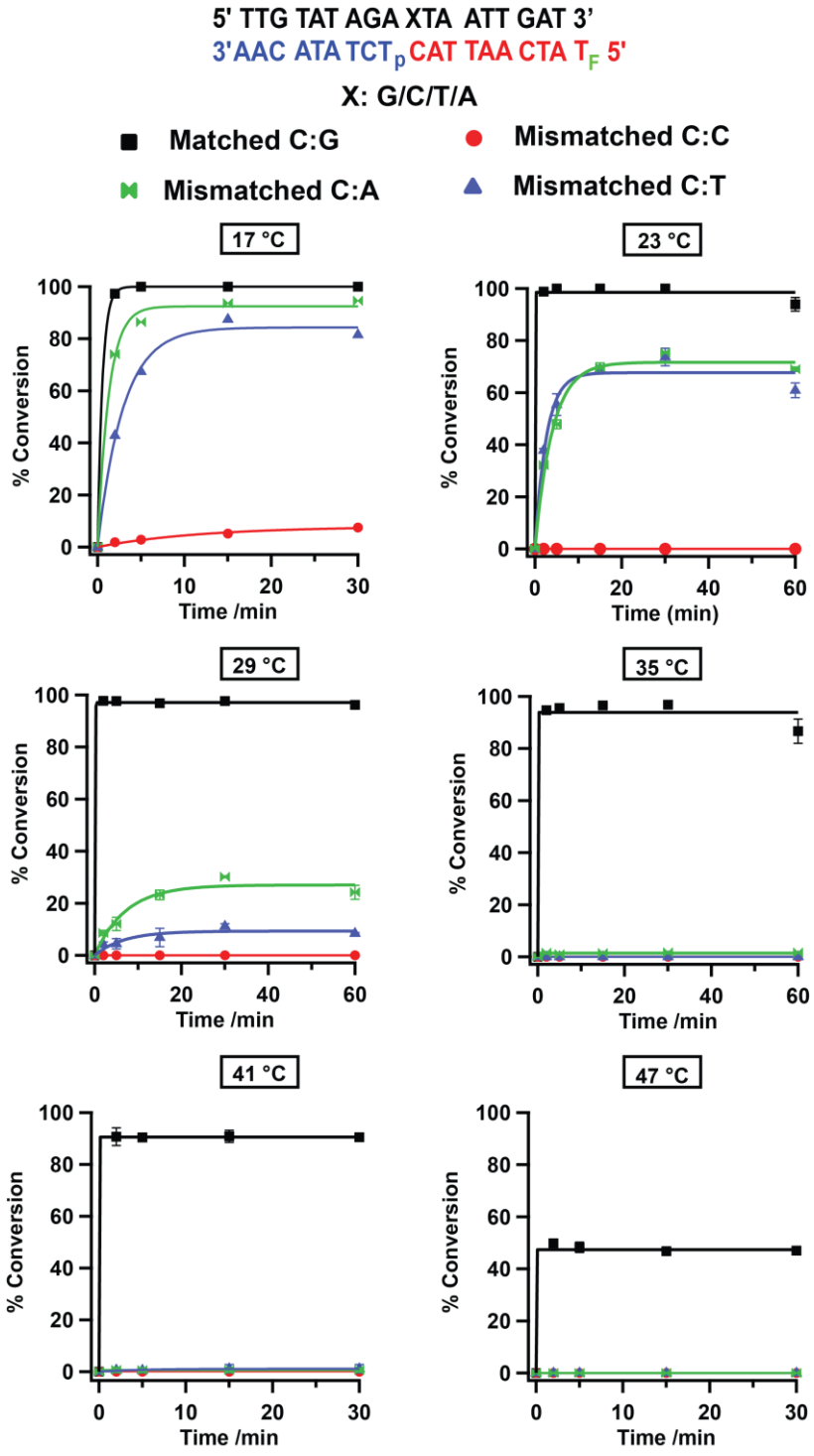

Figure 3.3 Reaction profile of DNA-templated enzymatic ligation in the presence and absence of SNP at various temperatures. *Experimental Conditions*: 1.4 µM matched or mismatched template, 2.8 µM 5'-phosphate ODN, 1.4 µM 3'-hydroxy-5' fluorescein ODN, T4 DNA ligase (400 cohesive end units, New England Biolabs) in ligase buffer (0.010 M $MgCl_2$, 50 mM Tris-HCl, pH 7.5).

3.3.2 SNP Selectivity Using High Concentration of T4 DNA Ligase

Next we explored the high enzyme concentration utilized in our earlier work, which is not as commonly chosen for SNP analysis with T4 DNA ligase but instead is used in rapid ligation for plasmid generation.[111] As previously mentioned, at 29 °C which lay at the T_m of the perfect system but above that of the mismatched duplexes, we observed worse selectivity for the high concentration enzyme (Figure 3.4) compared with the lower concentration (Figure 3.3). However, the selectivity increased dramatically at higher temperatures as was seen for the lower concentration of enzyme. The high concentration showed no mismatch ligation at 41 °C for the C:T, C:A, or C:C mismatch while the reaction reached 94% conversion within 5 minutes for the perfect matched system (Figure 3.4). At higher temperature of 47 °C, the high concentration yielded 88% for the perfect matched after 5 min and no mismatched ligation (Figure 3.4), while the low concentration of enzyme yielded only 49% for the perfect matched and no mismatched ligation at the same time point (Figure 3.3). These results indicated that using the higher enzyme concentration increased the range over where excellent selectivities were observed defined as temperatures where the perfect match yielded >80% and the mismatched template resulted in no discernable ligation (<2%) as this criteria was used in a recent screen of ligase fidelity.[100]

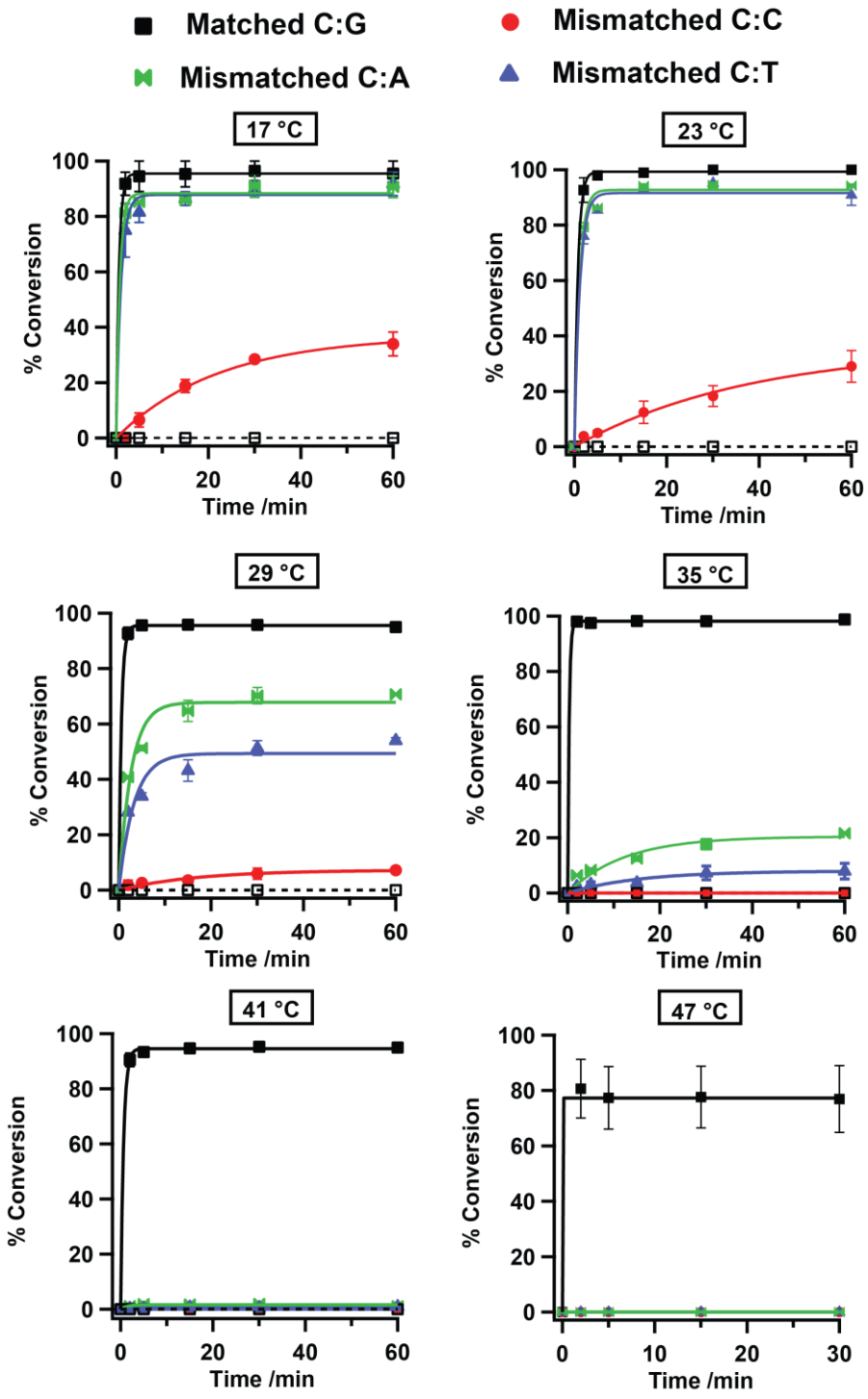

Figure 3.4 Reaction profile of DNA-templated enzymatic ligation in presence and absence of SNP at various temperatures. *Experimental Conditions*: 1.4 μM matched or mismatched template, 2.8 μM 5'-phosphate ODN, 1.4 μM 3'-hydroxy-5' fluorescein ODN, T4 DNA ligase (2000 cohesive end units, New England Biolabs) in ligase buffer (0.010 M $MgCl_2$, 50 mM Tris-HCl, pH 7.5).

3.4 SNP Selectivity in the Presence of an Abasic Group and High Concentration of Ligase

One advantage of T4 DNA ligase over other enzymes often chosen for ligase-based SNP detection is that it works well at lower temperatures. This is an advantage as one goal of point-of-care diagnostics outlined by the World Health Organization is that assays be "Equipment-Free" (the E in the ASSURED criteria). A simple way to remove the requirement for temperature control is to have the assay operate at room temperature. Unfortunately, many enzymatic nucleic acid based tests require carefully controlled temperatures above room temperature. Using T4 DNA ligase, our lab has been able to make our DNA amplification method LIDA facile at room temperature by using combinations of destabilizing groups, one of which is always a 5'-phosphate abasic modification.[97-98] As such, we decided to explore the temperature dependence of SNP selectivity using this abasic containing strand.

First we measured the thermal dissociation curves for all of the nicked duplexes based on the 5'-abasic phosphate system (Figure 3.5A). Interestingly, the nicked duplex formed with the complementary 3'-hydroxy probe exhibited a similar dissociation temperature for the 5'-abasic phosphate or the 5'-thymidine phosphate (Figure 3.5B). This similarity in nicked duplex T_m for the 5'-abasic and 5'-thymidine was also observed for a different sequence.[104]

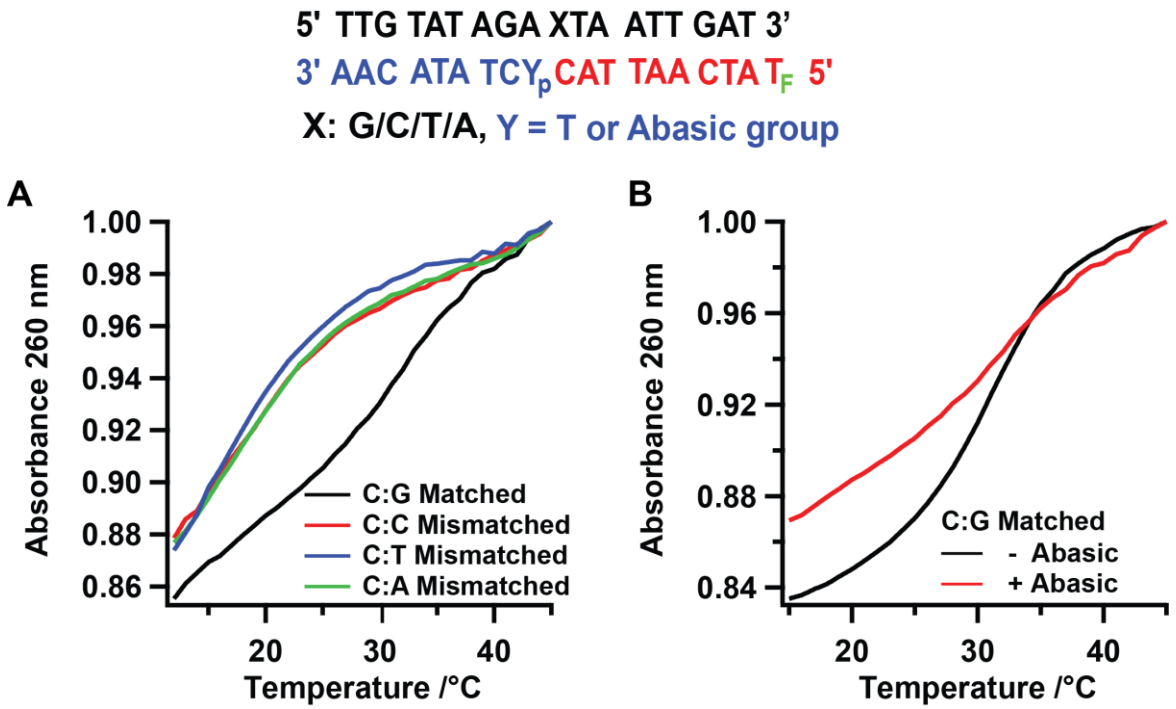

Figure 3.5 Thermal dissociation curves for nicked duplexes formed with the matched and mismatched templates. A) In presence of an abasic group. B) The matched template with and without an abasic group. *Experimental conditions*: 1.3 nmol from each DNA (template, 5' phosphate-abasic probe or 5' phosphate probe and 3'-hydroxy- 5' fluorescein probe), 10 mM $MgCl_2$, 10 mM PBS.

As shown in Figure 3.6, we observed highly selective discrimination from 29-35 °C with >95% conversion for the matched template and negligible ligation of any of the explored mismatches. This temperature range was >7 °C than the probe:template duplex dissociation temperature for the matched template using the abasic-containing probe.

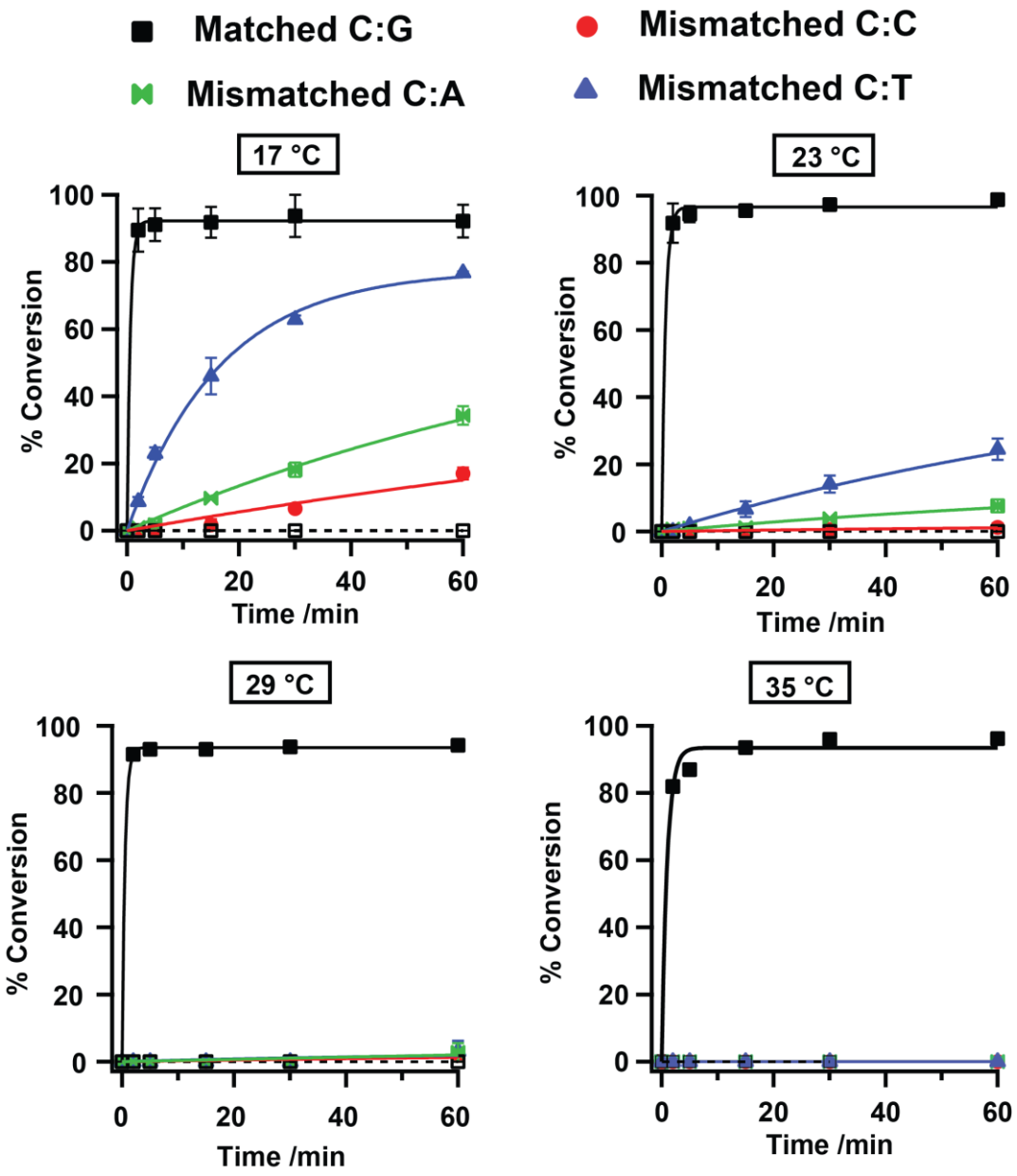

Figure 3.6 Reaction profile of DNA-templated enzymatic ligation in presence and absence of SNP. *Experimental Conditions*: 1.4 μM matched or mismatched template, 2.8 μM 5'abasic-phosphate ODN, 1.4 μM 3'-OH-5' fluorescein ODN, T4 DNA ligase (2000 cohesive end units, New England Biolabs) in ligase buffer (0.010 M $MgCl_2$, 50 mM Tris-HCl, pH 7.5).

3.5 Temperature Range of Optimal Selectivity and T_m Values for 5'-Abasic and 5'-Thymidine Systems

Table 3.1 lists all of the experimental dissociation temperatures and the temperature range where optimal selectivity was observed (>80% for the perfect and negligible ligation for the

mismatched). As a point of reference we calculated the melting temperature of each probe:template duplex for the perfect matched system using OligoAnalyzer on Integrated DNA Technology's (IDT) website similar to a previous report to estimate the nicked duplex temperature.[100] The probe:template duplexes had T_m value of 29 °C; all of our temperature ranges are with respect to this , and all our results are compared to this temperature.

From the results we see high selectivity 7-13 degrees above the melting temperature of the nicked duplex of the perfectly matched template (28 °C) with the use of 1.3 unit enzyme but a higher temperature range is required to observed such selectivity (13-19 degrees above the T_m) when 6.5 unit enzyme was used. This suggested that T4 DNA ligase appears to stabilize the perfect system more strongly compared to the mismatches and perhaps allows for ligation even at higher temperatures.

Moreover, for this system, the abasic-modified strand did seem to impart even greater selectivity than the strands containing the 5'-thymidine terminus as that system only exhibited selectivity > 13 °C above its T_m. However, the T_m parameter might not fully reflect the influence of the abasic group on the structure of the nicked duplex. For example, the absorbance curves at 260 nm show much less absorbance change for the abasic-containing system in comparison to that with the complementary 5'-thymidine phosphate (Figure 3.5B) suggesting that the duplex is not as well formed. The less ordered structure of the nicked duplex with the abasic site might exacerbate the interactions of the enzyme with the nicked duplex that contains both the abasic and the mismatched based at the 3'-hydroxy terminus, leading to greater selectivity at lower temperatures with respect to the T_m. It is unclear whether this is a general phenomenon, but we note that our previous work exhibited excellent selectivities with the 5'-abasic phosphate for a different 18-mer sequence.[104]

Table 3.1 The experimental dissociation temperatures and the temperature range for optimal selectivity.

Basepair at 3'-OH terminus and template	**C:G**	**C:C**	**C:T**	**C:A**
Nicked duplex T_m with 5'-phosphate abasic (°C)	31	19	23	20
Nicked duplex T_m with 5'-phosphate thymidine (°C)	31	15	15	15
% Conversion with 1 unit enzyme at 35- 41 °C with 5'-phosphate thymidine	>80%	0	<2%	<2%
% Conversion with 6.5 unit enzyme (35- 47 °C) with 5'-phosphate thymidine	>80%	0	<2%	<2%
% Conversion with 6.5 unit enzyme with abasic (29-35 °C) with 5'-phosphate abasic	>80%	0	<2%	<2%

3.6 Assessing Probe Adenylation at High Concentration of Enzyme and a Temperature Far Above the T_m of the Nicked Duplexes

To understand the temperature dependence of SNP selectivity, we consider the mechanism of ligation by T4 DNA ligase, which is an adenosine triphosphate (ATP)-dependent ligase. First, the enzyme docks onto the nicked duplex. Next adenosine monophosphate (AMP) is loaded onto the enzyme by reaction of the enzyme with ATP, and then the AMP is transferred to the 5'-phosphate group of the ligating strand.[112-115] Finally, ligation occurs by activation of the 3'-hydroxy group by the enzyme, which facilitates nucleophilic attack at the 5'-AMP-phosphate end and loss of ADP. The rate-determining step in DNA ligation reactions is the ligation step after adenylation of the 5'-phosphate probe by the AMP-loaded ligase. However, if ligation is very slow, then the enzyme can reload with AMP prior to ligation. This AMP-loaded enzyme has

a weaker affinity for the nicked duplex and cannot catalyze ligation of the adenylated probe. Consequently, oligonucleotides that are difficult for the enzyme to ligate, like RNA fragments, require lower ATP concentrations for optimal ligation.[109, 116]

At higher temperature and higher enzyme concentration the relative amount of AMP-loaded enzyme and the rate of adenylation of the 5'-phosphate strand is increased relative to lower temperatures. We speculate that this increase in AMP-loaded enzyme and possibly 5'-phosphate adenylation leads to an increase in AMP reloading before the 5'-adenylated phosphate strand can be ligated. This situation should occur more frequently for the mismatched duplexes because ligation with the mismatched 3'-hydroxy is quite slow relative to the perfect matched system. Figure 3.7 reveals the formation of the AMP-modified 5'-phosphate abasic strand band on top of the reactant band over time in the presence and absence of mismatches at 29 °C using the high enzyme concentration. We did observe a steady increase in the AMP-modified 5'-phosphate abasic for the mismatched systems. These data provide some support that the selectivity stems from slower ligation of the mismatches compared to the matched system after 5' adenylation of the ligating strand.

To understand the temperature dependence of the system with higher enzyme concentration, we consider how the enzyme shifts the equilibrium toward hybridization as it binds selectively to the duplex rather than the single-stranded form of DNA. As such, the increased enzyme concentration should increase the amount of nicked duplex. This would explain why greater temperatures are required to achieve selectivity when high enzyme concentration is used because a new temperature has to be found where the rate of ligation, which depends on the concentration of nicked duplex, is much faster for the matched than mismatched duplexes.

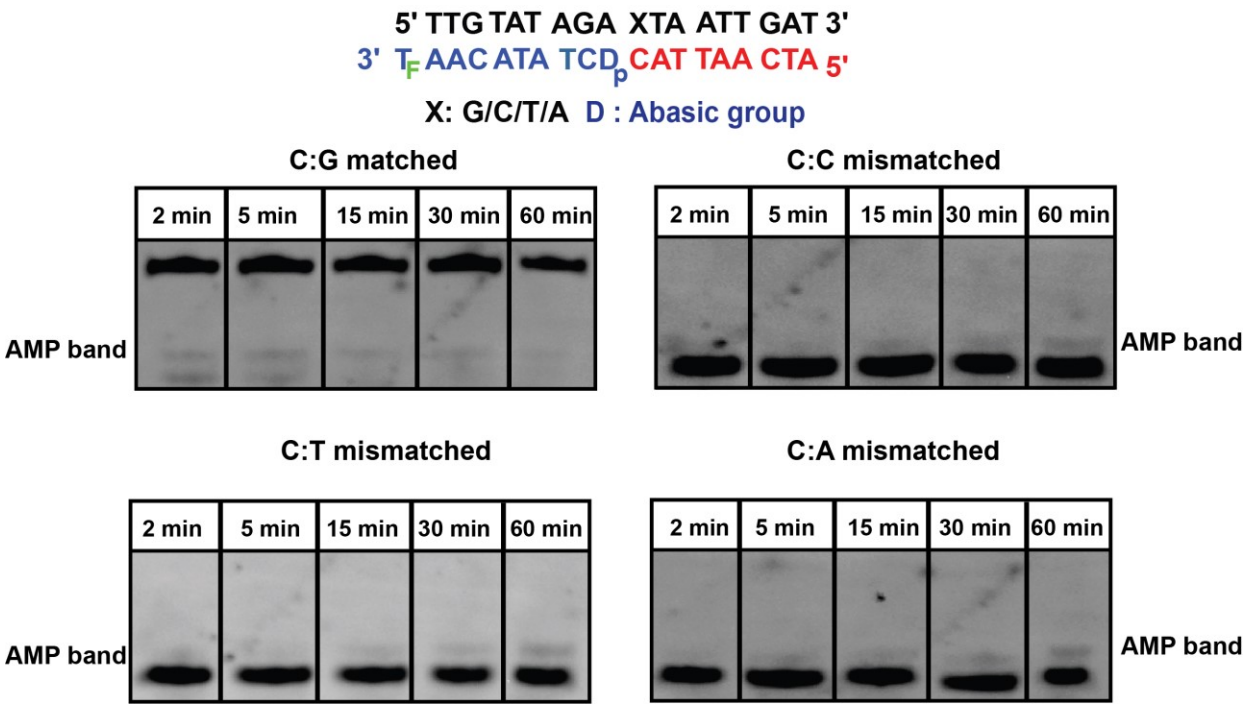

Figure 3.7 Gel images of the AMP formation of the DNA-templated enzymatic ligation using an abasic group. *Experimental Conditions*: 1.4 μM matched or mismatched template, 1.4 μM 5'abasic-phosphate-3' fluorescein ODN, 1.4 μM 3'-hydroxy-5' fluorescein ODN, T4 DNA ligase (2000 cohesive end units, New England Biolabs) in ligase buffer (0.010 M $MgCl_2$, 50 mM Tris-HCl, pH 7.5), 29 °C.

3.7 Conclusions

In conclusion, contrary to conventional thought, T4 DNA ligase can be made quite selective for mismatches at the 3'-hydroxy site of ligation. Increasing the temperature to 7-13 °C above the probe:template duplex T_m of the perfect system, we observe facile ligation of the perfect match (> 90% conversion) while significantly mitigating ligation of the mismatched duplex. Increasing the enzyme concentration shifted the temperature range where the excellent % conversion and excellent selectivity were observed to higher temperatures of 13-19 °C above the T_m. For future work, we will explore higher temperature ranges (> 47 °C) to see the temperature at which the high concentration enzyme will no longer be selective.

Finally, the ideal temperature range for selective ligation can be tuned to lower temperatures including room temperature with the use of a 5'-phosphate abasic ligating strand. The presence of this abasic site either enhances or maintains the excellent selectivity of T4 DNA ligase at elevated temperature. As such, these modifications can be utilized to control the assay temperature as they significantly influence the T_m of the nicked duplex. Given the commercial availability of the abasic modification as well as the two concentrations used of enzyme, these results should be easily incorporated into ligase-based assays for SNP detection.

3.8 Experimental Section

3.8.1 General

All the DNA synthesis reagents were purchased from Glen Research. 40% Acrylamide/bisacrylamide solution, 19:1 (cat. #1610144) was purchased from Bio-Rad. T4 DNA ligase enzyme (2,000,000 cohesive end units/mL, cat. #M0202T) and ligase buffer were purchased from New England Biolabs.

Table 3.2 DNA sequences used in this study

Name	**Sequence**
Template	5' TTG TAT AGA GTA ATT GAT 3'
Mismatched Template	5' TTG TAT AGA XTA ATT GAT 3' X= C, T, A
5'- Abasic Phosphate ODN	5' P –DCT ATA CAA- 3'
5'-Phosphate ODN	5' P –TCT ATA CAA- 3'
3'-Hydroxy- 5' Fluorescein ODN	5' T_F- ATC AAT TAC 3'
5'-Abasic Phosphate-3' Fluorescein ODN	5' P –DCT ATA CAA- F 3'

P = phosphate, D = abasic group, F = fluorescein.

3.8.2 Enzymatic Ligation Method

The matched or mismatched template, 5'-phosphate ODN and 3'-hydroxy ODN- 5' fluorescein were added to an Eppendorf tube and diluted 10 μL MQ H_2O. The mixture was allowed to incubate in a covered thermal incubator at the specific temperature. A master mix (5

μL), with T4 DNA ligase (400 or 2000 cohesive end units, New England Biolabs) and the provided buffer (1.5 μL) was added to the previous mixture and timing started. The final volume was 15 μL and the DNA concentrations were: 1.4 μM matched or mismatched template, 2.8 μM 5' phosphate ODN and 1.4 μM 3'-hydroxy ODN-5' fluorescein. At different times of the reaction, aliquots (2 μL) were taken from the reaction mixture and put in an Eppendorf tube containing a running dye (0.25% w/v bromophenol blue with 80% w/v sucrose in 0.5 M EDTA (aq) (2 μL). Samples were analyzed by 15% denaturing PAGE as described previously.[23]

3.8.3 T_m Measurements

1.3 nmol of each DNA strand (template and ligating ODN) were diluted in a 1 ml of 0.01 M $MgCl_2$. The sample was hybridized in the fridge for around 1 hour. UV melting curves were measured using an HP 8453 diode-array spectrophotometer with an HP 89090A Peltier temperature controller instrument were measured at 260 nm with a heating range between 12-50 °C with 1 °C intervals, and 100 rpm stirring.

3.8.4 DNA Synthesis and Purification

The synthesis of the DNA strands were done using Glen Research reagents on an ABI solid-phase synthesizer, Model 392. Strands were purified following DMT-On GlenPak purification protocol using GlenPak DNA cartridges (cat. 60-5200-01). Standard DNA phosphoramidite, CPG's and the following modifications: chemical phosphorylation reagent II (cat. 10-1901-90)], fluorescein-dT phosphoramidite (cat.10-1056-95), dSpacer CE phosphoramidite (cat. 10-1914-90), and 3'-(6-FAM) cat. 20-2961-41 were used (Figure 3.8).

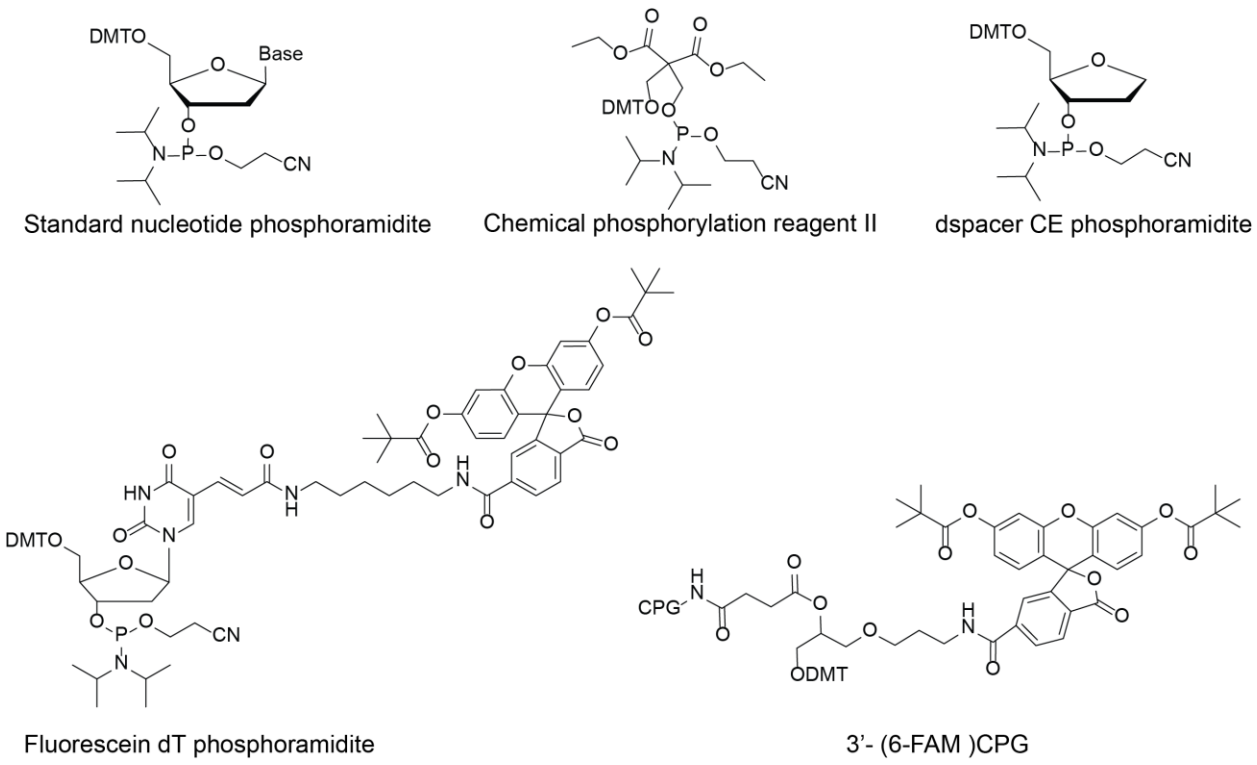

Figure 3.8 The chemical structures of the phosphoramidites and CPG used in this study. Dmt is dimethoxytrityl.

3.8.5 MALDI-TOF Characterization

Synthesised DNA strands were analyzed by MALDI-TOF. First a matrix solution of 3-hydroxypicolinic acid in 1:1 acetonitrile:water was prepared (25 mg/mL) as well as an ammonium citrate solution in water (25 mg/mL). These two solutions were mixed in a 9:1 ratio to yield the final matrix mixture. The synthesized DNA (5 nmol) was desalted using ZipTip (ZTC18S096) purchased from Millipore Sigma and was mixed in a 1:1 ratio with the matrix mixture. The measurements were carried out on a Voyager Elite (Applied BioSystems, Foster City, CA, USA) time of flight-mass spectrometer.

3.8.6 Denaturing Polyacrylamide Gel Electrophoresis

A denaturing 15% polyacrylamide gel was prepared by dissolving urea (4.8 g) in 40% Acrylamide/Bis Solution 19:1 (3.75 mL) (Bio-Rad Cat.161-0144) and 5 x TBE buffer (1 mL), then diluted to 10 mL with MQ water. Tetramethylethylenediamine (10.7 µL, TEMED) and aqueous ammonium persulfate (80 µL) were added after urea was dissolved to induce polymerization. A portion of the aliquot and running dye mixture (3 µL) was loaded into a denaturing 15% polyacrylamide gel (8 M urea in 0.5 X TBE, 37.5 vol% of 40% acrylamide/bisacrylamide solution, 0.75 mm thick, 10 wells). PAGE was run at 150 V for 80 min. A fluorescent image was taken of the gel using a fluorescent imager with trans-UV illumination using an ImageQuant RT ECL instrument from GE Healthcare Life Science. Quantification of the fluorescence emitted by each band was analysed by using ImageQuant TL analysis software. The %con was determined based on the ratio of the fluorescence intensity of the product band over the sum of the fluorescence intensity of the product and reactant bands multiplied by 100%.[22]

The equation is as follow:

$$\%\ Yield = \frac{I_{\text{Product Band}}}{I_{\text{Product Band}} + I_{\text{Reactant Band}}} \times 100\%$$

3.8.7 Testing the Purity of the Synthesized DNA Probes by Stains-All

The DNA strands were loaded into 15% denaturing PAGE then stained with Stains-All (Aldrich cat # E9379). The Stains-All solution was prepared by dissolving Stains-All (25 mg) in 50 mL mixture of 1:1 (MilliQ H_2O: Formamide). The PAGE is placed in a container contained

the Stains-All solution, covered with foil and placed in a shaker for 15 min. The presence of one band only for each strand is an indication of the purity of the DNA strand.

Chapter Four

Amplification of O^6-Methyl Guanine on the KRAS Gene by Lesion Induced DNA Amplification

4.1 Introduction

Epigenetics is the study of the transmitted changes in gene function or expression that are not based on changes to the DNA sequence of the gene.[117] Some examples of epigenetic modification of genomic DNA are methylation,[118] acetylation,[119] phosphorylation,[120] and sumoylation.[121] This Chapter will focus on methylation of DNA. DNA methylation can occur endogenously or exogenously. Examples of endogenous methylating agents are nitrosation products[122-123] and S-adenosylmethionine.[124] Exogenous methylating agents may originate from diet, environment, or toxins.

One common type of methylation is the methylation of cytosine, which is the introduction of a methyl group into the 5 position of cytosine in CpG dinucleotides to form 5-methyl cytosine (^{5Me}dC).[125-127] This modification plays an important role in gene expression, gene silencing, and cellular reprograming.[128-130] Levels of methylation vary in cancer cells: it can be less than the normal cells (hypomethylation) or higher than the normal cells (hypermethylation).[131-132] Hypomethylation activates proto-oncogenes by allowing transcription, while hypermethylation on the tumor suppressor genes lead to gene silencing.[133-135] Moreover, ^{5Me}dC can undergo further deamination, resulting in thymidine, which in turn results in a G:T mismatch which could lead to a mutation .[136-137]

Another important example of methylation is the methylation of the 6-oxygen on the guanine base (O^6-MeG), which occurs after exposure to exogenous or endogenous methylating agents.[138] This modification has been found in the KRAS gene, a gene that regulates cellular growth and is a key controller for the epidermal growth factor receptor that is expressed highly in many cancer cells. Mutations in the KRAS gene, especially in codon 12 and 13, have a negative impact on cell proliferation and could lead to tumor cells resistant to epidermal growth factor

receptor therapies.[139-141] This methylated DNA damage site often can be repaired by O^6-methylguanine transferase enzyme, which removes the methyl group from the damaged site and incorporates it onto a cysteine residue. Otherwise, DNA polymerase often introduces a thymidine base opposite to O^6-MeG instead of cytosine, resulting in a G to A transition that could lead to cancer.[142]

One of the challenges of O^6-MeG mutation is the lack of appropriate methods of detection or quantification due to the low abundance of methyl guanine in the genome.[143-144] O^6-MeG was detected using different methods such as ultra-high performance liquid chromatography coupled with mass spectroscopy (UPLC-MS), [145] or high resolution mass spectrometry (UPLC-HRMS/MS), [146] immunoassay[143, 147] and ^{32}P-postlabeling.[144, 148] Despite the selectivity and sensitivity of these methods, they involve digestion of the DNA sample in order to perform the analysis, hindering the detection of the O^6-MeG quantity in specific positions of the genome.

A reasonable approach for in-gene detection and quantification of alkylated bases is the use of a chemically modified nucleoside that recognizes the adduct DNA by forming a strong H-bond. Saski and co-workers developed a method for detecting O^6-MeG using an unnatural nucleoside with a transferable group that mediated the labeling of O^6-MeG with FAM (carboxyfluorescein) when it is placed on the opposite site to O^6-MeG. This method was useful in the detection and quantification of O^6-MeG, however, the authors did not mention the ability of this method to detect the methylated DNA adduct in the presence of other DNA targets.[149] The Sturla group developed a method for detecting and sensing O^6-MeG in the KRAS gene at codon 12 and 13.[150] They synthesized unnatural nucleosides for in-gene detection, and one of the first examples shown was perimidinone-derived nucleoside (Per) (Scheme 4.1A).[151] The Per probe

was found to bind more strongly to O^6-benzylguanine (O^6-BnG), resulting in a more stable duplex than when it binds to G. They attributed the formation of a stable duplex when Per is placed opposite to O^6-BnG to the different conformation that Per adopts, a syn conformation when it is opposite to O^6-BnG and an anti conformation when it is opposite to the G.[151] For better hybridization and duplex stability, the Sturla lab synthesized 1′-β-[1-naphtho[2,3-d]imidazol-2(3H)-one)]-2′-deoxy-D-ribofuranose (ExBenzi) and 1′-β-[1-naphtho[2,3-d]-imidazole]-2′-deoxy-D-ribofuranose (ExBIM) (Scheme 4.1B) that bind more strongly to O^6-MeG compared to guanine when they are placed opposite to them. Colorimetric detection was achieved after incorporating ExBenzi and ExBIM nucleotide derivatives into DNA-modified gold nanoparticles to form nanoprobes. The presence of O^6-MeG DNA in the DNA gene induced the aggregation of gold nanoparticles due to the formation of a stable DNA duplex with the modified nucleobases, which led to a color change to purple. However, no color change was observed for the bulk DNA that was not methylated, indicating that ExBIM was selective to the methylated template.[150] The sensitivity of ExBIM nanoprobes to the presence of O^6-MeG target was assessed in a background of human genomic DNA and non-methylated G target. The ratio of the concentration of O^6-MeG to the total DNA concentration was 0 to 2.8%, the ExBIM was able to binds to 0.24% of the O^6-MeG in the total DNA indicating that ExBIM is sensitive to the presence of O^6-MeG even in a background of genomic DNA.[150]

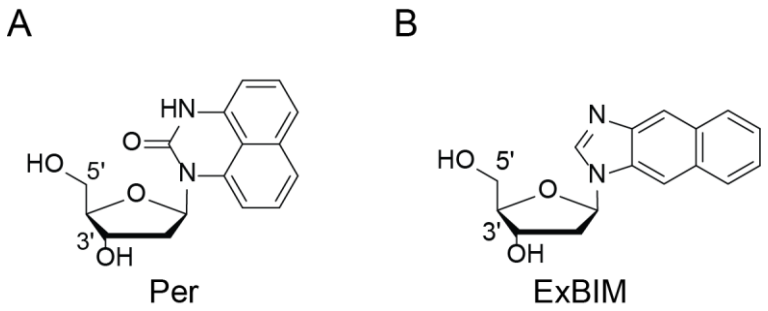

Scheme 4.1 Structure of the unnatural nucleosides that selectively recognize O^6-alkylated guanine. A) Perimidinone-modified nucleoside (Per). B) ExBIM-modified nucleoside (ExBIM).

The occurrence of O^6-MeG in genomic DNA is very low, hence, there is a need for an amplification method to enable the detection of such small amounts. Finding the right amplification method that can discriminate between the affected methylated gene and the wild type will assist in the early detection of cancer. We have collaborated with Sturla lab to investigate the amplification of O^6-MeG in the KRAS gene using the isothermal amplification method that was developed in our group (Scheme 4.2, Chapter 1.1.1.2).[22-23] In this Chapter, we synthesized an 18-mer KRAS template that is rich in GC content and contained O^6-methylated guanines as they have been implicated in the tendency of KRAS to become mutated. We then attempted to amplify it using our LIDA approach. We started with the synthesis of two methylated templates, O^6-MeG with the methyl G on the 11 or 14 base of the 18-mer template. Nilforoushan Arman from the Sturla lab synthesized one of the complementary DNA probes with the ExBIM opposite to the methylated guanine, and all the other DNA probes were synthesized in our lab. Our hypothesis was that in the presence of an ExBIM probe, the methylated template would be amplified by LIDA, while no or little amplification would occur for the non-methylated template due to the higher affinity of the ExBIM probe to the O^6-MeG template.

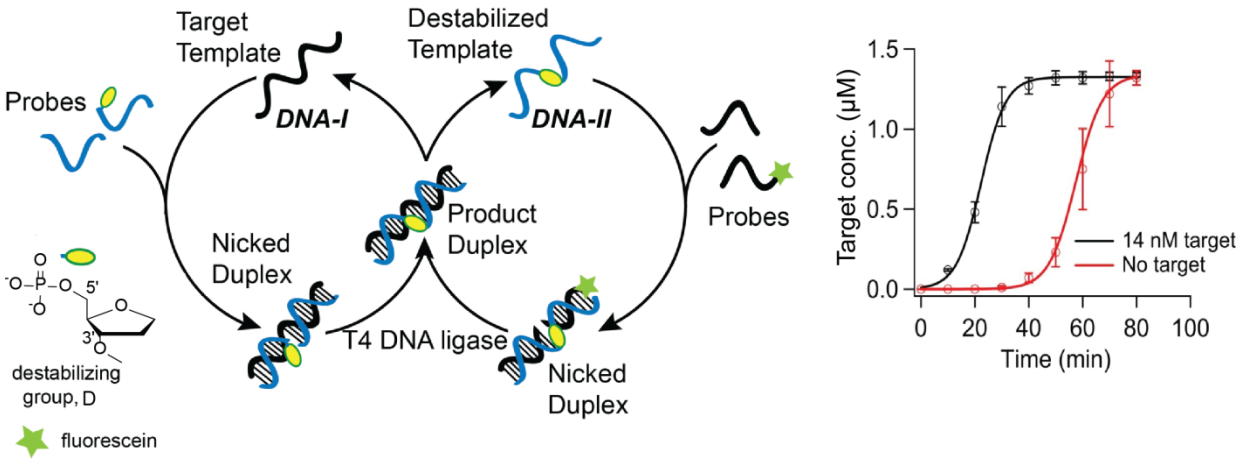

Scheme 4.2 Lesion induced DNA amplification (LIDA) and the kinetics of the cross-catalysis amplification when 14 nM or 0 nM of initial target is present.

4.2 Stoichiometric Experiments for the Methylated and the Non-methylated Template Using an Internal ExBIM Modification (Away from the Ligation Site)

We started our project by running stoichiometric experiments to test if T4 DNA ligase could ligate the two complementary probes even when one contained an ExBIM instead of a cytosine. The templated reaction of the two complementary DNA probes: the 3'-hydroxy probe containing the internal ExBIM and the 5'-phosphate probe containing two abasic groups and a fluorescein at the 3'-terminus was performed with either the methylated or non-methylated template in the presence of T4 DNA ligase at 12, 15, and 18 °C (Figure 4.1). We evaluated the percent conversions using polyacrylamide gel electrophoresis and fluorescent imaging. (These experiments were conducted in collaboration with Anyeld Ubeda, a graduate student in our group). The percent conversion refers to the percent of ligation of the limiting fluorescent labeled probe, which was always lower in concentration by a factor of two with respect to the one or three other probes used in stoichiometric or cross-catalysis reactions, respectively. The results revealed that T4 DNA ligase was able to ligate the two probes, even when one included an internal ExBIM modification (Figure 4.1). Not only that, at 15 and 18 °C around 60% ligation

product was observed for the reaction containing the methylated template while less than 5% product resulted for the non-methylated template (Figure 4.1 B and C). The selectivity for the methylated template was not as significant at 12 °C (Figure 4.1 A). Since the stoichiometric reaction worked, we moved on to the cross-catalysis experiments.

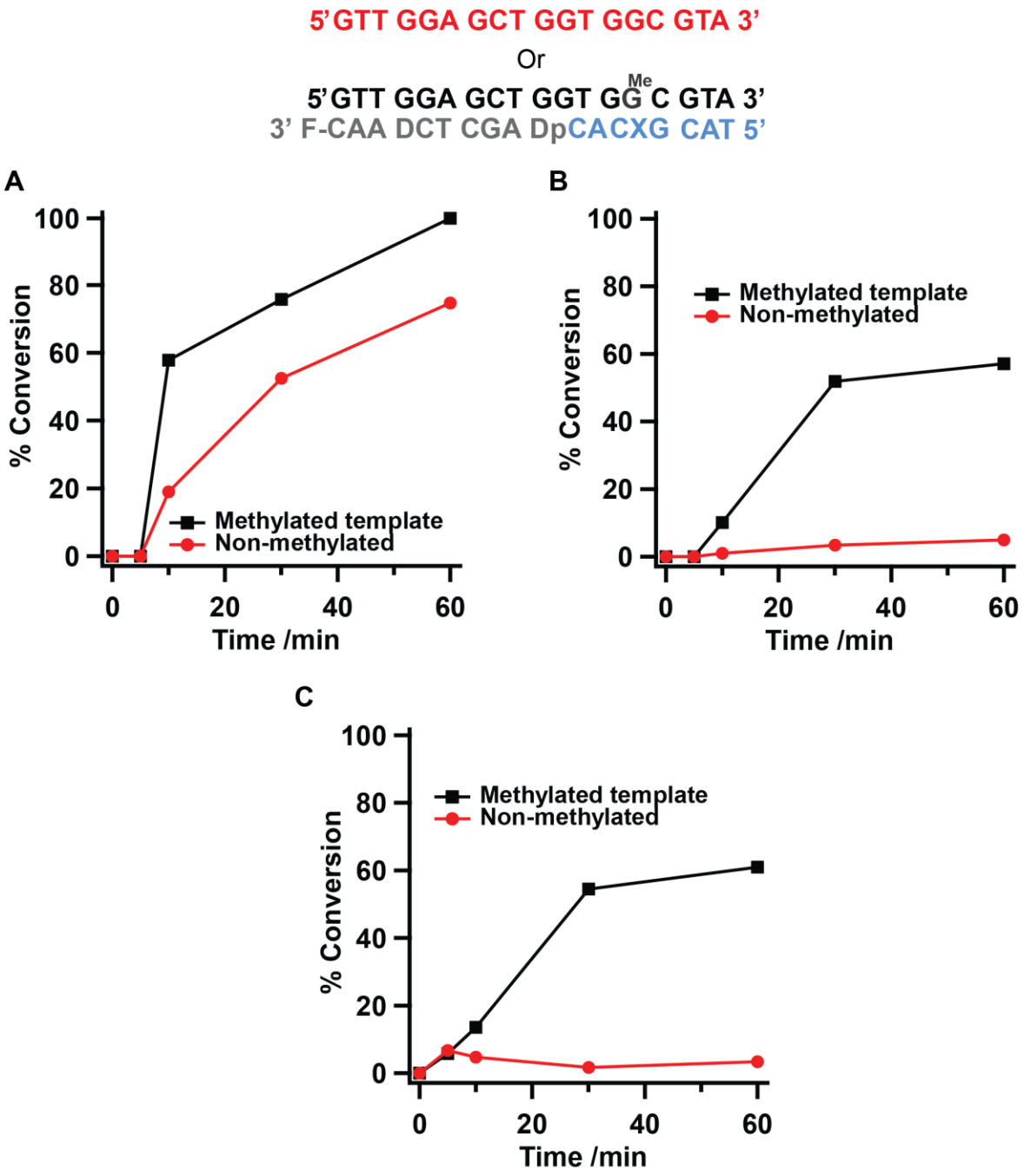

Figure 4.1 Stoichiometric DNA-templated ligation using a 5'phosphate abasic$_2$- 3' fluorescein probe, 3'-hydroxy probe with an internal ExBIM modification and either methylated or non-methylated template at: A) 12 °C B) 15 °C and C) 18 °C. G^{Me} = O^6-MeG, X = ExBIM, D = abasic group, p = 5'-phosphate group, F = 6-carboxyfluorescein. *Experimental conditions*: O^6-MeG14-Template (1.4 µM), 5'-phosphate abasic$_2$- 3' fluorescein (grey) probe (1.4 µM), 3'-hydroxy ExBIM-G14 (blue) probe (2.8 µM), T4 DNA ligase (2,000 CEU per 7.5 µL), 0.01 M $MgCl_2$.

4.3 Amplification of the Non-methylated KRAS Template in the Presence of a 5'-Phosphate Probe with One Abasic Group

The wild type (wt) KRAS has more GC content (55% GC) than the anthrax template (16% GC) previously amplified by LIDA.[23] Hence, we decided to amplify it first before testing the methylated version of the same template. The complementary DNA probes were synthesized, the 5' phosphate containing one abasic destabilizing group and the 3'-hydroxy probe (these probes are for the first cycle). The second cycle of DNA probes were synthesized as well, one with a 3'-hydroxy-5'fluorescein DNA probe and the other one with a 5'-phosphate DNA probe.

We based our results in this chapter on the % conversion which is calculated from the percentage of the limiting probe (fluorescein-labeled 3'-OH probe) that was converted to the ligation product (see Chapter 4.10.4). For a cross-catalysis reaction, the target amplification factor is this % conversion divided by the mol% of the initial target template. For example, 70% conversion for a cross-catalysis reaction initiated by 1 mol% of the wt KRAS target is equivalent to an amplification factor of 70.

First, we explored the cross-catalysis reaction using a small initial concentration (1 mol%) of the wt KRAS target with excess of the four probes at 30, 33, 37, and 40 °C. No amplified product was detected on the polyacrylamide gel for the reaction at 30 °C after 17 h (Figure 4.2 green) nor at 33 °C after 17 h (Figure 4.2 blue). However, the reaction at 37 °C yielded around 15% after 17 h (Figure 4.1 red), while the reaction at 40 °C yielded around 20% after 17 h (Figure 4.2 black).

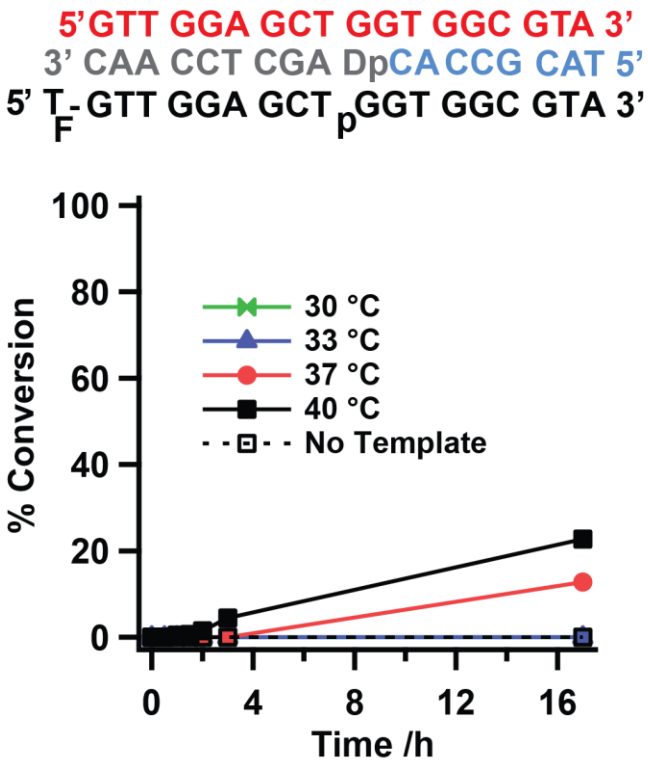

Figure 4.2 Cross-catalysis of the wt KRAS template using one abasic group. D = abasic group, p = phosphate group, T_F = dT fluorescein. *Experimental conditions*: K-Template (14 nM), 5'phosphate-abasic (grey) probe (2.8 µM), 3'-hydroxy (blue) probe (2.8 µM), 3'-hydroxy-5' fluorescein (black) probe (1.4 µM), 5'-phosphate (black) probe (2.8 µM), T4 DNA ligase (2,000 CEU per 7.5 µL) at 30, 33, 37, 40 ºC, 0.01 M $MgCl_2$.

We attributed the low yield even at relatively high temperature (40 °C) to the high GC content, which increases the T_m of the duplex and makes it hard to amplify with only one abasic group. For that reason, we introduced another abasic group on the 3'-hydroxy DNA probe (5' TAC GCC AC 3') shown in blue in Figure 4.2 to decrease the temperature of amplification to a relatively low temperature. The cross-catalysis reaction was run for the wt KRAS template (1 mol%) using this new probe at temperatures between 15 and 34 °C. The reactions did not reveal any ligation product by PAGE analysis indicating that no amplification had occurred.

4.4 Amplification of the Non-methylated KRAS Template in the Presence of Two Abasic Groups on the 5' Phosphate DNA Probe

Given the previous results, we reasoned that the lack of cross-catalysis did not originate from the shorter 3'-OH probe as that was only 8 nucleotides unlike the 5'-phosphate abasic probe that was 10 nucleotides in length. If the shorter 3'-OH probe was too stable then cross-catalysis should have improved when we introduced an abasic group, which was not the case. Consequently, another set of cross-catalysis probes were assembled with the introduction of two rather than one abasic group on the same DNA probe (5'-phosphate-abasic$_2$ probe = 5' pDAG CTC DAA C 3') to increase destabilization and cross-catalysis of the non-methylated KRAS target. The cross-catalysis of the non-methylated template (1 mol%) yielded no ligation product detected at 21 and 24 °C after 26 h. However, the reaction at 27, 30, and 33 °C yielded 5, 87, and 53% ligation product (ie more of the KRAS target), corresponding to a target amplification factor of 5, 87, and 53, respectively, after 28 h. We narrowed the range and tried this reaction at one degree intervals between 27 and 33 °C to determine the optimum temperature (Figure 4.3). At 28, 29, 30, 31, and 32 °C the reaction yielded 10, 56, 90, 80, and 42%, respectively (corresponding to a target amplification factor of 10, 56, 90, 80, and 42), after 26 h, indicating the highest yield was at 30 °C. Since the cross-catalysis for the wt KRAS worked, we decided to next explore the amplification reaction using the methylated template.

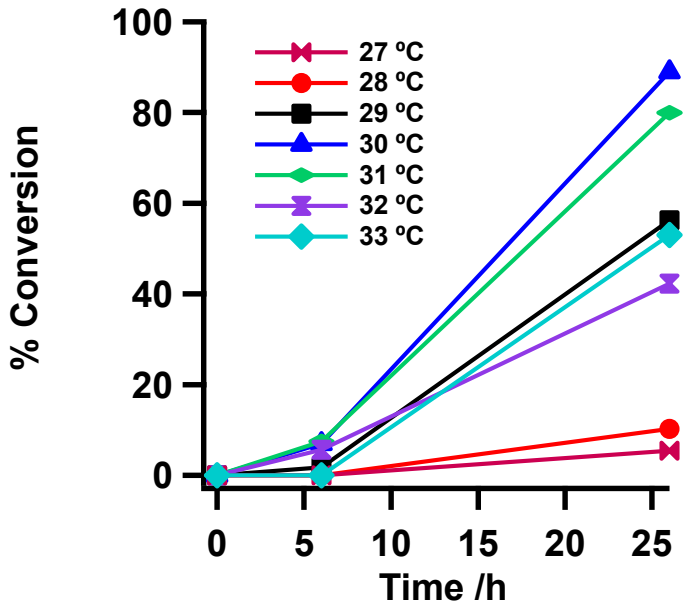

Figure 4.3 Temperature optimization of cross-catalytic amplification of the wt KRAS template using one more abasic group in the destabilizing probe. D = abasic group, p = phosphate group, T_F = fluorescein-dT. *Experimental conditions*: K-Template (14 nM), 5'-phosphate abasic$_2$ (grey) probe (2.8 µM), 3'-hydroxy (blue) probe (2.8 µM), 3'-hydroxy-5' fluorescein (black) probe (1.4 µM), 5'-phosphate (black) probe (2.8 µM), T_4 DNA ligase (2,000 CEU per 7.5 µL) at various temperatures in 0.01 M $MgCl_2$.

4.5 Amplification of O^6-Methyl Guanine (O^6-Me G) KRAS Template

Two methylated KRAS templates with methylated guanine at two different positions (11 and 14) were synthesized as well as the corresponding methylated 5'-phosphate probes using a modified guanine base (O^6-MeG) on the solid-phase synthesizer. The template that contains O^6-Me on the 11 base (O^6-MeG11) results in O^6-MeG at the 3' end of the ligation site during cross-catalysis. The other template with the methylated group on the 14 base (O^6-MeG14) results in the O^6-MeG in the middle of one of the probes 4 positions away from the ligation site during cross-catalysis. The complementary DNA probes that have an 1′-β-[1-naphtho[2,3-d]-imidazole]-2′-deoxy-D-ribofuranose (ExBIM) across from the O^6-MeG were synthesized by our collaborator Nilforoushan Arman in the Sturla lab.[150] The probe complementary to the O^6-MeG11 template

we refer to as 3'-hydroxy ExBIM-G11 DNA probe, and 3'-hydroxy ExBIM-G14 is the probe complementary to the O^6-MeG14 template. Sturla and co-workers showed that ExBIM binds slightly stronger to the O^6-MeG template (T_m = 54 °C) compared to the wt template containing natural G (T_m = 51.7 °C). With this in mind, we aimed to amplify the methylated KRAS template by LIDA, hoping that we could find a temperature where the methylated template would initiate amplification using the ExBIM probes whereas only the background process would be observed for the non-methylated template.

4.6 Amplification of the Methylated KRAS Template O^6-MeG11 with the MeG at the Ligation Site

Previous work in our group revealed that the ideal amplification temperature was ~4 °C below the dissociation, or melting, temperature (T_m) of the product duplex.[22-23] As such, an important parameter to know prior to attempting amplification is the melting temperature, which helps in determining the range of temperatures that should be explored. To determine this dissociation temperature, we prepared the ligation product that would form between the destabilizing probe containing two abasic groups and the probe containing the C rather than the ExBIM across from the O^6-MeG (this substitution was made owing to the small amount of material available for making ExBIM modified strands). The T_m for the methylated KRAS template (O^6-MeG11) with this mostly complementary DNA was 35 °C. Therefore, we decided to run the amplification reaction between 27 and 33 °C. Sturla and co-workers had shown that the T_m of a strand with the O^6-MeG:C is very similar to that with the O^6-MeG:ExBIM (55.2 and 54.0 °C, respectively).[150] First, we explored the cross-catalysis of the methylated template (1 mol%) O^6-MeG11 at 27, 30, and 33 °C that required the ligation of a 3'-terminal ExBIM group in the catalytic cycle. No product was detected after 28 h when cross-catalysis was performed at

any of these temperatures. We suspected that the T4 DNA ligase was not able to ligate the 3'-hydroxy ExBIM-G11 terminated probe or the 5'-phosphate O^6-MeG terminated probe owing to the unnatural basepair at the ligation site.[152] To confirm that, we collaborated with Anyeld Ubeda for testing the stoichiometric reaction for the methylated target, and indeed no ligation of the 3'-hydroxy ExBIM probe was detected at 10, 13 and 16 °C. We performed the stoichiometric reaction at temperatures below the dissociation temperature of the nicked duplex to facilitate ligation. Consequently, we decided to try the other KRAS template with the methylated guanine further from the ligation site.

4.7 Amplification of the Methylated KRAS Template (O^6-MeG14) Using ExBIM-G14 Probe

Similar to above, the melting temperature was first determined for the methylated template O^6-MeG14 with the mostly complementary DNA strand containing two abasic groups and a C in place of the ExBIM. The T_m was 37 °C; therefore, we decided to run the reaction at a temperature lower than 37 °C. The cross-catalysis for the O^6-MeG14 template (1 mol%) with its cycle 1 probes (one containing the ExBIM) and cycle 2 DNA probes was performed at 27, 30, 33, and 35 °C. No ligation product was observed at these temperatures after 33 h. As cross-catalysis is a combination of two steps, ligation and dissociation, the reason that the amplification of the O^6-MeG14 template with the ExBIM probe did not work may be due to the dissociation step as the ExBIM probe lacked any destabilizing group. In other words, perhaps the product duplex was very stable and could not dissociate spontaneously. For future work, we will introduce another abasic group into the 3'-hydroxy ExBIM-G14 DNA probe to help in the spontaneous dissociation.

4.8 Amplification of the Methylated KRAS Template (O^6-MeG14) Using the C-G14 Probe

Having an ExBIM group across from the methylated G did not lead to any amplification under any of the tested conditions, therefore, the next step was to carry out the reaction using cytosine across from the methylated G instead of the modified ExBIM nucleobase. We decided to explore this C-G14 probe instead of ExBIM as we hypothesized that the DNA-templated reaction of the methylated template should work faster compared to the reaction with ExBIM. To test this hypothesis we ran a stoichiometric reaction with 1 eq of the methylated template, 1 eq of 5'-phosphate abasic$_2$- 3'fluorescein probe, and 2 eq of the 3'-hydroxy probe with and without ExBIM. The reaction with C-G14 probe gave a faster reaction ~ 61% in 15 min (Figure 4.4, black square), compared to the reaction with the ExBIM probe that yielded 20% after the same time (Figure 4.4, red circle) at 16 °C. As the rate of ligation has been shown to influence the cross-catalysis (see Chapter 1.5), we hypothesized that the C-G14 probe would be able to undergo cross-catalysis more effectively.

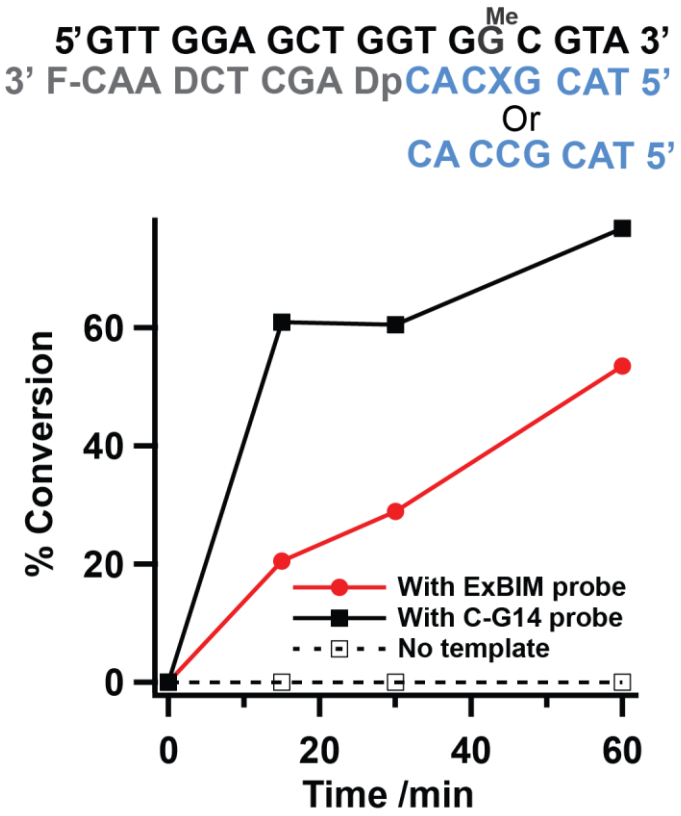

Figure 4.4 Stoichiometric DNA-templated ligation using the methylated target at 16 °C. G^{Me} = O^6-MeG, X = ExBIM, D = abasic group, p = 5'-phosphate group, F = 6-carboxyfluorescein. *Experimental conditions*: O^6-MeG14-Template (1.4 μM), 5'-phosphate abasic$_2$- 3' fluorescein (grey) probe (1.4 μM), 3'-hydroxy ExBIM-G14 (blue) probe, 3'-hydroxy DNA (blue) probe (2.8 μM), T4 DNA ligase (2,000 CEU per 7.5 μL), 0.01 M $MgCl_2$.

Cross-catalysis was performed with the 3'-hydroxy DNA probe with C across from the methylated G (C-G14 probe) and sub-stoichiometric amounts of the methylated O^6-MeG14 template (140 nM, 10 mol% with respect to the limiting fluorescein-labeled 3'-OH probe). As a point of comparison, the same conditions were used except that 10% of the non-methylated KRAS template was used instead to initiate the reaction. At 23 °C, we were pleased to observe amplification but it was slower compared to the other temperatures and yielded 39% of the methylated target after 3 h for the reaction initiated with methylated target (corresponding to a target amplification factor of 3.9) and 9% of methylated target for the reaction initiated with the

non-methylated target. After 6 h, the conversion had increased to 88% and 12% for the reaction initiated by the methylated and the non-methylated template, respectively (Figure 4.5 A). At 24 °C, the reaction was faster, yielding 88% for the methylated and 14% for the non-methylated initial template within 4 hours. This yield increased to 100% and 69% after 8 h for the methylated and non-methylated initial template, respectively, (Figure 4.5 B). The reaction at 25 °C yielded 94% for the methylated and 20% for the non-methylated template after 3 h, which increased to 100% and 85%, respectively, after 6 h (Figure 4.5 C). The fastest reaction was the reaction at 26 °C, which resulted in 89% and 69% for the methylated and the non-methylated template, respectively, after 3 h. At this temperature, the reaction showed less discrimination between the reaction initiated with the methylated and the non-methylated template (Figure 4.5 D). Therefore, the optimal reaction temperature was 24 °C for the methylated system, providing the best balance of fast kinetics and discrimination between the reaction initiated with the methylated and the non-methylated template.

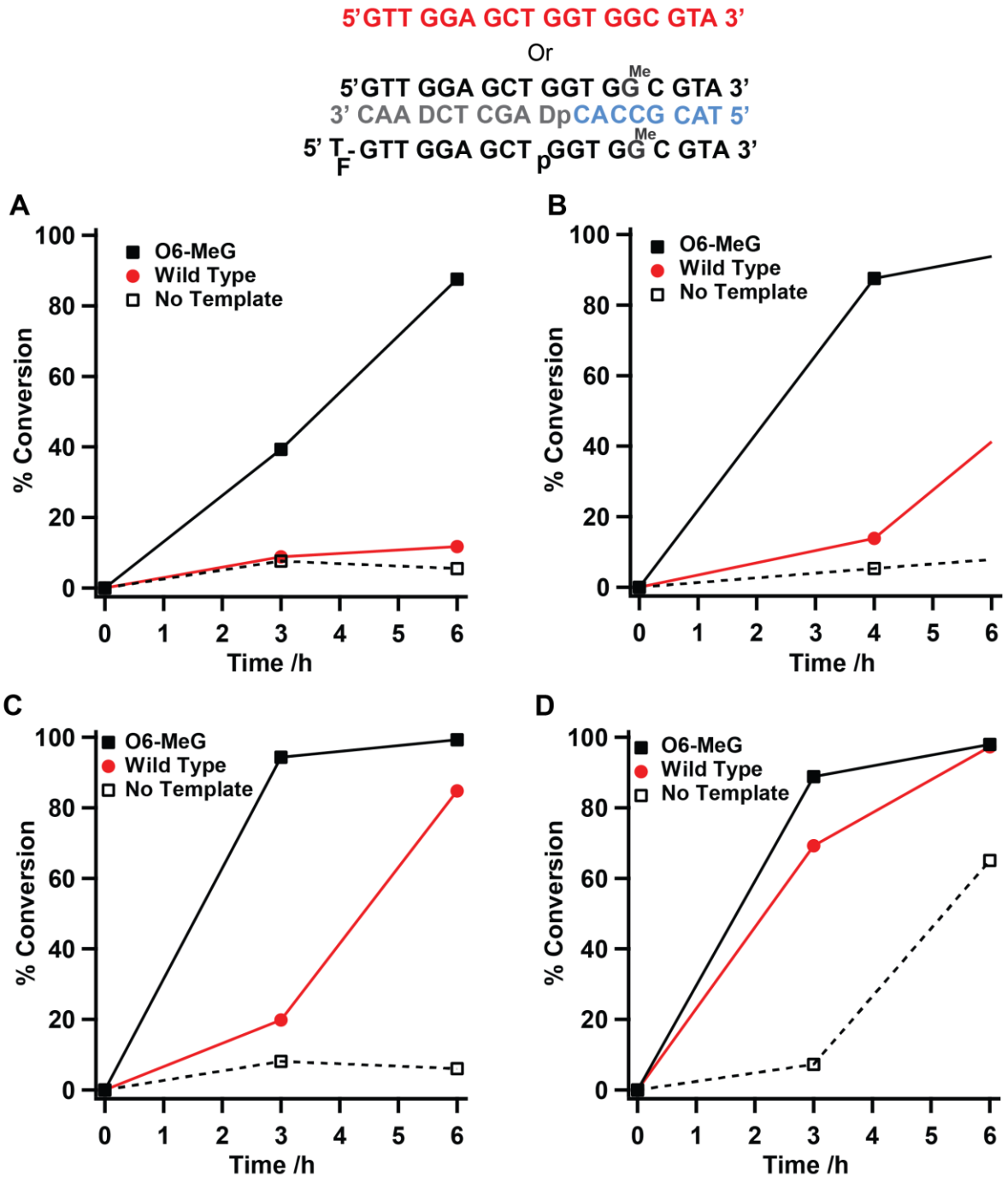

Figure 4.5 Cross-catalysis of a 10% methylated and non-methylated template. A) 23 °C B) 24 °C C) 25 °C D) 26 °C. G^{Me} = O^6-MeG14, D = abasic group, p = phosphate group, T_F = fluorescein-dT. *Experimental conditions*: K-Template (140 nM), 5'phosphate abasic$_2$ (grey) probe (2.8 µM), 3'-hydroxy (blue) probe (2.8 µM), 3'-hydroxy-5' fluorescein (black) probe (1.4 µM), 5'-phosphate (black) probe (2.8 µM), T4 DNA ligase (2,000 CEU per 7.5 µL), 0.01 M $MgCl_2$.

Next, we decreased the template concentration to 14 nM (1 mol%) and ran another set of cross-catalysis reactions for the methylated and non-methylated template at the optimum temperature of 24 °C. The reaction yielded around 70% for the methylated (corresponding to a target amplification factor of 70) and around 10% for the non-methylated template after 6 h (Figure 4.6A). The non-templated reaction also yielded around 10%. Lowering the concentration of the template to 1.4 nM (0.1 mol%) also showed selectivity for the methylated over the non-methylated template, with a yield of 93% for the methylated (an amplification factor of ~930), 28% for the non-methylated initial template, and 15% for the background reaction when no template was initially present (Figure 4.6B). The % conversion of the methylated target formed from the reactions initiated by the non-methylated template or no initial template (the background triggered process) are close to each other, suggesting that the non-methylated template is responsible for only some self-replication similar in magnitude to that initiated by the background-triggered process.

The stability of the duplex resulted from the first cycle using the methylated template is lower compared to the duplex with the non-methylated template due to the weaker binding of O^6-MeG:C compared to G:C. This stability has a significant effect on the second step of cross-catalysis, the dissociation of the duplex, to produce the template again that could initiate the second cycle. The formed duplex stability is also sensitive to the reaction temperature, as in the presence of a destabilizing group, the melting temperature of the nicked duplex and the product duplex will be close to each other and that helps in the spontaneous dissociation as we saw in a previous report by our group.[23] Therefore, the amplification worked faster in the case of the methylated template compared to the non-methylated template.

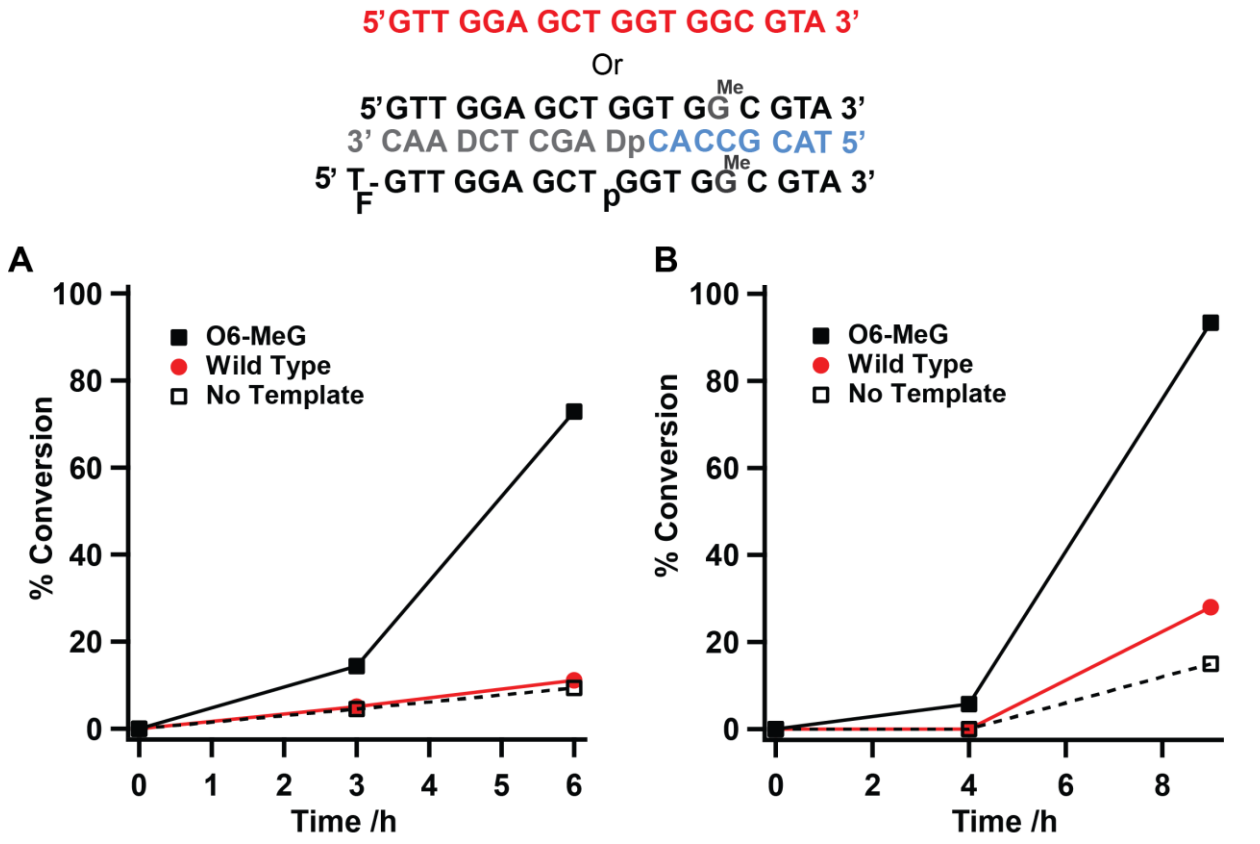

Figure 4.6 Cross-catalytic replication of the methylated KRAS target initiated by methylated and non-methylated KRAS template. A) 14 nM template B) 1.4 nM template. G^{Me} = O^6-MeG14, D = abasic group, p = phosphate group, T_F = fluorescein-dT. *Experimental conditions*: K-Template (140 nM), 5'-phosphate $abasic_2$ (grey) probe (2.8 µM), 3'-hydroxy (blue) probe (2.8 µM), 3' hydroxy-5' fluorescein (black) probe (1.4 µM), 5' phosphate (black) probe (2.8 µM), T4 DNA ligase (2,000 CEU per 7.5 µL), 0.01 M $MgCl_2$, 24 °C.

4.9 Conclusions

Amplification of the O^6-MeG KRAS template with methylated G at the ligation site or internally did not lead to an amplification product at different temperatures using the modified nucleoside ExBIM in the complementary probe. For future work, introducing another abasic group on the ExBIM probe may be required to help in the spontaneous dissociation of the DNA duplex and the isothermal amplification of O^6-MeG using these "complementary" ExBIM probes.

The amplification of O^6-MeG occurred, however, when a cytosine rather than the ExBIM was present on the probe across from O^6-MeG, and we were able to achieve good discrimination between the reactions initiated by the methylated versus the non-methylated template. The best discrimination ratio between the reactions initiated with methylated and the non-methylated templates was observed at 24 °C yielding 93% for the methylated and 28% for the non-methylated template after 9 hours, which corresponded to a net amplification factor of 650 (amplification factor resulting from initial methylated target minus that from the reaction with initial non-methylated target). Under these conditions, we were also able to discriminate as low as 1.4 nM of the methylated template. For a better assessment of this method's ability to selectively identify the methylated DNA target, templates with a single mutation in place of O^6-MeG are required to test if this method can recognize the methylated DNA target with high efficiency compared to the other targets. If this succeeds, this method could emerge as a tool for the sequence selective detection of O^6-MeG alkylated adducts on target DNA in point-of-care diagnostics.

4.10 Experimental Section

4.10.1 General

All the DNA phosphoramidite and DNA synthesizer reagents were purchased from Glen Research. T4 DNA ligase enzyme (2,000,000 cohesive end units/mL, cat. #M0202T) and ligase buffer were purchased from New England Biolabs. Magnesium chloride and ammonium persulfate were purchased from Sigma-Aldrich. Tris base, boric acid, EDTA, Stains-All (cat. # E9379), and tetramethylethylenediamine (cat. #T9281) were purchased from Fisher. 40% Acrylamide/bisacrylamide solution, 19:1 (cat. #1610144) was purchased from Bio-Rad.

4.10.2 Synthesis of DNA Strands

The synthesis of the DNA strands were done using Glen Research reagents on an ABI solid-phase synthesizer, Model 392. Strands were purified following DMT-On GlenPak purification protocol using GlenPak DNA cartridges (cat. 60-5200-01). Standard DNA phosphoramidite, CPG's and the following mdifications: dSpacer CE phosphoramidite (cat. 10-1914-90), fluorescein-dT phosphoramidite (cat. 10-1056-95), 3'-(6-FAM) CPG (cat. 20-2961-41), chemical phosphorylation reagent II (cat. 10-1901-90), O^6-Me-dG-CE phosphoramidite (cat. 10-1070-90) were used (Figure 4.7). For synthesizing strands with the latter, ibu-dG-CE phosphoramidite (cat. 10-1020-05) were used (Figure 4.7).

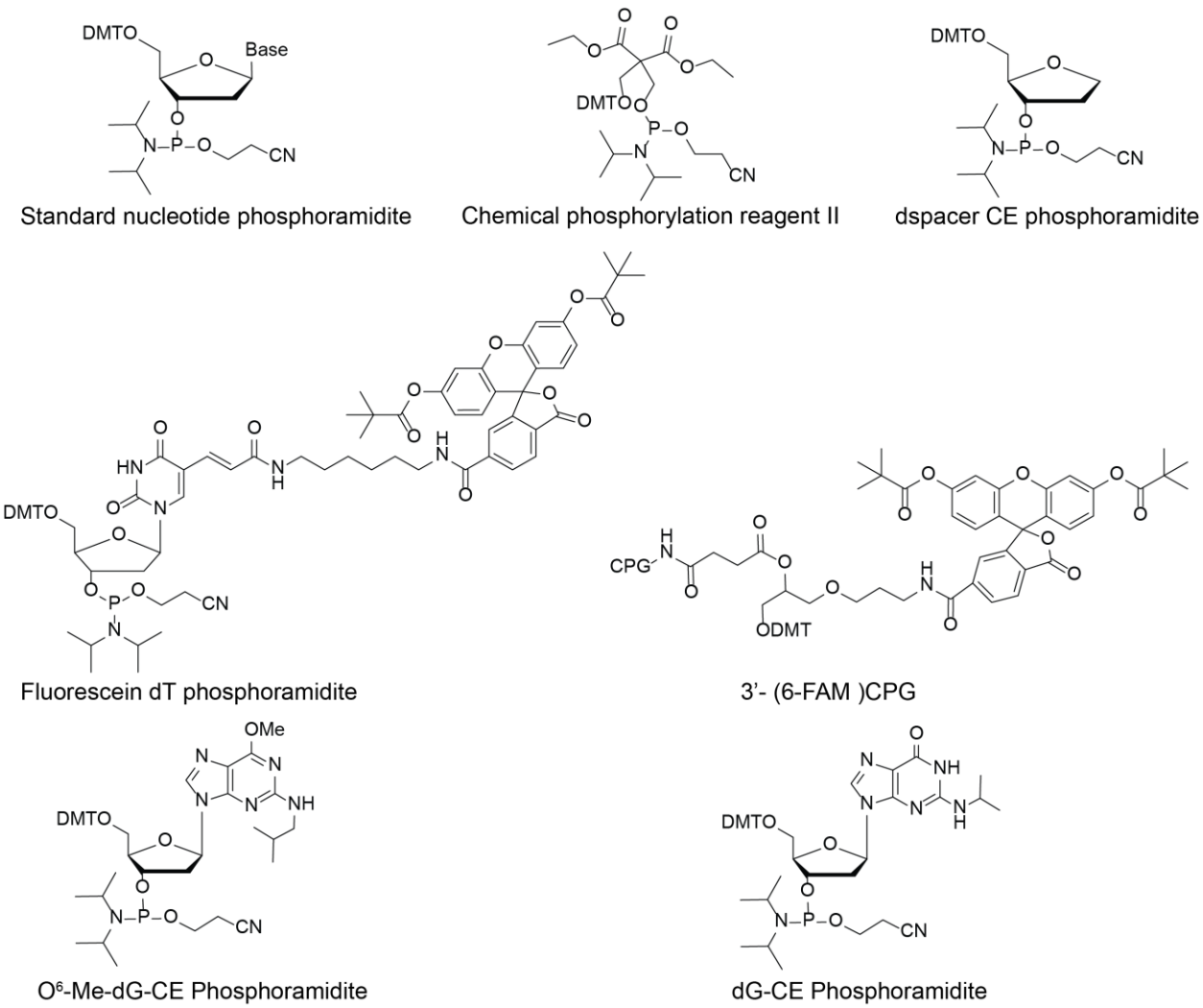

Figure 4.7 The chemical structures of the phosphoramidites and CPG used in this study. Dmt is dimethoxytrityl.

Table 4.1 DNA Sequences Used in This Study

Name	**Sequence**
K template	5' GTT GGA GCT GGT GGC GTA 3'
K(O^6-MeG14) template	5' GTT GGA GCT GGT G**G**$^{\mathbf{Me}}$C GTA 3'
K(O^6-Me-G11) template	5' GTT GGA GCT G**G**$^{\mathbf{Me}}$T GGC GTA 3'
5'-phosphate-abasic$_2$ probe (Cycle 1)	5' p**D**AG CTC **D**AA C 3'
3'-hydroxy DNA probe (Cycle 1)	5' TAC GCC AC 3'
3'-hydroxy ExBIM-G14 DNA probe (Cycle 1)	5' TAC C**X**C AC 3'

5'-phosphate DNA probe (Cycle 2)	5' pGGT GGC GTA 3'
3'-hydroxy-5' fluorescein DNA probe (Cycle 2)	5' T_{F-} GTT GGA GCT 3'
5'-phosphate-O^6-MeG14 DNA probe (Cycle 2)	5' pGGT G**G^{Me}**C GTA 3'
3'-hydroxy ExBIM-G11 DNA probe (Cycle 1)	5' TAC GCC A**X** 3'
5'-phosphate-O^6-MeG11 DNA probe (Cycle 2)	5' pG**G^{Me}**T GGC GTA 3'
3'-hydroxy-abasic probe (Cycle 1)	5' TAC **D**CC AC 3'
complementary K_c target with one abasic group	5' TAC GCC AC**D** AGC TCC AAC 3'
Complementary K_c target with two abasic groups	5' TAC GCC AC**D** AGC TC**D** AAC 3'

X = ExBIM, **G^{Me}**= O^6-MeG, **D** = abasic group, p = phosphate group, T_F = fluorescein-dT

4.10.2 Mass Analysis of the DNA Strands

Synthesized DNA strands were analyzed by MALDI-TOF. First a matrix solution of 3-hydroxypicolinic acid in 1:1 acetonitrile:water was prepared (25 mg/mL) as well as an ammonium citrate solution in water (25 mg/mL). These two solutions were mixed in a 9:1 ratio to yield the final matrix mixture. The synthesized DNA (5 nmol) was desalted using ZipTip (ZTC18S096) purchased from Millipore Sigma and was mixed in a 1:1 ratio with the matrix mixture. The measurements were carried out on a Voyager Elite (Applied BioSystems, Foster City, CA, USA) time of flight-mass spectrometer.

4.10.3 Ligation Experiments

4.10.3.1 Stoichiometric Enzymatic Ligation Procedure

The methylated or non-methylated template (1.4 μM), 5' phosphate (ExBIM or C probe) (2.8 μM), and 3'-hydroxy-5'-fluorescein DNA probe (1.4 μM) were added to the tube containing milliQ H_2O (2.5 μL) and incubated at 16, 19, or 21 °C. The master mix (1X T4 DNA ligase (6.5 unit μL-1, NEB), 1.5 X NEB buffer, 2.5 X MQ H2O) was added to a total volume of 15 μL, and the reaction was started. The ligation mixture (3 μL) were taken at different times and added to a

tube containing a running dye (0.25% w/v bromophenol blue with 80% w/v sucrose in 0.5 M EDTA (aq)) (2 μL). Then, the previous solution was loaded into a 15% polyacrylamide gel electrophoresis (PAGE), and run for 70 min on a 175 V electrophoresis.

4.10.3.2 Cross-Catalysis Enzymatic Ligation Procedure

0.1, 0.01, and 0.001 equivalents of the methylated or non-methylated template, 3'-hydroxy ExBIM DNA probe, 5' 5'phosphate-abasic2 DNA probe, 5' phosphate-O^6-MeG DNA probe, and 3'-hydroxy-5' fluorescein DNA probe were added to a tube containing MQ water. The DNA strands were incubated at a specific temperature. The master mix (1X T4 DNA ligase (6.5 unit μL^{-1}, NEB), 1.5 X NEB buffer, 2.5 X MQ H2O) was added to a total volume of 15 μL, and the reaction was started. 2 μL of the ligation mixture were taken at different times and added to an eppendorf tube containing a running dye (2 μL). Then, the previous solution was loaded into a 15% polyacrylamide gel electrophoresis (PAGE).

4.10.4 Denaturing Polyacrylamide Gel Electrophoresis

A denaturing 15% polyacrylamide gel was prepared by dissolving urea (4.8 g) in 40% Acrylamide/Bis Solution 19:1 (3.75 mL) (Bio-Rad Cat.161-0144) and 5 x TBE buffer (1 mL), then diluted to 10 mL with MQ water. Tetramethylethylenediamine (10.7 μL, TEMED) and aqueous ammonium persulfate (80 μL) were added after urea was dissolved to induce polymerization. A portion of the aliquot and running dye mixture (3 μL) was loaded into a denaturing 15% polyacrylamide gel (8 M urea in 0.5 X TBE, 37.5 vol% of 40% acrylamide/bisacrylamide solution, 0.75 mm thick, 10 wells). PAGE was run at 150 V for 80 min. A fluorescent image was taken of the gel using a fluorescent imager with trans-UV illumination using an ImageQuant RT ECL instrument from GE Healthcare Life Science. Quantification of the fluorescence emitted by each band was analysed by using ImageQuant TL

analysis software. The %con was determined based on the ratio of the fluorescence intensity of the product band over the sum of the fluorescence intensity of the product and reactant bands multiplied by 100%.[22]

The equation is as follow:

$$\%conversion = \frac{I\ product\ band}{I\ product\ band + I\ reactant\ band} \times 100\%$$

4.10.5 Testing the Purity of the Synthesized DNA Probes by Stains-All

The DNA strands were loaded into 15% denaturing PAGE then stained with Stains-All (Aldrich cat # E9379). The Stains-All solution was prepared by dissolving Stains-All (25 mg) in 50 mL mixture of 1:1 (MilliQ H2O: Formamide). The PAGE is placed in a container contained the Stains-All solution, covered with foil and placed in a shaker for 15 min. The presence of one band only for each strand is an indication of the purity of the DNA strand.

Chapter Five

General Conclusions and Future Plans

5.1 General Conclusions

The ultimate goal for this thesis was to develop an enzyme-free self-replicating system for point-of-care diagnostics. Although we did not achieve this goal, the work herein helped in getting a better understanding about the design of a non-enzymatic DNA replicator. One of the most important steps that we realized in order to develop such a system is the ligation step. The ligation step has to be rapid in the presence of the template and no reaction should occur when no template is present.

In chapter two, I discussed how we achieved DNA-templated CuAAC ligation that was as rapid and more selective as DNA-templated enzymatic ligation. We have assessed the reaction rate using 3'-propargyl ether and 5'-azide modifications under aerobic conditions as these modifications result in the most biocompatible triazole linkage to date.[43-44] The k_{obs} for the optimized reaction at 23 °C was 1.1 min^{-1} similar to that of the reaction catalyzed by T4 DNA ligase at high enzyme concentration. The selectivity of the reaction to a single nucleotide polymorphism on the ligation site of 3'-propargyl probe was studied and compared to the enzymatic ligation. We found that CuAAC was able to discriminate most mismatches better than T4 DNA ligase at temperatures slightly below the T_m of the nicked duplex of the perfect matched and higher than the T_m of the mismatched.

In chapter three, I discussed how we developed a single nucleotide polymorphism assay to improve the selectivity of DNA-templated ligation using T4 DNA ligase at a temperature far from the dissociation temperature of the nicked duplex of the perfect matched template. We used T4 DNA ligase, which is known of having low fidelity in discriminating between mismatches especially at the 3'-hydroxy site of the ligation. We observed facile ligation of the perfect match (> 80% conversion) while significantly mitigating ligation of the mismatched duplex. The

requirements are a temperature of ~ 7 °C above the nicked duplex dissociation temperature of the matched template. This temperature range can be extended to 13-19 °C if a higher concentration of enzyme was used. For testing the feasibility of the SNP assay at room temperature, an abasic group should be used which allows for a great discrimination around the T_m of the nicked duplex of the perfect matched template.

In chapter four, I discussed how we investigated the amplification of O^6-MeG in the KRAS gene using the lesion induced DNA amplification (LIDA). Mutations in the KRAS gene, especially in codon 12 and 13, have a negative impact on cell proliferation and could lead to tumor cells resistant to epidermal growth factor receptor therapies. The KRAS sequence is rich in GC content, thus we introduced another abasic group on the abasic LIDA system. The amplification of the methylated template was successful when a probe containing 2 abasic groups and a C across from the methylated group on the template was used. The most significant differences in amount of the methylated target produced when the reaction was initiated with 0.1 mol% of the methylated or non-methylated target was 93% for the methylated and 28% for the non-methylated template after 9 hours at 24 °C. Under these conditions, we were also able to amplify as low as 1.4 nM of the methylated template. With more investigation, this method could emerge as a tool for the sequence selective detection of O^6-MeG alkylated adducts on target DNA in point-of-care diagnostics.

5.2 Future Plans

5.2.1 Turnover Amplification with DNA-Templated Strain Promoted Alkyne-Azide Cycloaddition (SPAAC) Isothermally

As we discussed earlier in the introduction that one of the requirement for turnover is that the reaction is rapid. And to facilitate turnover experiment even more we thought of trying a reaction where no catalyst needed which could potentially help in point-of-care-diagnostic. We chose to investigate Cu free alkyne-azide cycloaddition DNA ligation which was reported by the Brown's group.[46] In this reaction, the alkyne is internal rather than terminal and located in a large ring which is dibenzocyclooctyne (DIBO). This ring is a strained molecule that relieves its strain by undergoing a click reaction involving cycloaddition of the internal alkyne with an azide (Scheme 1.8).[46] The author reported the templated reaction to be rapid and almost completed in 1 min at room temperature.

We followed the previous report and designed a DNA probe dibenzocyclooctyne (DIBO) at the 3'-with a fluorescein on the 5' position and a 5'-azide DNA probe (Scheme 5.1). The stoichiometric reaction was rapid as well same to what was reported.

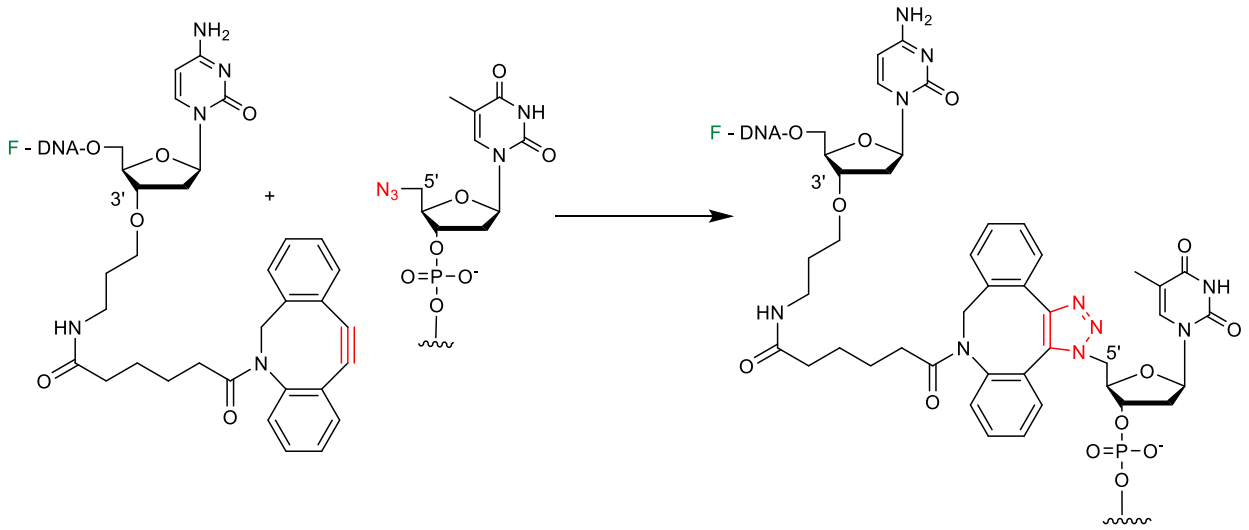

Scheme 5.1 DNA-templated strain promoted alkyne-azide cycloaddition.

5.2.1.1 Turnover in the Presence of an Abasic Group

We will introduce an abasic group on the 5' azide DNA probe to help with the spontaneous dissociation of the double stranded DNA as we have seen in a previous report by our group.[23] From the previous stoichiometric study on SPAAC, we determined 23 °C to be the optimum temperature. The next step, we will reduce the concentration of the template to 0.1, 0.01 and 0.001 eq and try the reaction. If this reaction works, it will be a great tool for amplification in point of care diagnostic since it does not require any catalyst and it works well at room temperature.

5.2.1.2 Salt Driven Turnover in DNA-Templated Ligation

As we have seen in Appendix I, we achieved 6 cycles of hybridization and dehybridization using Mg-EDTA cycling for an 18-mer duplex. We can apply the same idea to achieving turnover in a DNA-templated ligation. The addition of Mg salt will hybridize a nicked duplex (template and the two probes) allowing the reaction like SPAAC to occur, then we add EDTA to dehybridize the double stranded DNA product. The template will be in

substoichiometric concentration. By cycling the Mg-EDTA, we can achieve a good number of turnovers. If this reaction works, it could be a great tool for turnover as it can be applied with other reactions too and not only with SPAAC.

5.2.2 Turnover Amplification with DNA-templated Strain Promoted Alkyne-Azide Cycloaddition (SPAAC) with Thermocycling

Another strategy for SPAAC turnover that we will try if the isothermal reaction does not work is to produce turnover with temperature cycling. This work was done previously by Ito and co-workers (Chapter 1.3.1).[12] Temperature cycling requires a relatively low temperature where the nicked duplex will be hybridized (and the reaction can occurs), and a high temperature (higher than the melting temperature of the product duplex) to denature the duplex. We will work with 23 °C (optimized for this reaction) and since the reaction is rapid then we can have it at this temperature for 2- 3 min then heat up at 70 °C for 5 min. And repeat these cycles many times to achieve turnover.

References

1. Xu, Y.; Kool, E. T., High sequence fidelity in a non-enzymatic DNA autoligation reaction. *Nucleic Acids Research* **1999,** *27* (3), 875-81.

2. Xu, Y.; Karalkar, N. B.; Kool, E. T., Nonenzymatic autoligation in direct three-color detection of RNA and DNA point mutations. *Nature biotechnology* **2001,** *19*, 148.

3. Sando, S.; Kool, E. T., Imaging of RNA in Bacteria with Self-Ligating Quenched Probes. *Journal of the American Chemical Society* **2002,** *124* (33), 9686-9687.

4. Sando, S.; Kool, E. T., Quencher as Leaving Group: Efficient Detection of DNA-Joining Reactions. *Journal of the American Chemical Society* **2002,** *124* (10), 2096-2097.

5. Pianowski, Z. L.; Winssinger, N., Fluorescence-based detection of single nucleotide permutation in DNAvia catalytically templated reaction. *Chemical Communications* **2007,** (37), 3820-3822.

6. Sando, S.; Abe, H.; Kool, E. T., Quenched auto-ligating DNAs: multicolor identification of nucleic acids at single nucleotide resolution. *Journal of the American Chemical Society* **2004,** *126* (4), 1081-7.

7. Ficht, S.; Dose, C.; Seitz, O., As fast and selective as enzymatic ligations: unpaired nucleobases increase the selectivity of DNA-controlled native chemical PNA ligation. *ChemBioChem* **2005,** *6* (11), 2098-103.

8. Brunner, J.; Mokhir, A.; Kraemer, R., DNA-Templated Metal Catalysis. *Journal of the American Chemical Society* **2003,** *125* (41), 12410-12411.

9. Ma, Z.; Taylor, J.-S., Nucleic acid-triggered catalytic drug release. *Proceedings of the National Academy of Sciences* **2000,** *97* (21), 11159-11163.

10. Mirkin, C. A.; Letsinger, R. L.; Mucic, R. C.; Storhoff, J. J., A DNA-based method for rationally assembling nanoparticles into macroscopic materials. *Nature* **1996,** *382*, 607.

11. Alivisatos, A. P.; Johnsson, K. P.; Peng, X.; Wilson, T. E.; Loweth, C. J.; Bruchez Jr, M. P.; Schultz, P. G., Organization of 'nanocrystal molecules' using DNA. *Nature* **1996,** *382*, 609.

12. Abe, H.; Kondo, Y.; Jinmei, H.; Abe, N.; Furukawa, K.; Uchiyama, A.; Tsuneda, S.; Aikawa, K.; Matsumoto, I.; Ito, Y., Rapid DNA chemical ligation for amplification of RNA and DNA signal. *Bioconjugate Chemistry* **2008,** *19* (1), 327-33.

13. Patzke, V.; McCaskill, J. S.; von Kiedrowski, G., DNA with 3′-5′-Disulfide Links—Rapid Chemical Ligation through Isosteric Replacement. *Angewandte Chemie International Edition* **2014,** *53* (16), 4222-4226.

14. Sanzone, A. P.; El-Sagheer, A. H.; Brown, T.; Tavassoli, A., Assessing the biocompatibility of click-linked DNA in Escherichia coli. *Nucleic Acids Research* **2012,** *40* (20), 10567-75.

15. Seckute, J.; Yang, J.; Devaraj, N. K., Rapid oligonucleotide-templated fluorogenic tetrazine ligations. *Nucleic Acids Research* **2013,** *41* (15), e148.

16. Shelbourne, M.; Chen, X.; Brown, T.; El-Sagheer, A. H., Fast copper-free click DNA ligation by the ring-strain promoted alkyne-azide cycloaddition reaction. *Chemical Communications* **2011,** *47* (22), 6257-6259.

17. Vázquez, O.; Seitz, O., Templated native chemical ligation: peptide chemistry beyond protein synthesis. *Journal of Peptide Science* **2014,** *20* (2), 78-86.

18. Xu, Y.; Kool, E. T., A Novel 5'-Iodonucleoside Allows Efficient Nonenzymatic Ligation of Single-stranded and Duplex DNAs. *Tetrahedron Letters* **1997,** *38* (32), 5595-5598.

19. Achilles, T.; von Kiedrowski, G., A Self-Replicating System from Three Starting Materials. *Angewandte Chemie International Edition in English* **1993,** *32* (8), 1198-1201.

20. Sievers, D.; von Kiedrowski, G., Self-replication of complementary nucleotide-based oligomers. *Nature* **1994,** *369*, 221.

21. Grossmann, T. N.; Strohbach, A.; Seitz, O., Achieving Turnover in DNA-Templated Reactions. *ChemBioChem* **2008,** *9* (14), 2185-2192.

22. Kausar, A.; McKay, R. D.; Lam, J.; Bhogal, R. S.; Tang, A. Y.; Gibbs-Davis, J. M., Tuning DNA Stability To Achieve Turnover in Template for an Enzymatic Ligation Reaction. *Angewandte Chemie International Edition* **2011,** *50* (38), 8922-8926.

23. Kausar, A.; Mitran, C. J.; Li, Y.; Gibbs-Davis, J. M., Rapid, Isothermal DNA Self-Replication Induced by a Destabilizing Lesion. *Angewandte Chemie International Edition* **2013,** *52* (40), 10577-10581.

24. Alladin-Mustan, B. S.; Mitran, C. J.; Gibbs-Davis, J. M., Achieving room temperature DNA amplification by dialling in destabilization. *Chemical Communications* **2015,** *51* (44), 9101-4.

25. Abe, H.; Kool, E. T., Destabilizing Universal Linkers for Signal Amplification in Self-Ligating Probes for RNA. *Journal of the American Chemical Society* **2004,** *126* (43), 13980-13986.

26. Velema, W. A.; Kool, E. T., Fluorogenic Templated Reaction Cascades for RNA Detection. *Journal of the American Chemical Society* **2017,** *139* (15), 5405-5411.

27. Goodwin, J. T.; Lynn, D. G., Template-directed synthesis: use of a reversible reaction. *Journal of the American Chemical Society* **1992,** *114* (23), 9197-9198.

28. Zhan, Z.-Y. J.; Lynn, D. G., Chemical Amplification through Template-Directed Synthesis. *Journal of the American Chemical Society* **1997,** *119* (50), 12420-12421.

29. Luo, P.; Leitzel, J. C.; Zhan, Z.-Y. J.; Lynn, D. G., Analysis of the Structure and Stability of a Backbone-Modified Oligonucleotide: Implications for Avoiding Product Inhibition in Catalytic Template-Directed Synthesis. *Journal of the American Chemical Society* **1998,** *120* (13), 3019-3031.

30. Dose, C.; Ficht, S.; Seitz, O., Reducing Product Inhibition in DNA-Template-Controlled Ligation Reactions. *Angewandte Chemie International Edition* **2006,** *45* (32), 5369-5373.

31. Devaraj, N. K.; Weissleder, R.; Hilderbrand, S. A., Tetrazine-Based Cycloadditions: Application to Pretargeted Live Cell Imaging. *Bioconjugate Chemistry* **2008,** *19* (12), 2297-2299.

32. Blackman, M. L.; Royzen, M.; Fox, J. M., Tetrazine Ligation: Fast Bioconjugation Based on Inverse-Electron-Demand Diels−Alder Reactivity. *Journal of the American Chemical Society* **2008,** *130* (41), 13518-13519.

33. Devaraj, N. K.; Upadhyay, R.; Haun, J. B.; Hilderbrand, S. A.; Weissleder, R., Fast and Sensitive Pretargeted Labeling of Cancer Cells through a Tetrazine/trans-Cyclooctene Cycloaddition. *Angewandte Chemie International Edition* **2009,** *48* (38), 7013-7016.

34. Devaraj, N. K.; Hilderbrand, S.; Upadhyay, R.; Mazitschek, R.; Weissleder, R., Bioorthogonal Turn-On Probes for Imaging Small Molecules inside Living Cells. *Angewandte Chemie International Edition* **2010,** *49* (16), 2869-2872.

35. Peng, T.; Hang, H. C., Site-Specific Bioorthogonal Labeling for Fluorescence Imaging of Intracellular Proteins in Living Cells. *Journal of the American Chemical Society* **2016,** *138* (43), 14423-14433.

36. El-Sagheer, A. H.; Cheong, V. V.; Brown, T., Rapid chemical ligation of oligonucleotides by the Diels-Alder reaction. *Organic & Biomolecular Chemistry* **2011,** *9* (1), 232-5.

37. Rostovtsev, V. V.; Green, L. G.; Fokin, V. V.; Sharpless, K. B., A Stepwise Huisgen Cycloaddition Process: Copper(I)-Catalyzed Regioselective "Ligation" of Azides and Terminal Alkynes. *Angewandte Chemie International Edition* **2002,** *41* (14), 2596-2599.

38. Tornøe, C. W.; Christensen, C.; Meldal, M., Peptidotriazoles on Solid Phase: [1,2,3]-Triazoles by Regiospecific Copper(I)-Catalyzed 1,3-Dipolar Cycloadditions of Terminal Alkynes to Azides. *The Journal of Organic Chemistry* **2002,** *67* (9), 3057-3064.

39. Gartner, Z. J.; Grubina, R.; Calderone, C. T.; Liu, D. R., Two Enabling Architectures for DNA-Templated Organic Synthesis. *Angewandte Chemie International Edition* **2003,** *42* (12), 1370-1375.

40. Kumar, R.; El-Sagheer, A.; Tumpane, J.; Lincoln, P.; Wilhelmsson, L. M.; Brown, T., Template-Directed Oligonucleotide Strand Ligation, Covalent Intramolecular DNA Circularization and Catenation Using Click Chemistry. *Journal of the American Chemical Society* **2007,** *129* (21), 6859-6864.

41. Guerre, M.; Semsarilar, M.; Totee, C.; Silly, G.; Ameduri, B.; Ladmiral, V., Self-assembly of poly(vinylidene fluoride)-block-poly(2-(dimethylamino)ethylmethacrylate) block copolymers prepared by CuAAC click coupling. *Polymer Chemistry* **2017,** *8* (34), 5203-5211.

42. El-Sagheer, A. H.; Brown, T., Click chemistry with DNA. *Chemical Society Reviews* **2010,** *39* (4), 1388-1405.

43. El-Sagheer, A. H.; Brown, T., Synthesis and Polymerase Chain Reaction Amplification of DNA Strands Containing an Unnatural Triazole Linkage. *Journal of the American Chemical Society* **2009,** *131* (11), 3958-3964.

44. El-Sagheer, A. H.; Sanzone, A. P.; Gao, R.; Tavassoli, A.; Brown, T., Biocompatible artificial DNA linker that is read through by DNA polymerases and is functional in *Escherichia coli*. *Proceedings of the National Academy of Sciences of the United States of America* **2011,** *108* (28), 11338-11343.

45. El-Sagheer, A. H.; Brown, T., Single tube gene synthesis by phosphoramidate chemical ligation. *Chemical Communications* **2017,** *53* (77), 10700-10702.

46. Shelbourne, M.; Chen, X.; Brown, T.; El-Sagheer, A. H., Fast copper-free click DNA ligation by the ring-strain promoted alkyne-azide cycloaddition reaction. *Chemical Communications* **2011,** *47* (22), 6257-9.

47. Baskin, J. M; et al. Copper-free click chemistry for dynamic in vivo imaging. *The National Academy of Sciences of the USA* **2007,** *104* (43), 16793-97.

48. Abe, H.; Kondo, Y.; Jinmei, H.; Abe, N.; Furukawa, K.; Uchiyama, A.; Tsuneda, S.; Aikawa, K.; Matsumoto, I.; Ito, Y., Rapid DNA chemical ligation for amplification of RNA and DNA signal. *Bioconjugate Chemistry* **2008,** *19* (1), 327-33.

49. Melkonyan, H. S.; Feaver, W. J.; Meyer, E.; Scheinker, V.; Shekhtman, E. M.; Xin, Z.; Umansky, S. R., Transrenal nucleic acids: from proof of principle to clinical tests. *Annals of the New York Academy of Sciences* **2008,** *1137*, 73-81.

50. Shekhtman, E. M.; Anne, K.; Melkonyan, H. S.; Robbins, D. J.; Warsof, S. L.; Umansky, S. R., Optimization of transrenal DNA analysis: detection of fetal DNA in maternal urine. *Clinical Chemistry* **2009,** *55* (4), 723-9.

51. Sun, H.; Peng, X., Template-Directed Fluorogenic Oligonucleotide Ligation Using "Click" Chemistry: Detection of Single Nucleotide Polymorphism in the Human p53 Tumor Suppressor Gene. *Bioconjugate Chemistry* **2013,** *24* (7), 1226-1234.

52. Zhou, Q.-Y.; Yuan, F.; Zhang, X.-H.; Zhou, Y.-L.; Zhang, X.-X., Simultaneous multiple single nucleotide polymorphism detection based on click chemistry combined with DNA-encoded probes. *Chemical Science* **2018,** *9* (13), 3335-3340.

53. Dose, C.; Seitz, O., Single nucleotide specific detection of DNA by native chemical ligation of fluorescence labeled PNA-probes. *Bioorganic & Medicinal Chemistry* **2008,** *16* (1), 65-77.

54. Mattes, A.; Seitz, O., Mass-Spectrometric Monitoring of a PNA-Based Ligation Reaction for the Multiplex Detection of DNA Single-Nucleotide Polymorphisms. *Angewandte Chemie International Edition* **2001,** *40* (17), 3178-3181.

55. Peng, X.; Li, H.; Seidman, M., A Template-Mediated Click–Click Reaction: PNA–DNA, PNA–PNA (or Peptide) Ligation, and Single Nucleotide Discrimination. *European Journal of Organic Chemistry* **2010,** *2010* (22), 4194-4197.

56. Rostovtsev, V. V.; Green, L. G.; Fokin, V. V.; Sharpless, K. B., A stepwise huisgen cycloaddition process: copper(I)-catalyzed regioselective "ligation" of azides and terminal alkynes. *Angewandte Chemie International Edition Engl* **2002,** *41* (14), 2596-9.

57. Tornøe, C. W.; Christensen, C.; Meldal, M., Peptidotriazoles on Solid Phase: [1,2,3]-Triazoles by Regiospecific Copper(I)-Catalyzed 1,3-Dipolar Cycloadditions of Terminal Alkynes to Azides. *Journal of Organic Chemistry* **2002,** *67* (9), 3057-3064.

58. Sletten, E. M.; Bertozzi, C. R., Bioorthogonal Chemistry: Fishing for Selectivity in a Sea of Functionality. *Angewandte Chemie International Edition* **2009,** *48* (38), 6974-6998.

59. Kolb, H. C.; Finn, M. G.; Sharpless, K. B., Click Chemistry: Diverse Chemical Function from a Few Good Reactions. *Angewandte Chemie International Edition Engl* **2001,** *40* (11), 2004-2021.

60. Haque, M. M.; Peng, X., DNA-associated click chemistry. *Science China-Chemistry* **2014,** *57* (2), 215-231.

61. El-Sagheer, A. H.; Brown, T., Click Nucleic Acid Ligation: Applications in Biology and Nanotechnology. *Accounts of Chemical Research* **2012,** *45* (8), 1258-1267.

62. El-Sagheer, A. H.; Brown, T., Click chemistry with DNA. *Chemical Society Reviews* **2010,** *39* (4), 1388-405.

63. Gutsmiedl, K.; Fazio, D.; Carell, T., High-Density DNA Functionalization by a Combination of Cu-Catalyzed and Cu-Free Click Chemistry. *Chemistry – A European Journal* **2010,** *16* (23), 6877-6883.

64. Burley, G. A.; Gierlich, J.; Mofid, M. R.; Nir, H.; Tal, S.; Eichen, Y.; Carell, T., Directed DNA Metallization. *Journal of American Chemical Society* **2006,** *128* (5), 1398-1399.

65. Gierlich, J.; Burley, G. A.; Gramlich, P. M. E.; Hammond, D. M.; Carell, T., Click Chemistry as a Reliable Method for the High-Density Postsynthetic Functionalization of Alkyne-Modified DNA. *Organic Letters* **2006,** *8* (17), 3639-3642.

66. Seela, F.; Sirivolu, V. R., DNA Containing Side Chains with Terminal Triple Bonds: Base-Pair Stability and Functionalization of Alkynylated Pyrimidines and 7-Deazapurines. *Chemistry and Biodiversity* **2006,** *3* (5), 509-514.

67. Kocalka, P.; Andersen, N. K.; Jensen, F.; Nielsen, P., Synthesis of 5-(1,2,3-triazol-4-yl)-2'-deoxyuridines by a click chemistry approach: stacking of triazoles in the major groove gives increased nucleic acid duplex stability. *ChemBioChem* **2007,** *8* (17), 2106-16.

68. Kumar, R.; El-Sagheer, A.; Tumpane, J.; Lincoln, P.; Wilhelmsson, L. M.; Brown, T., Template-Directed Oligonucleotide Strand Ligation, Covalent Intramolecular DNA Circularization and Catenation Using Click Chemistry. *Journal of American Chemical Society* **2007,** *129* (21), 6859-6864.

69. Devaraj, N. K.; Miller, G. P.; Ebina, W.; Kakaradov, B.; Collman, J. P.; Kool, E. T.; Chidsey, C. E. D., Chemoselective Covalent Coupling of Oligonucleotide Probes to Self-Assembled Monolayers. *Journal of American Chemical Society* **2005,** *127* (24), 8600-8601.

70. Weller, R. L.; Rajski, S. R., DNA Methyltransferase-Moderated Click Chemistry. *Organic Letters* **2005,** *7* (11), 2141-2144.

71. Seo, T. S.; Li, Z.; Ruparel, H.; Ju, J., Click Chemistry to Construct Fluorescent Oligonucleotides for DNA Sequencing. *Journal of Organic Chemistry* **2003,** *68* (2), 609-612.

72. Chen, Y.; Xianyu, Y.; Wu, J.; Yin, B.; Jiang, X., Click Chemistry-Mediated Nanosensors for Biochemical Assays. *Theranostics* **2016,** *6* (7), 969-985.

73. Hu, Q.; Deng, X.; Kong, J.; Dong, Y.; Liu, Q.; Zhang, X., Simple and fast electrochemical detection of sequence-specific DNA via click chemistry-mediated labeling of hairpin DNA probes with ethynylferrocene. *Analyst* **2015,** *140* (12), 4154-4161.

74. Presolski, S. I.; Hong, V.; Cho, S.-H.; Finn, M. G., Tailored Ligand Acceleration of the Cu-Catalyzed Azide−Alkyne Cycloaddition Reaction: Practical and Mechanistic Implications. *Journal of American Chemical Society* **2010,** *132* (41), 14570-14576.

75. Sharma, A. K.; Kent, A. D.; Heemstra, J. M., Enzyme-Linked Small-Molecule Detection Using Split Aptamer Ligation. *Analytical Chemistry* **2012,** *84* (14), 6104-6109.

76. Abel, G. R.; Cao, B. H.; Hein, J. E.; Ye, T., Covalent, sequence-specific attachment of long DNA molecules to a surface using DNA-templated click chemistry. *Chemical Communications* **2014,** *50* (60), 8131-8133.

77. El-Sagheer, A. H.; Brown, T., A triazole linkage that mimics the DNA phosphodiester group in living systems. *Quarterly Reviews of Biophysics* **2015,** *48* (4), 429-36.

78. El-Sagheer, A. H.; Brown, T., Efficient RNA synthesis by in vitrotranscription of a triazole-modified DNA template. *Chemical Communications* **2011,** *47* (44), 12057-12058.

79. Kukwikila, M.; Gale, N.; El-Sagheer, A. H.; Brown, T.; Tavassoli, A., Assembly of a biocompatible triazole-linked gene by one-pot click-DNA ligation. *Nature Chemistry* **2017,** *9*, 1089.

80. Rodionov, V. O.; Presolski, S. I.; Gardinier, S.; Lim, Y.-H.; Finn, M. G., Benzimidazole and Related Ligands for Cu-Catalyzed Azide−Alkyne Cycloaddition. *Journal of American Chemical Society* **2007,** *129* (42), 12696-12704.

81. Rodionov, V. O.; Presolski, S. I.; Díaz Díaz, D.; Fokin, V. V.; Finn, M. G., Ligand-Accelerated Cu-Catalyzed Azide−Alkyne Cycloaddition: A Mechanistic Report. *Journal of American Chemical Society* **2007,** *129* (42), 12705-12712.

82. Presolski, S. I.; Hong, V. P.; Finn, M. G., Copper-Catalyzed Azide–Alkyne Click Chemistry for Bioconjugation. *Current Protocols in Chemical Biology* **2011,** *3* (4), 153-162.

83. New England Biolab https://content.neb.com/faqs/2012/01/14/what-is-the-concentration-of-t4-dna-ligase-provided-in-the-quick-ligation-kit. (accessed 17 May, 2018).

84. Kočalka, P.; El-Sagheer, A. H.; Brown, T., Rapid and Efficient DNA Strand Cross-Linking by Click Chemistry. *ChemBioChem* **2008,** *9* (8), 1280-1285.

85. Siemsen, P.; Livingston, R. C.; Diederich, F., Acetylenic Coupling: A Powerful Tool in Molecular Construction. *Angewandte Chemie International Edition* **2000,** *39* (15), 2632-2657.

86. Jia, X.; Yin, K.; Li, C.; Li, J.; Bian, H., Copper-catalyzed oxidative alkyne homocoupling without palladium, ligands and bases. *Green Chemistry* **2011,** *13* (8), 2175-2178.

87. Fry, S. C., Oxidative scission of plant cell wall polysaccharides by ascorbate-induced hydroxyl radicals. *Biochemical Journal* **1998,** *332* (Pt 2), 507-515.

88. Saito, F.; Noda, H.; Bode, J. W., Critical Evaluation and Rate Constants of Chemoselective Ligation Reactions for Stoichiometric Conjugations in Water. *ACS Chemial Biology* **2015,** *10* (4), 1026-1033.

89. Pritchard, C. E.; Southern, E. M., Effects of base mismatches on joining of short oligodeoxynucleotides by DNA ligases. *Nucleic Acids Research.* **1997,** *25* (17), 3403-3407.

90. Liu, P.; Burdzy, A.; Sowers, L. C., DNA ligases ensure fidelity by interrogating minor groove contacts. *Nucleic Acids Research.* **2004,** *32* (15), 4503-4511.

91. Pack, S. P.; Doi, A.; Choi, Y. S.; Kodaki, T.; Makino, K., Biomolecular response of oxanine in DNA strands to T4 polynucleotide kinase, T4 DNA ligase, and restriction enzymes. *Biochemical and Biophysical Research Communications* **2010,** *391* (1), 118-122.

92. Wiaderkiewicz, R.; Ruiz-Carrillo, A., Mismatch and blunt to protruding-end joining by DNA ligases. *Nucleic Acids Research* **1987,** *15* (19), 7831-7848.

93. Goffin, C.; Bailly, V.; Verly, W. G., Nicks 3′ or 5′ to AP sites or to mispaired bases, and one-nucleotide gaps can be sealed by T4 DNA ligase. *Nucleic Acids Research* **1987,** *15* (21), 8755-8771.

94. M. Tsiapalis, C.; A. Narang, S., On the fidelity of phage T4-induced polynucleotide ligase in the joining of chemically synthesized deoxyribooligonucleotides. *Biochemical and Biophysical Research Communication* 1970; Vol. 39, p 631-6.

95. Wu, D. Y.; Wallace, R. B., Specificity of the nick-closing activity of bacteriophage T4 DNA ligase. *Gene* **1989,** *76* (2), 245-54.

96. Kim, J.; Mrksich, M., Profiling the selectivity of DNA ligases in an array format with mass spectrometry. *Nucleic Acids Research* **2010,** *38* (1), e2-e2.

97. Lamarche, B. J.; Showalter, A. K.; Tsai, M. D., An error-prone viral DNA ligase. *Biochemistry* **2005,** *44* (23), 8408-17.

98. Cherepanov, A.; Yildirim, E.; de Vries, S., Joining of short DNA oligonucleotides with base pair mismatches by T4 DNA ligase. *Journal of Biochemistry* **2001,** *129* (1), 61-8.

99. Alexander, R. C.; Johnson, A. K.; Thorpe, J. A.; Gevedon, T.; Testa, S. M., Canonical nucleosides can be utilized by T4 DNA ligase as universal template bases at ligation junctions. *Nucleic Acids Research* **2003,** *31* (12), 3208-3216.

100. Lohman, G. J.; Bauer, R. J.; Nichols, N. M.; Mazzola, L.; Bybee, J.; Rivizzigno, D.; Cantin, E.; Evans, T. C., Jr., A high-throughput assay for the comprehensive profiling of DNA ligase fidelity. *Nucleic Acids Research* **2016,** *44* (2), e14.

101. Barany, F.; Gelfand, D. H., Cloning, overexpression and nucleotide sequence of a thermostable DNA ligase-encoding gene. *Gene* **1991,** *109* (1), 1-11.

102. Jang, E. K.; Yang, M.; Pack, S. P., Highly-efficient T4 DNA ligase-based SNP analysis using a ligation fragment containing a modified nucleobase at the end. *Chemical Communications* **2015,** *51* (66), 13090-13093.

103. TriLink BioTechnologies, https://www.trilinkbiotech.com/work/Ligation.pdf.

104. Kausar, A.; Osman, E. A.; Gadzikwa, T.; Gibbs-Davis, J. M., The presence of a 5′-abasic lesion enhances discrimination of single nucleotide polymorphisms while inducing an isothermal ligase chain reaction. *Analyst* **2016,** *141* (14), 4272-4277.

105. Wang, H.; Li, J.; Wang, Y.; Jin, J.; Yang, R.; Wang, K.; Tan, W., Combination of DNA Ligase Reaction and Gold Nanoparticle-Quenched Fluorescent Oligonucleotides: A Simple and Efficient Approach for Fluorescent Assaying of Single-Nucleotide Polymorphisms. *Analytical Chemistry* **2010,** *82* (18), 7684-7690.

106. Luo, J.; Bergstrom, D. E.; Barany, F., Improving the fidelity of Thermus thermophilus DNA ligase. *Nucleic Acids Research* **1996,** *24* (15), 3071-3078.

107. Kim, S.; Misra, A., SNP genotyping: technologies and biomedical applications. *Annual Review of Biomedical Engineering* **2007,** *9*, 289-320.

108. Pack, S. P.; Morimoto, H.; Makino, K.; Tajima, K.; Kanaori, K., Solution structure and stability of the DNA undecamer duplexes containing oxanine mismatch. *Nucleic Acids Research* **2012,** *40* (4), 1841-1855.

109. Rossi, R.; Montecucco, A.; Ciarrocchi, G.; Biamonti, G., Functional characterization of the T4 DNA ligase: a new insight into the mechanism of action. *Nucleic Acids Research* **1997,** *25* (11), 2106-2113.

110. Landegren, U.; Kaiser, R.; Sanders, J.; Hood, L., A ligase-mediated gene detection technique. *Science* **1988,** *241* (4869), 1077-1080.

111. New England Biolabs, https://international.neb.com/faqs/2012/01/14/what-is-the-concentration-of-t4-dna-ligase-provided-in-the-quick-ligation-kit. **2018**.

112. Weiss, B.; Jacquemin-Sablon, A.; Live, T. R.; Fareed, G. C.; Richardson, C. C., Enzymatic breakage and joining of deoxyribonucleic acid. VI. Further purification and properties of polynucleotide ligase from Escherichia coli infected with bacteriophage T4. *The Journal of Biological Chemistry* **1968,** *243* (17), 4543-55.

113. Olivera, B. M.; Hall, Z. W.; Lehman, I. R., Enzymatic joining of polynucleotides, V. A DNA-adenylate intermediate in the polynucleotide-joining reaction. *Proceedings of the National Academy of Sciences of the United States of America* **1968,** *61* (1), 237-244.

114. Olivera, B. M.; Hall, Z. W.; Anraku, Y.; Chien, J. R.; Lehman, I. R., On the mechanism of the polynucleotide joining reaction. *Cold Spring Harbor symposia on quantitative biology* **1968,** *33*, 27-34.

115. Harvey, C. L.; Gabriel, T. F.; Wilt, E. M.; Richardson, C. C., Enzymatic breakage and joining of deoxyribonucleic acid. IX. Synthesis and properties of the deoxyribonucleic acid adenylate in the phage T4 ligase reaction. *The Journal of Biological Chemistry* **1971,** *246* (14), 4523-30.

116. Nilsson, M.; Antson, D.-O.; Barbany, G.; Landegren, U., RNA-templated DNA ligation for transcript analysis. *Nucleic Acids Research* **2001,** *29* (2), 578-581.

117. Dupont, C.; Armant, D. R.; Brenner, C. A., Epigenetics: Definition, Mechanisms and Clinical Perspective. *Seminars in reproductive medicine* **2009,** *27* (5), 351-357.

118. K, L. D. H.; R, M. E., DNA methylation: a form of epigenetic control of gene expression. *The Obstetrician & Gynaecologist* **2010,** *12* (1), 37-42.

119. Javaid, N.; Choi, S., Acetylation- and Methylation-Related Epigenetic Proteins in the Context of Their Targets. *Genes* **2017,** *8* (8), 196.

120. Rossetto, D.; Avvakumov, N.; Côté, J., Histone phosphorylation: A chromatin modification involved in diverse nuclear events. *Epigenetics* **2012,** *7* (10), 1098-1108.

121. Vranych, C. V.; Rivero, M. R.; Merino, M. C.; Mayol, G. F.; Zamponi, N.; Maletto, B. A.; Pistoresi-Palencia, M. C.; Touz, M. C.; Ropolo, A. S., SUMOylation and deimination of proteins: two epigenetic modifications involved in Giardia encystation. *Biochimica et Biophysica Acta* **2014,** *1843* (9), 1805-17.

121. Harrison, K. L.; Jukes, R.; Cooper, D. P.; Shuker, D. E., Detection of concomitant formation of O^6-carboxymethyl- and O6-methyl-2'-deoxyguanosine in DNA exposed to nitrosated glycine derivatives using a combined immunoaffinity/HPLC method. *Chemical Research in Toxicology* **1999,** *12* (1), 106-111.

123. Sedgwick, B., Nitrosated peptides and polyamines as endogenous mutagens in O6-alkylguanine-DNA alkyltransferase deficient cells. *Carcinogenesis* **1997,** *18* (8), 1561-1567.

124. Rydberg, B.; Lindahl, T., Nonenzymatic methylation of DNA by the intracellular methyl group donor S-adenosyl-L-methionine is a potentially mutagenic reaction. *The EMBO Journal* **1982,** *1* (2), 211-216.

125. Jones, P. A.; Laird, P. W., Cancer epigenetics comes of age. *Nature Genetics* **1999,** *21* (2), 163-7.

126. Plass, C., Cancer epigenomics. *Human Molecular Genetics* **2002,** *11* (20), 2479-88.

127. Laird, P. W., The power and the promise of DNA methylation markers. *Nature Reviews Cancer* **2003,** *3* (4), 253-66.

128. Sasaki, H.; Matsui, Y., Epigenetic events in mammalian germ-cell development: reprogramming and beyond. *Nature Reviews Genetics* **2008,** *9* (2), 129-40.

129. Law, J. A.; Jacobsen, S. E., Establishing, maintaining and modifying DNA methylation patterns in plants and animals. *Nature reviews. Genetics* **2010,** *11* (3), 204-220.

130. Chen, K.; Zhao, Boxuan S.; He, C., Nucleic Acid Modifications in Regulation of Gene Expression. *Cell Chemical Biology* **2016,** *23* (1), 74-85.

131. Feinberg, A. P.; Vogelstein, B., Hypomethylation distinguishes genes of some human cancers from their normal counterparts. *Nature* **1983,** *301*, 89-92.

132. Baylin, S. B.; Hoppener, J. W.; de Bustros, A.; Steenbergh, P. H.; Lips, C. J.; Nelkin, B. D., DNA methylation patterns of the calcitonin gene in human lung cancers and lymphomas. *Cancer Research* **1986,** *46* (6), 2917-22.

133. Kulis, M.; Esteller, M., DNA methylation and cancer. *Advances in Genetics* **2010,** *70*, 27-56.

134. Jones, P. A., DNA methylation errors and cancer. *Cancer Research* **1996,** *56* (11), 2463-2467.

135. Counts, J. L.; Goodman, J. I., Alterations in DNA methylation may play a variety of roles in carcinogenesis. *Cell* **1995,** *83* (1), 13-15.

136. Cooper, D. N.; Krawczak, M., The mutational spectrum of single base-pair substitutions causing human genetic disease: patterns and predictions. *Human Genetics* **1990,** *85* (1), 55-74.

137. Sved, J.; Bird, A., The expected equilibrium of the CpG dinucleotide in vertebrate genomes under a mutation model. *Proceedings of the National Academy of Sciences of the United States of America* **1990,** *87* (12), 4692-4696.

138. Sharma, V.; Collins, L. B.; Clement, J. M.; Zhang, Z.; Nakamura, J.; Swenberg, J. A., Molecular dosimetry of endogenous and exogenous O(6)-methyl-dG and N7-methyl-G adducts following low dose [D3]-methylnitrosourea exposures in cultured human cells. *Chemical Research in Toxicology* **2014,** *27* (4), 480-482.

139. Karapetis, C. S.; Khambata-Ford, S.; Jonker, D. J.; O'Callaghan, C. J.; Tu, D.; Tebbutt, N. C.; Simes, R. J.; Chalchal, H.; Shapiro, J. D.; Robitaille, S.; Price, T. J.; Shepherd, L.; Au, H. J.; Langer, C.; Moore, M. J.; Zalcberg, J. R., K-ras mutations and benefit from cetuximab in advanced colorectal cancer. *The New England Journal of Medicine* **2008,** *359* (17), 1757-1765.

140. Amado, R. G.; Wolf, M.; Peeters, M.; Van Cutsem, E.; Siena, S.; Freeman, D. J.; Juan, T.; Sikorski, R.; Suggs, S.; Radinsky, R.; Patterson, S. D.; Chang, D. D., Wild-type KRAS is required for panitumumab efficacy in patients with metastatic colorectal cancer. *Journal of Clinical Oncology* **2008,** *26* (10), 1626-1634.

141. Waldner, M. J.; Neurath, M. F., The molecular therapy of colorectal cancer. *Molecular Aspects of Medicine* **2010,** *31* (2), 171-8.

142. O'Reilly, S. M.; et al., Temozolomide: a new oral cytotoxic chemotherapeutic agent with promising activity against primary brain tumours. *European Journal of Cancer* **1993,** *29a* (7), 940-942.

143. Foiles, P. G.; Miglietta, L. M.; Akerkar, S. A.; Everson, R. B.; Hecht, S. S., Detection of O^6-Methyldeoxyguanosine in Human Placental DNA. *Cancer Research* **1988,** *48* (15), 4184-4188.

144. Kang, H.-i.; Konishi, C.; Kuroki, T.; Huh, N.-h., Detection of O6-methylguanine, O4-methylthymine and O4-ethylthymine in human liver and peripheral blood leukocyte DNA. *Carcinogenesis* **1995,** *16* (6), 1277-1280.

145. Ma, F.; Zhang, Z.; Jiang, J.; Hu, J., Chromium (VI) potentiates the DNA adducts (O(6)-methylguanine) formation of N-nitrosodimethylamine in rat: implication on carcinogenic risk. *Chemosphere* **2015,** *139*, 256-9.

146. Hemeryck, L. Y.; Decloedt, A. I.; Vanden Bussche, J.; Geboes, K. P.; Vanhaecke, L., High resolution mass spectrometry based profiling of diet-related deoxyribonucleic acid adducts. *Analytica Chimica Acta* **2015,** *892*, 123-31.

147. Kreimer, A. R.; Villa, A.; Nyitray, A. G.; Abrahamsen, M.; Papenfuss, M.; Smith, D.; Hildesheim, A.; Villa, L. L.; Lazcano-Ponce, E.; Giuliano, A. R., The epidemiology of oral HPV infection among a multinational sample of healthy men. *Cancer epidemiology, biomarkers & prevention : a publication of the American Association for Cancer Research, cosponsored by the American Society of Preventive Oncology* **2011,** *20* (1), 172-182.

148. Kang, H.-i.; Konishi, C.; Eberle, G.; Rajewsky, M. F.; Kuroki, T.; Huh, N.-h., Highly Sensitive, Specific Detection of O^6-Methylguanine, O^4-Methylthymine, and O^4-Ethylthymine by the Combination of High-Performance Liquid Chromatography Prefractionation, ^{32}P Postlabeling, and Immunoprecipitation. *Cancer Research* **1992,** *52* (19), 5307-5312.

149. Onizuka, K.; Nishioka, T.; Li, Z.; Jitsuzaki, D.; Taniguchi, Y.; Sasaki, S., An efficient and simple method for site-selective modification of O6-methyl-2[prime or minute]-deoxyguanosine in DNA. *Chemical Communications* **2012,** *48* (33), 3969-3971.

150. Trantakis, I. A.; Nilforoushan, A.; Dahlmann, H. A.; Stäuble, C. K.; Sturla, S. J., In-gene Quantification of O(6)-Methylguanine with Elongated Nucleoside Analogues on Gold Nanoprobes. *Journal of American Chemical Society* **2016,** *138* (27), 8497-8504.

151. Gong, J.; Sturla, S. J., A synthetic nucleoside probe that discerns a DNA adduct from unmodified DNA. *Journal of American Chemical Society* **2007,** *129* (16), 4882-4883.

152. V., C. A.; Simon, d. V., Dynamic mechanism of nick recognition by DNA ligase. *European Journal of Biochemistry* **2002,** *269* (24), 5993-5999.

Appendix I

Towards Fuel-Driven DNA Hybridization/Dehybridization Cycles

AI.1 Introduction

DNA is an excellent candidate in nanotechnology and nanoswitch devices due to its versatility, flexibility and, more importantly, its sequence-specific hybridization in a well-defined double helix.[1-4] These properties allow the DNA to self-assemble in nanostructures, forming the building blocks of different nanomachines, such as DNA walkers, DNA tweezers, and DNA gears.[5-8] Such DNA nanomachines have different applications in molecular sensing, nanomedicine, and drug delivery.[9-11] They change their motion, structure, hybridization state (switching between hybridization and dehybridization) as a result of a response to external stimuli, such as a change in pH, conformation, etc. Researchers have been working in finding different ways to control DNA hybridization and dehybridization to expand the application of such switches in nanotechnology.

AI.1.1 Light Driven DNA Hybridization and Dehybridization

One way to control the hybridization and dehybridization of DNA is by light. The dsDNA has been modified with a photoresponsive molecule that changes its conformation when it absorbs light. These molecules include spiropyran,[12] stilbene,[13] diarylethene,[14] and azobenzene. The azobenzene family is the most common one among them and has many applications due to its simple synthesis as well as its commercial availability and is tolerance to the multiple photon irradiations.[15] When a DNA is modified with azobenzene, it forms a trans conformation in the dsDNA, and when it is irradiated with UV light (~ 340 nm), it changes to the cis form, causing the double stranded DNA to dehybridize. Irradiating it again with visible light (> 400 nm) leads to a change in the geometric isomerism back to the trans form, and the DNA will be hybridized.

Light driven DNA hybridization and dehybridization of a DNA containing azobenzene was used to construct different nanomachines. Photoswitchable molecular glues were achieved by the hybridization and dehybridization of dsDNA containing azobenzene upon applying photoirradiation UV and visible light on the duplex (Scheme AI.1 A).[16] Photoresponsive tweezers with an exchangeable toehold were designed. The tweezer will be in the closed form when the DNA containing azobenzene molecules in the trans configuration is hybridized to the toehold. Photoirradiation with 340 nm UV light changes the azobenzene to the cis isomer, causing dehybridization and opening the tweezer (Scheme AI.1B).[17]

Another photoresponsive device was designed by Hiroyuki's group. The authors designed a photoresponsive DNAzyme with a catalytic loop, an RNA region hybridized to part of the two arms, and the extended arms were modified with azobenzene molecules. The photoisomerization of azobenzene initiated the switching on and off the DNAzyme activity and the cleavage of the RNA (Scheme A.1C).[18-19]

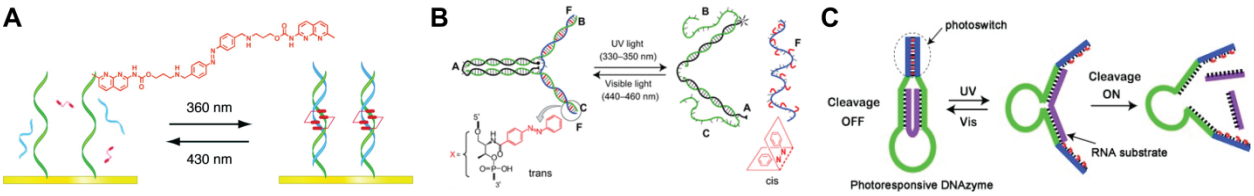

Scheme AI.1. Light driven DNA hybridization and dehybridization in nanoswitches. A) Photoswitchable molecular glues. B) Photoresponsive tweezers. C) Photoresponsive DNAzyme. Image A regenerated with the permission from ref. 16, Copyright © 2007, American Chemical Society. Image B regenerated with the permission from ref. 17, Copyright © 2008, John Wiley and Sons. Image B regenerated with the permission from ref. 18, Copyright © 2010, John Wiley and Sons.

Despite the great advantages of photoirradiation of azobenzene and the great applications in nanomachines, there are some limitations. Photoisomerization has low quantum yields, the cis form of azobenzene is thermally unstable, and the transformation does not exceed 80%.[20]

AI.1.2 pH Driven DNA Hybridization and Dehybridization

Another method to control the hybridization and dehybridization of DNA that has applications in nanodevices is by a change in pH. A switchable DNA nanotriangle was designed by three ssDNAs. The first strand, called M, has three different complementary parts, two parts of which are complementary to the second strand F, which has a fluorophore on one end and a quencher on the other end. The third strand is C, which is complementary to the middle part of strand M. DNA C and DNA M have three mismatches between them. In a neutral or basic medium, the three DNA strands hybridize together forming the triangle (open state). In an acidic medium, strand C will dehybridize from strand M, and the latter will form an i-motif[22-23] between the cytosine bases in the middle part of the strand (close state of the triangle). The authors controlled the opening and closing of the triangle by changing the pH, and the fluorescence signal is detected when it is open. This nanodevice could have potential use in a drug delivery system as well as a building block for more complex nanostructures.[21]

Another example of a pH dependent nanodevice was done by the Jiang group. They designed DNA nanoswitche with a pH-responsive carrier that attaches or releases gold nanoparticles on mesoporous silica.[24] The system was designed by attaching ssDNA (I) on mesoporous silica, whose pores are loaded with small molecules of rhodamine, and another ssDNA (II) with gold nanoparticles, which is partially complementary to strand I. In a basic medium, the two strands will hybridize to each other, and the gold nanoparticle will seal the pores, keeping the small molecules inside the pores. In an acidic medium, strand II will dehybridize from strand I and fold into an i-motif, resulting in the release of rhodamine molecules from the pores. These DNA nanoswitches have applications in the acidic release of drugs for the treatment of tumors or other affected tissues.[24]

pH driven DNA hybridization and dehybridization has wide applications in DNA nanodevices for drug delivery. However, there is always room to explore simple methods that can help in developing the applications.[25] In this Chapter we have looked into different strategies of controlling DNA hybridization and dehybridization for potential use in nanodevices and/or DNA amplification strategies, which could allow for isothermal turnover in microfluidic devices that could provide the timed introduction of fuel.

AI.2 Fuel Driven DNA Hybridization and Dehybridization

One strategy that we tried for inducing and controlling DNA hybridization is by the use of a fuel as a driving agent. In this regard, we collaborated with the Boekhoven group that has developed a method of self-assembly and disassembly of supramolecular materials using ethyl-3-(3-dimethylaminopropyl) carbodiimide (EDC).[26] They used different precursors based on two amino acids, aspartate (D) and glutamate (E), bearing a hydrophobic group of (fluoren-9-ylmethoxycarbonyl, Fmoc). In the presence of a fuel such as EDC, these precursors are self-assembled, forming an anhydride. In a reversible step, the anhydride can go back to the original dicarboxylate upon hydrolysis (Scheme AI.2). The concentration of the fuel controls how long the anhydride stage can last before the hydrolysis.

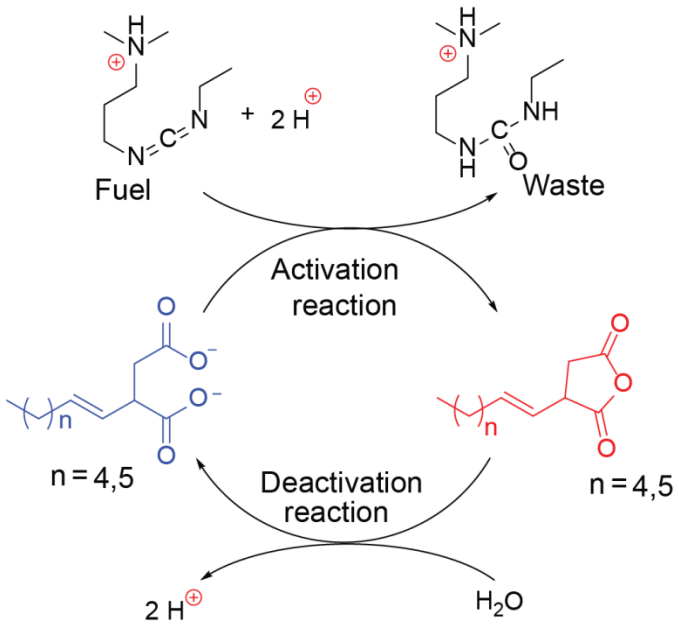

Scheme AI.2 Fuel driven self-assembly and disassembly of dicarboxylate precursors.

We synthesized a template by solid-phase synthesis that contained two dicarboxylate groups by preparing a DNA strand bearing two NHS carboxy groups, then reacting it with aspartic dimethyl chloride while the DNA was still bound to the controlled porous glass solid (Scheme AI.3). The idea here is that the two dicarboxylate groups on the DNA template will act as a precursor, which forms an anhydride upon reaction with EDC. This anhydride is neutral, allowing hybridization of two complementary probes (one with 5'-azide and the other one with 3'-alkyne-5' fluorescein); these two probes can form a triazole product in the presence of the Cu (I) catalyst. When the EDC is consumed, the anhydride will eventually be hydrolyzed by water back to the original dicarboxylate form, which is negatively charged. We hoped that the repulsion between the two strands should result in dehybridization and lead to turnover (Scheme A.4). The cycle can be reinitiated by the addition of another batch of EDC, then Cu(I) catalyst, and more cycles can be regenerated by the addition of EDC, followed by Cu(I) catalyst.

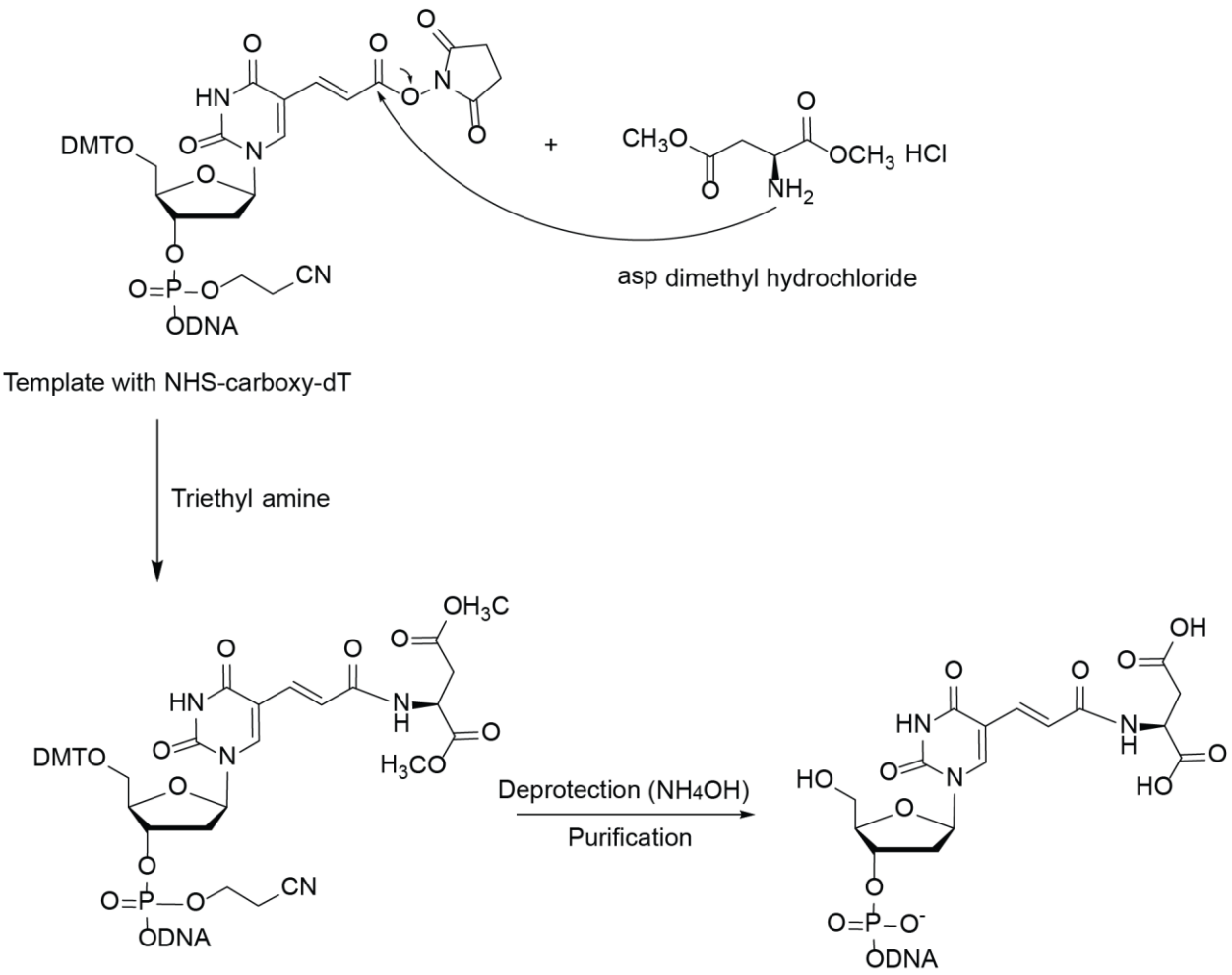

Scheme AI.3 Reaction scheme of the synthesis of a dicarboxylate template starting from NHS carboxy dT template and aspartic dimethyl chloride.

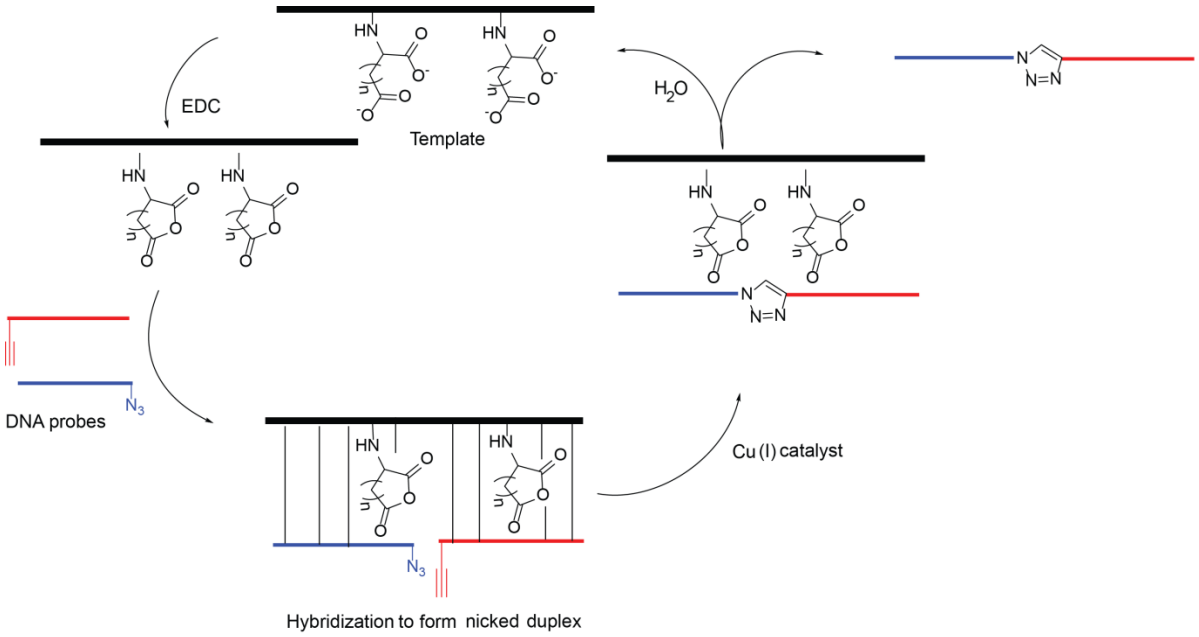

Scheme AI.4 Fuel driven turnover of dicarboxylate templated Cu(I) catalyzed azide-alkyne cycloaddition.

First, we wanted to test whether we could control the hybridization and dehybridization of the 18-mer template that had two dicarboxylate groups with an 18-mer complementary target by the addition of EDC (Scheme AI.4) and monitor this process by the absorbance at 260 nm using UV spectroscopy. The idea here is that when it is in the anhydride form, the duplex will be hybridized and the absorbance decreases, but when it is in the dicarboxylate form, the duplex is dehybridized and the absorbance increases. However, monitoring by UV was not possible since EDC has some absorption at 260 nm where DNA has its absorbance maximum, meaning that an increase in the absorbance occurs with the addition of EDC.

Later we realized another limitation of this strategy, which was that the difference in melting temperature between the duplex that had two dicarboxylate groups (46 °C) and a control duplex with no dicarboxylate groups (49 °C) was only 3 °C (Figure AI.1) suggesting that hydrolysis of the anhydrides would have a minor effect on duplex stability. One solution that we

could explore in the future would be to increase the number of the dicarboxylate groups on the template, maybe to 4—6 dicarboxylate groups.

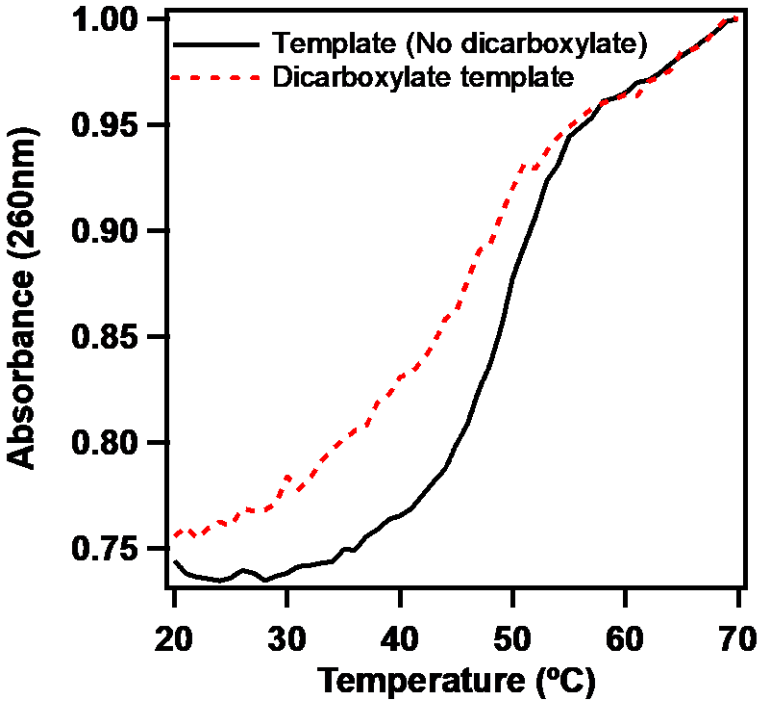

Figure AI.1 Melting temperature of DNA duplex with dicarboxylate template and its control with no dicarboxylate (Normalized). *Experimental conditions*: 1.4 µM of each DNA strand, 20 mM MOPS.

AI.3 Salt Driven DNA Hybridization and Dehybridization

It is known that metal ions affect the DNA structure when they interact with it causing some modifications, such as a decrease in the solubility (precipitation), an increase in its flexibility, an increase or decrease in its stability, and aggregation.[27] These interactions depend on many factors, including pH, [28-29] temperature, ionic strength,[30] and DNA sequence.[31] Metal ions increase the melting temperature of a DNA duplex by neutralizing the negative charges on the DNA backbone and by increasing its stability.[34-35]

We chose Mg^{2+} in this study as the metal ion since it is one of the most common metal ions in molecular biology. It has a direct effect on the amplification by polymerase chain reaction (PCR),[36] is a cofactor for many enzymes, and it has a direct effect on the stability of DNA duplex; therefore, we chose to use it to induce the hybridization of the DNA duplex. For inducing dehybridization of the DNA duplex, we used ethylenediaminetetraacetic acid (EDTA), which chelates with magnesium metal and reduces the stability of the DNA duplex. Since EDTA absorbs at 260 nm, we cannot use UV spectroscopy to monitor the hybridization and dehybridization of the DNA duplex. Thus, we decided to label the two complementary strands with a pair of fluorophores for a Förster Resonance Energy Transfer (FRET) study. FRET is a phenomenon for energy transfer between two fluorophores, one a donor and the other one an acceptor, depending on the distance between them. When the donor is excited, it emits light that excites the acceptor, and the latter will emit light or fluorescence that could be detected.[37-38] The pair we used was Cy3 as the donor and Cy5 as the acceptor. Cy3 has an excitation at 550 nm and an emission at 570 nm, while Cy5 has an excitation at 650 nm and an emission at 670 nm.

We synthesized a 23-mer DNA template with Cy3 fluorophore (5' TTG TAT AGA GTA ATT GAT TTT TT-Cy3 3') and its partial complementary an 18-mer strand that contains Cy5 (5' Cy5- ATC AAT TAC TCT ATA CAA 3'). The extra T's on the Cy3 strand were put to give a reasonable distance for the FRET pair in order not to quench each other.

We started by running melting temperature experiments to determine what temperature to use for the kinetic reactions. The melting temperature of the duplex in (3-(N-morpholino)propanesulfonic acid (MOPS) buffer that contains no salt was found to be 32 ºC (blue line, Figure AI.2), while the addition of 1 mM $MgCl_2$ raised the T_m to 52 ºC (black line, Figure AI.2). Furthermore, the addition of 10 mM EDTA to the previous duplex lowered the T_m

to 42 ºC (red line, Figure AI.2). The T_m is a bit high for this duplex, meaning that the kinetic study for monitoring the DNA hybridization and dehybridization has to be done at a higher temperature as well. Therefore, we synthesized a shorter Cy5 template (14-mer) with the sequence of Cy5 (5' Cy5- ATC AAT TAC TCT AT 3'). The melting temperature of the new duplex in MOPS buffer without salt is 24 ºC (blue line, Figure A.3), the addition of 1 mM $MgCl_2$ to the previous duplex in MOPS buffer raises the T_m to 40 ºC (black line, Figure AI.3), and the addition of 10 mM EDTA lowers the T_m to 26 ºC (red line, Figure AI.3). Thus, we identified 37 °C as the ideal temperature where we should be able to turn on and off hybridization by adding $MgCl_2$ then EDTA, respectively.

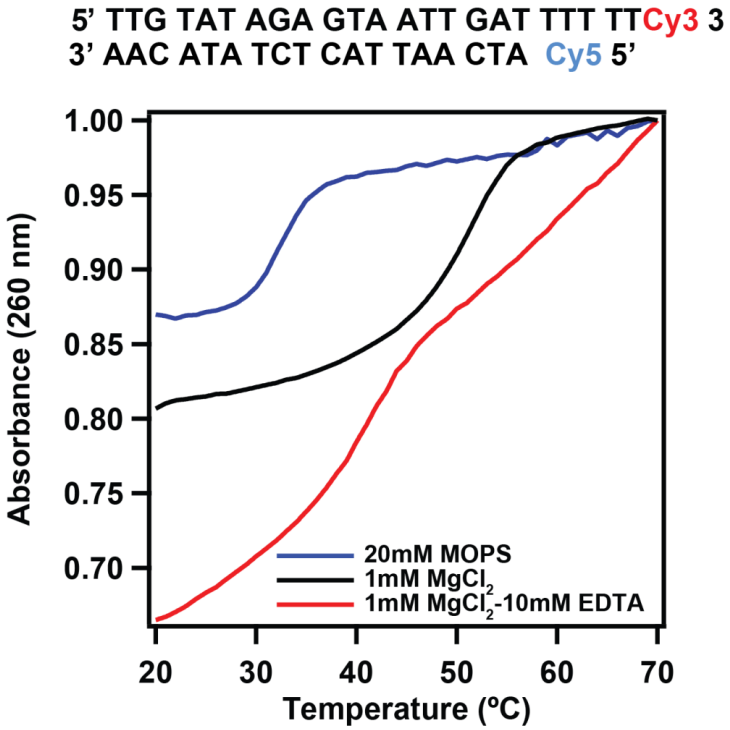

Figure AI.2 Melting temperature analysis (Normalized) of Cy5- Cy3 duplex. *Experimental conditions*: 1.4 µM of each DNA strand, 20 mM MOPS, $MgCl_2$ and EDTA if noted.

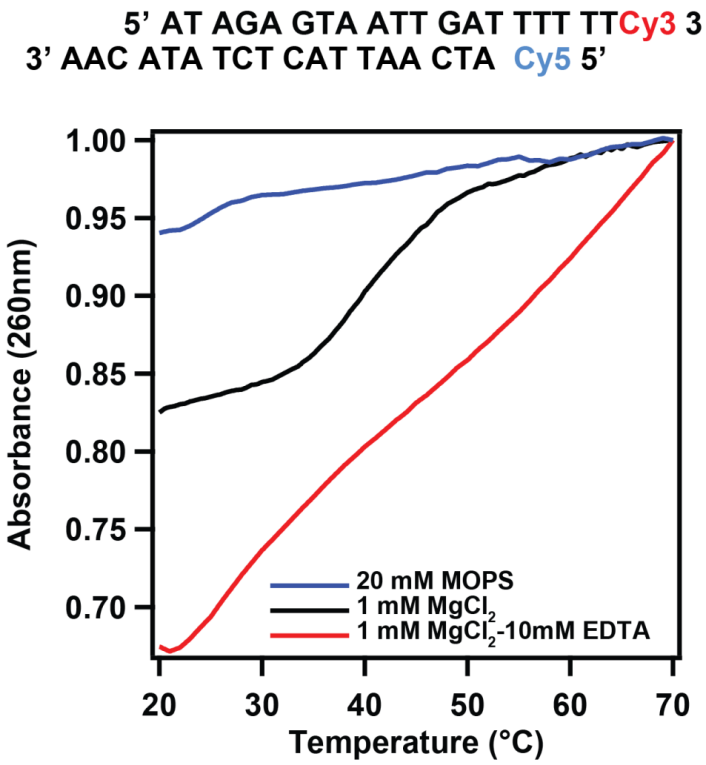

Figure AI.3 Normalized melting temperature analysis of shorter Cy5- Cy3 duplex. *Experimental conditions*: 1.4 µM of each DNA strand, 20 mM MOPS, $MgCl_2$ and EDTA if noted.

AI.3.1 Titration of Mg Chloride on DNA Duplex

First of all we needed to determine the minimum amount of Mg salt that could induce DNA hybridization. A titration of magnesium chloride ($MgCl_2$) on the DNA duplex was monitored with a fluorometer using a fixed excitation wavelength of 570 nm and a range of emission wavelength of 650—700 nm. Different concentrations of $MgCl_2$ were tested between 0.1 and 10 mM. From these results, the ratio of the fluorescence intensity between Cy5 at 662 nm to Cy3 at 656 nm was calculated (Figure AI.4B) with an increase in the ratio corresponding to DNA hybridization. From this analysis we determined that the minimum concentration of $MgCl_2$ required to induce hybridization of the DNA duplex at 37 °C was 0.25 mM (Figure AI.4 B).

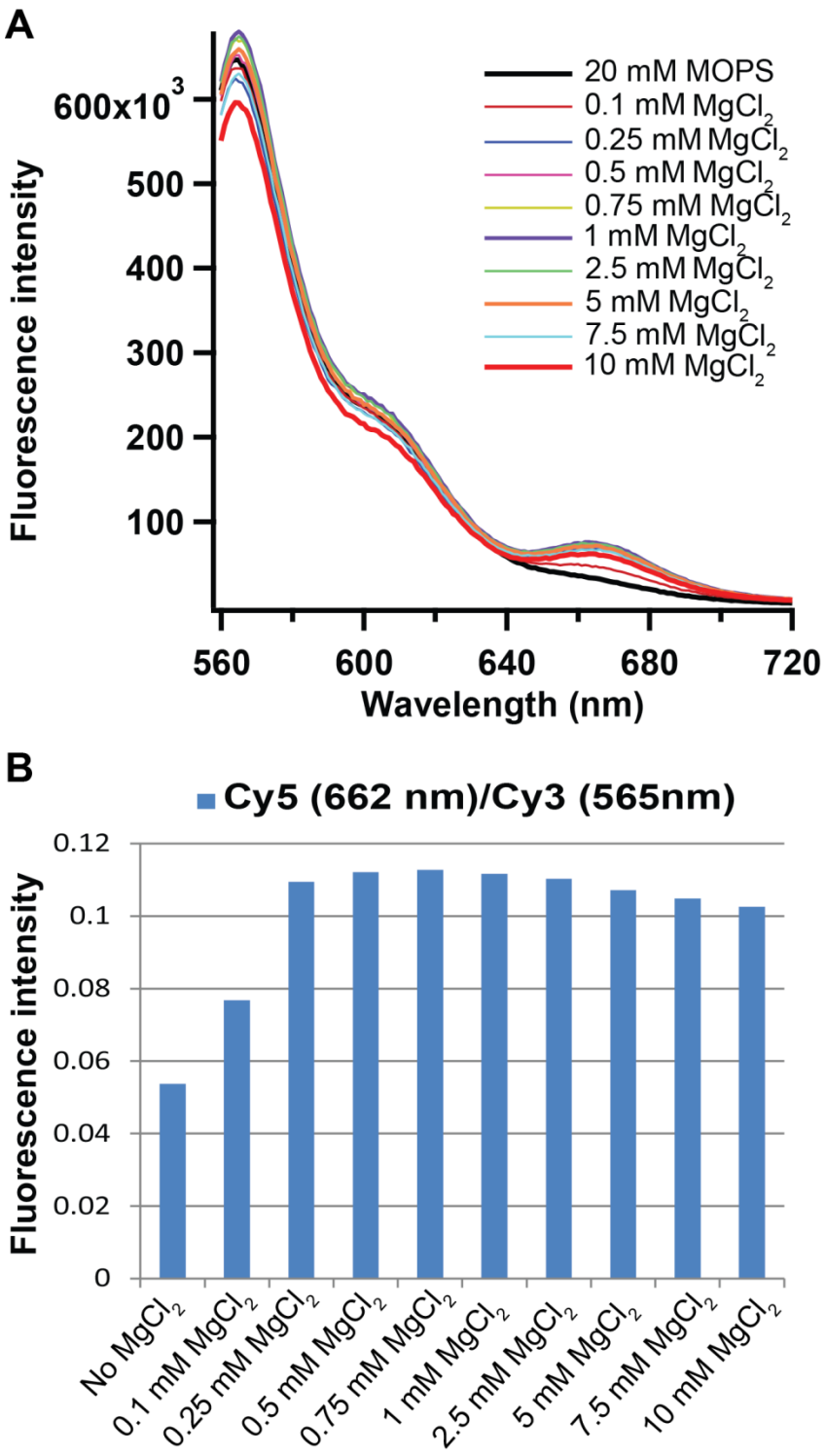

Figure AI.4. Titration of different concentrations of $MgCl_2$ on Cy5-Cy3 DNA duplex in MOPS buffer as monitored by fluorescence. A) Fluorescence emission spectra (λex = 570 nm). B) Plot of FRET efficiency (I_{662}/I_{565}) vs the concentration of $MgCl_2$. *Experimental conditions*: 1.4 µM of each DNA strand, 20 mM MOPS, various concentrations of $MgCl_2$ (mM), 37 °C.

AI.3.2 Titration of EDTA with 0.25 mM Magnesium Chloride

After identifying conditions that led to DNA hybridization, we next focused on determining how much EDTA needed to be added to afford dehybridization. The DNA duplex was diluted in MOPS buffer and 0.25 mM $MgCl_2$ was added, and a fluorescence spectra were measured. An increase of the FRET was attributed to the hybridization of the double stranded DNA. Disodium dihydrogen EDTA was added to the previous solution using different concentrations, and the fluorescence readings were taken after each addition (Figure AI.5). The ratio of the fluorescence intensity between Cy5 at 661 nm to Cy3 at 653 nm was calculated (Figure AI.5 B). Disodium dihydrogen EDTA concentrations of 1, 2.5 and 5 mM led to a decrease in the FRET based on the (I_{661}/I_{563}) intensity ratio indicating that it induces dehybridization of the duplex. However, higher concentrations of EDTA (10, 12.5, and 15 mM) did not induce the dehybridization instead the signal went up. We reasoned that adding this much EDTA introduced enough sodium salt into the solution that it could stabilize the duplex. From these results, the concentration of EDTA that induced dehybridization was determined to be 1 mM (Figure AI.5 A). With further optimization of EDTA concentrations, the minimum concentration for dehybridization of the DNA duplex in the presence of 0.25 mM $MgCl_2$ was found to be 0.33 mM EDTA.

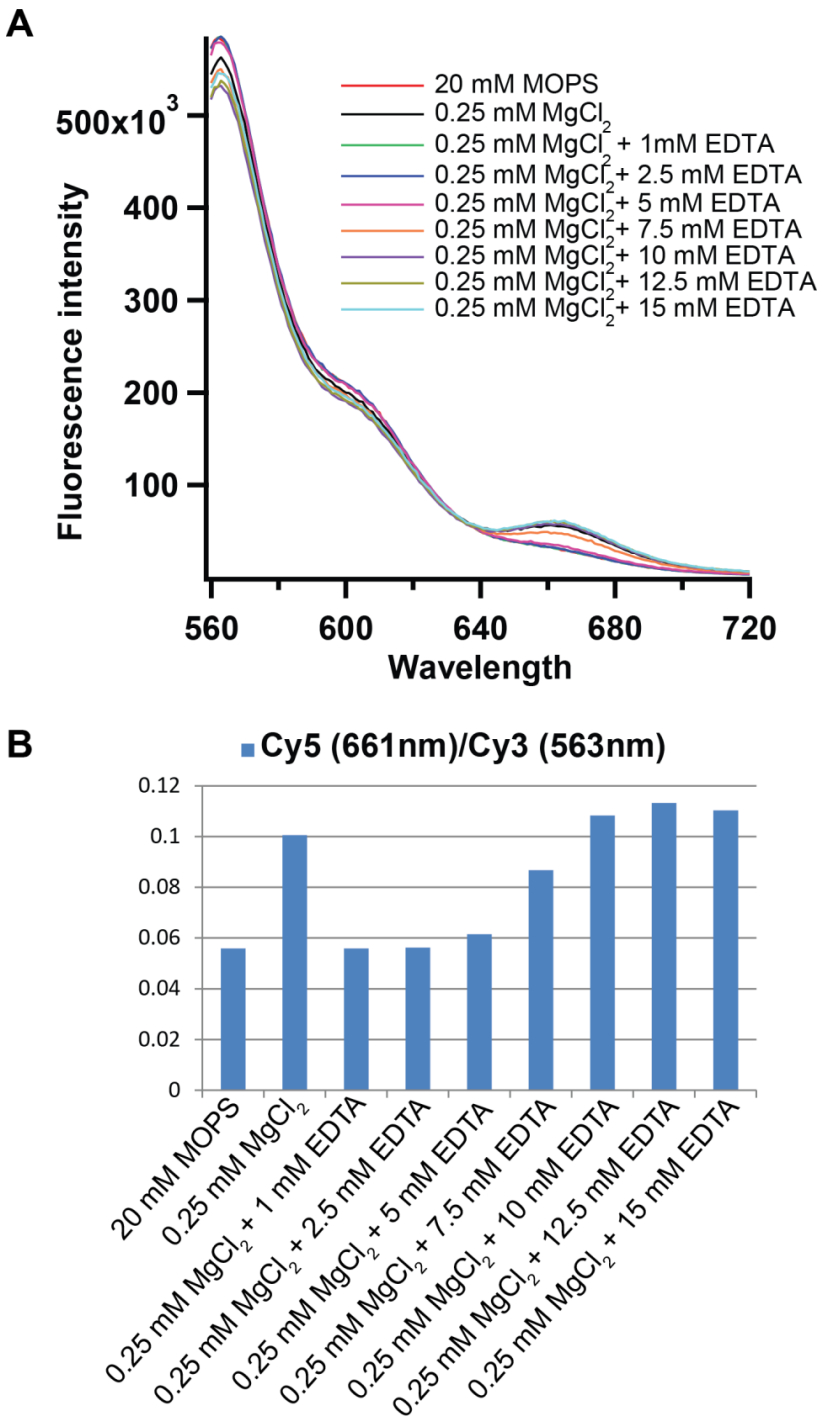

Figure AI.5 Titration of different concentrations of disodium dihydrogen EDTA vs 0.25 mM $MgCl_2$ in Cy5-Cy3 DNA duplex in MOPS buffer as monitored by fluorescence (λ_{ex} = 570 nm). A) Fluorescence emission spectra as a function of $MgCl_2$ or EDTA addition. B) Plot of FRET efficiency (I_{661}/I_{563}) vs the concentration of $MgCl_2$ and EDTA. *Experimental conditions*: 1.4 µM of each DNA strand, 20 mM MOPS, 0.25mM $MgCl_2$, various concentration of EDTA (mM) 37 °C.

AI.3.3 Driving DNA Hybridization and Dehybridization Using $MgCl_2$ and Disodium Dihydrogen EDTA

Now that we had identified minimal concentrations of $MgCl_2$ followed by EDTA that allowed for hybridization and dehybridization at 37 °C, respectively, we attempted to perform multiple hybridization/dehybridization cycles. The first cycle of hybridization was initiated by the addition of 0.25 mM $MgCl_2$, resulting in an increase of the fluorescence signal at 661 nm due to the hybridization of the DNA duplex. This was followed by the addition of 0.33 mM EDTA, resulting in a decrease of the FRET due to the dehybridization of the duplex (Scheme AI.5). Another cycle of $MgCl_2$, followed by EDTA, was monitored too. We were able to monitor two cycles of DNA hybridization and dehybridization (Figure AI.5). Adding more of disodium dihydrogen EDTA did not result in dehybridization of the DNA duplex, instead the signal increased. We attributed this increase to the sodium content on the EDTA solution that was used.

Scheme AI.5 FRET assay of hybridization and dehybridization of Cy5- Cy3 DNA duplex using Mg-EDTA assay.

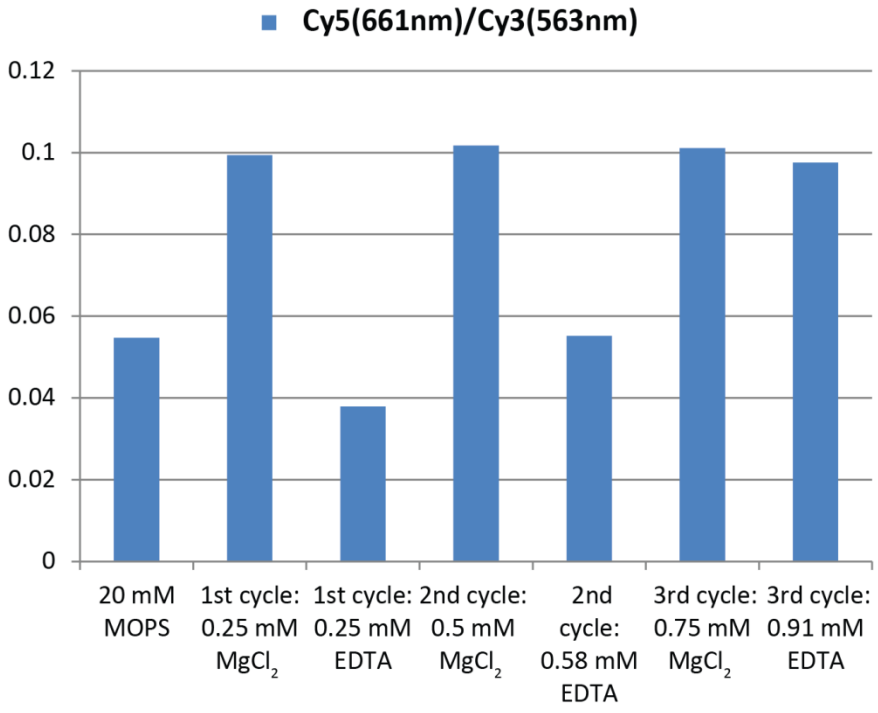

Figure AI.6 Cycling $MgCl_2$ and disodium dihydrogen ethylenediaminetetraacetate on Cy5-Cy3 DNA duplex in MOPS buffer as monitored by fluorometer. A) Fluorescence emission spectra (λ_{ex} = 570 nm) as a function of $MgCl_2$ or EDTA addition. B) Plot of FRET efficiency (I_{661}/I_{563}) vs the concentration of $MgCl_2$ and EDTA. *Experimental conditions*: 1.4 µM of each DNA strand, 20 mM MOPS, and various total concentrations of $MgCl_2$ and EDTA disodium salt, 37 °C.

A new solution was prepared using the EDTA of the acidic form without any sodium component, and the cycles were initiated again starting with the addition of 0.25 mM $MgCl_2$, which resulted in increasing the FRET signal due to hybridization of the DNA duplex. Then, addition of 0.25 mM EDTA resulted in less FRET signal due to the dehybridization of the DNA duplex after the chelation between Mg^{2+} and EDTA. Trying more cycles of $MgCl_2$, followed by EDTA, resulted in hybridization and dehybridization of Cy5- Cy3 DNA duplex; we were able to achieve six cycles (Figure AI.7 A). A plot of the FRET efficiency was calculated based on the ratio of the fluorescence intensity of Cy5 to the fluorescence intensity of Cy3 (Figure A.7B)

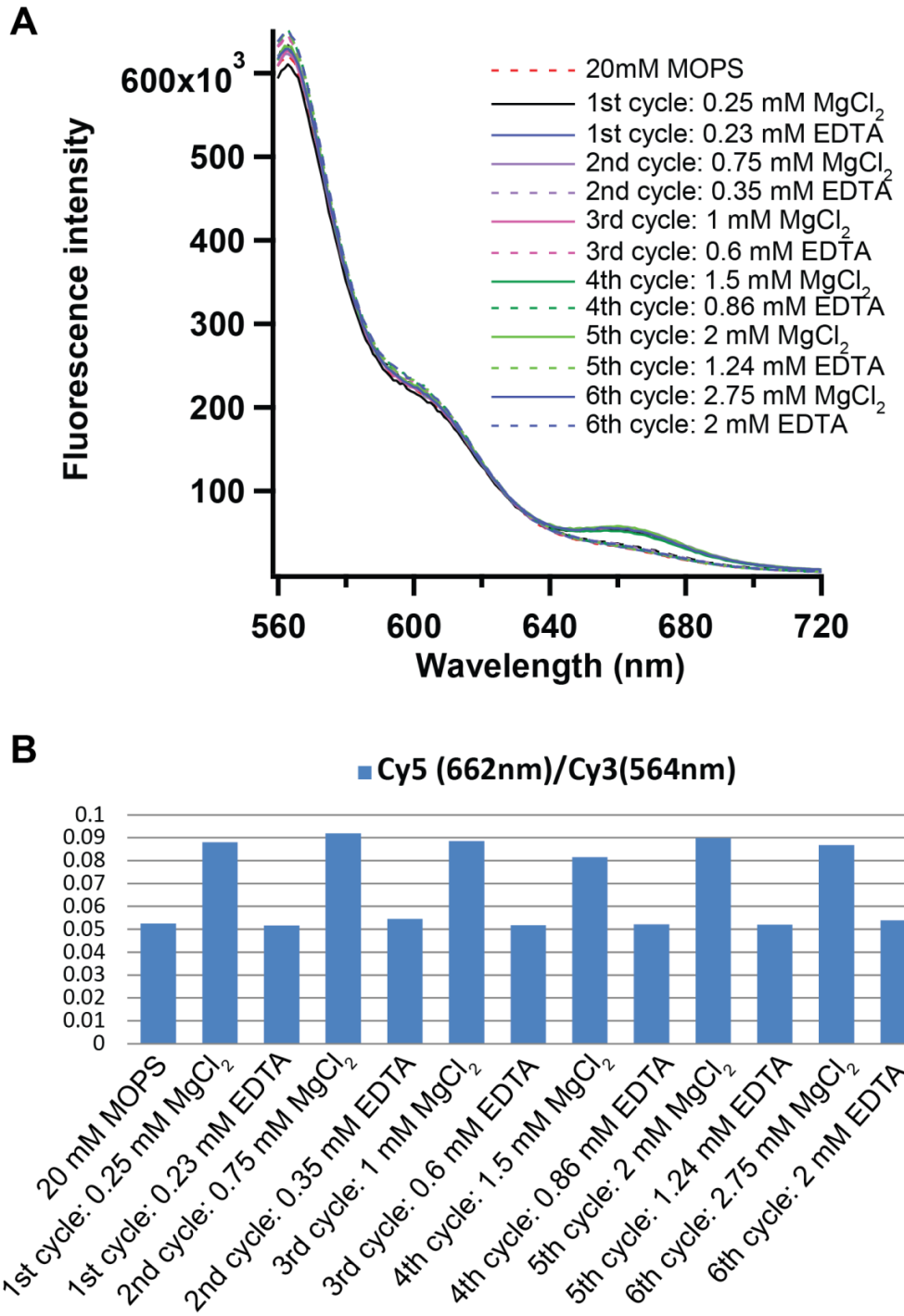

Figure AI.7 Cycling $MgCl_2$ and EDTA on Cy5-Cy3 DNA duplex in MOPS buffer as monitored by fluorometer. A) The emission spectrum spectra (λ_{ex}= 570 nm) as a function of $MgCl_2$ or EDTA addition. B) Plot of FRET efficiency (I_{662}/I_{564}) vs the concentration of $MgCl_2$ and EDTA**.** *Experimental conditions*: 1.4 µM of each DNA strand, 20 mM MOPS, various total concentrations of $MgCl_2$ and EDTA (acidic form), 37 °C.

Now, we have a system that could control DNA hybridization and dehybridization of DNA duplex and could potentially be used for turnover experiments in biosensors. For example using microfluidic devices, we could control the amount of EDTA or $MgCl_2$ present. Another option is to use EDTA-coated membranes and try to induce turnover by flowing through a series of membranes.

Additionally, we decided to explore combining this system with the EDC fuel-driven hybridization idea. Our strategy was to use the addition of EDC to generate the anhydride form of EDTA, which should be a weaker chelator of Mg^{2+}, allowing its release, which re-hybridizes the DNA duplex.

AI.3.4 Attempts at EDC-Driven DNA Hybridization by Turning On and Off Mg^{2+}/EDTA Chelation

The cycle was initiated by Mg^{2+} followed by EDTA, then EDC and monitored by FRET as in our previous experiments. We noticed an increase in the FRET signal upon the addition of EDC, indicating that EDC reacted with EDTA, thereby releasing Mg^{2+} (Figure AI.8). However, running a control experiment of DNA duplex in MOPS buffer, then adding EDC, also showed an increase of the fluorescence signal even when Mg^{2+} and EDTA were absent (Figure AI.9). This indicated that in the previous experiment, the increase of the FRET was due to the EDC interaction with the fluorophores.

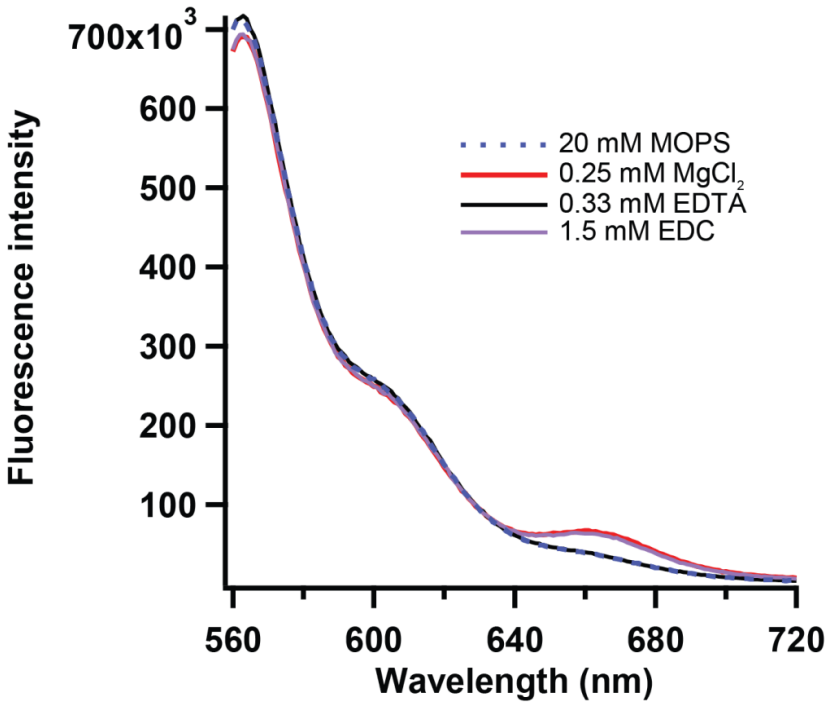

Figure AI.8 Cycling $MgCl_2$, EDTA, and EDC on Cy5-Cy3 DNA duplex in MOP buffer using the fluorometer. A) The fluorescence emission spectra (λ_{ex}= 570 nm) as a function of aqueous composition. *Experimental conditions:* 1.4 µM of each DNA strand, 20 mM MOPS, 0.25mM $MgCl_2$, 0.33 mM EDTA, 1.5 mM EDC, 37 °C.

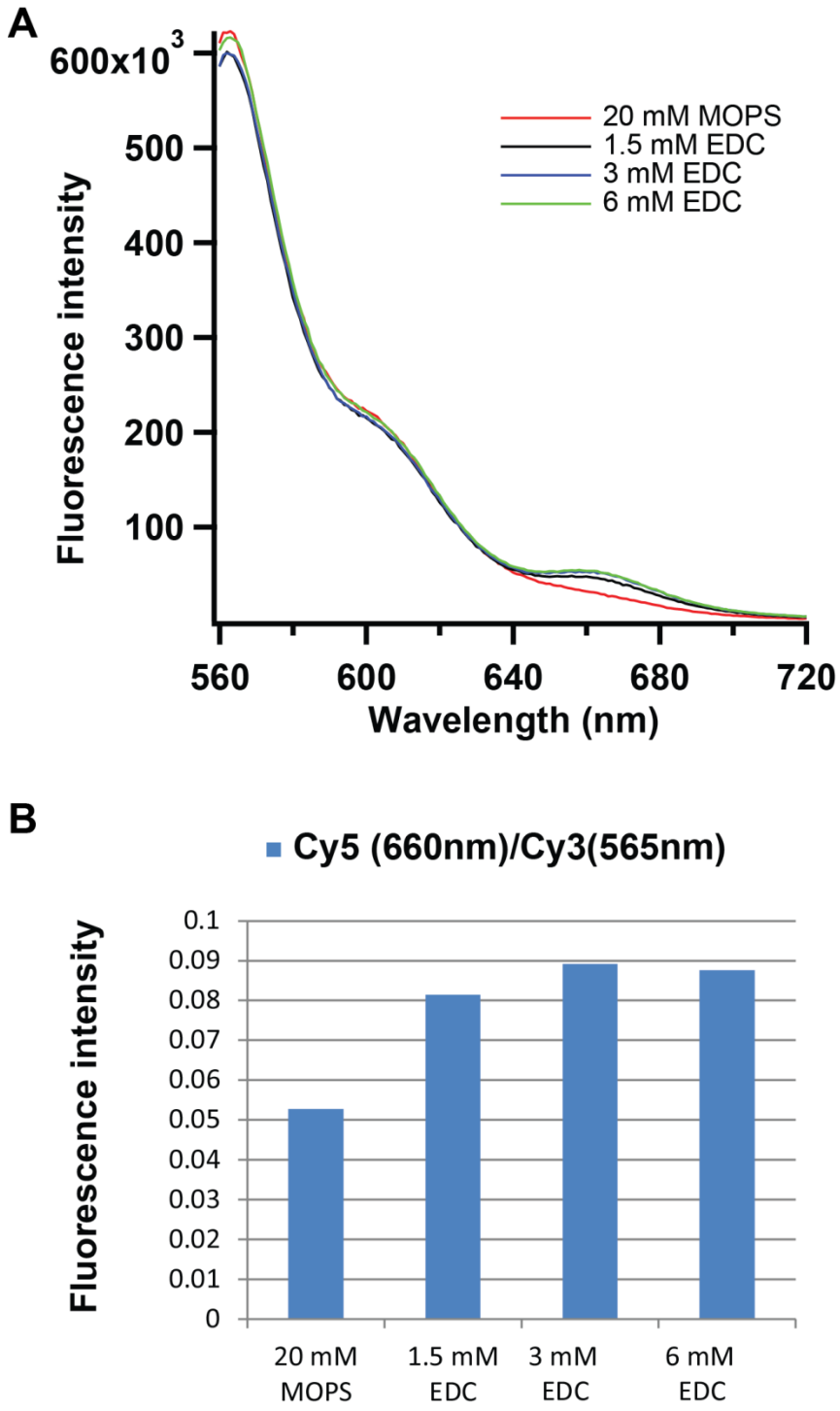

Figure AI.9 Control experiment of the addition of EDC to Cy5-Cy3 DNA duplex in MOPS buffer as monitored by the fluorometer. A) The emission spectra (λ_{ex}= 570 nm) as a function of EDC concentration. B) Plot of FRET efficiency (I_{660}/I_{565}) vs the concentration of $MgCl_2$. *Experimental conditions*: 1.4 µM of each DNA strand, 20 mM MOPS, 1.5, 3, and 6 mM EDC, 37 °C.

AI.4 Conclusions

In this Appendix, we discussed different strategies for controlling DNA hybridization and dehybridization. We have discussed EDC fuel driven DNA hybridization and dehybridization of a DNA duplex containing two dicarboxylate groups. The method was not successful due to the small difference in the melting temperature between the dicarboxylate duplex and the control duplex without dicarboxylate. For future work, a strand with more dicarboxylate groups, maybe 4-6 should be tested. Also, for monitoring the DNA hybridization and dehybridization, one of the strands should be labelled with a fluorophore and the other one with a quencher, and the kinetics could be monitored on a plate reader or fluorimeter.

Another strategy that we have developed is salt driven DNA hybridization and dehybridization of two strands of DNA labelled with Cy5 and Cy3 fluorophores using sequential additions of $MgCl_2$ and EDTA. Hybridization was monitored based on the FRET signal. The minimum concentration of $MgCl_2$ that caused the 14-mer DNA duplex to hybridize was found to be 0.25 mM at 37 °C, and the minimum concentration of EDTA that induced DNA duplex dehybridization was 0.33 mM. Many cycles of the addition of $MgCl_2$, followed by EDTA, were carried out; and we were able to achieve six cycles of DNA hybridization and dehybridization when the tetrahydrogen (sodium-free) form of the EDTA was used. This provides a simple strategy for cycling the hybridization state of DNA isothermally, which may be suitable for microfluidic devices. Finally, trying to turn on and off $Mg^{2+/}$EDTA chelation by the addition of EDC to indirectly influence DNA duplex stability was not successful. We attribute this to the strong affinity of Mg^{2+} for EDTA, which prevents reaction of the EDC with the chelator. Indeed, this lack of reactivity of the EDTA was confirmed by our collaborator Dr. Marta Tena-Solsona, in Boekhoven group at TUM.

AI.5 Experimental Section

AI.5.1 General

All the DNA phosphoramidite and DNA synthesizer reagents were purchased from Glen Research. Magnesium chloride and ammonium persulfate were purchased from Sigma-Aldrich. Tris base, boric acid, EDTA, Stains-All (cat. # E9379), and tetramethylethylenediamine (cat. #T9281) were purchased from Fisher. 40% Acrylamide/bisacrylamide solution, 19:1 (cat. #1610144) was purchased from Bio-Rad.

AI.5.2 Synthesis of DNA Strands

The synthesis of the DNA strands were done using Glen Research reagents on an ABI solid-phase synthesizer, Model 392. Strands were purified following DMT-On GlenPak purification protocol using GlenPak DNA cartridges (cat. 60-5200-01). Standard nucleotide phosphoramidite, CPG's and the following modifications were used for templates: Cy5 phosphoramidite (cat. 10-5915-95), Cy3 phosphoramidite (cat. 10-5913-95), and NHS carboxy dT phosphoramidite (cat. 10-1535-95), (Figure AI.10). Some of the strands needed more steps for the preparation after the synthesis by the synthesizer (see below).

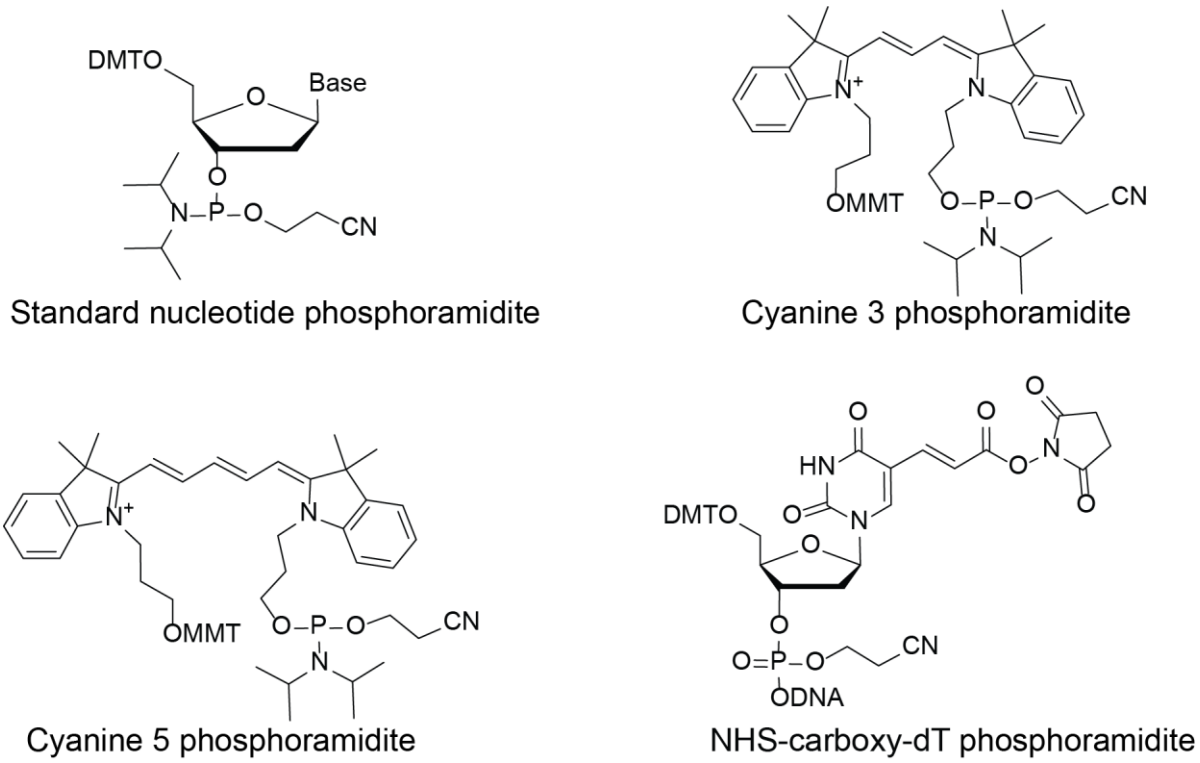

Figure AI.10 The chemical structures of the phosphoramidites and CPG used in this study.

Table AI.1 DNA Sequences Used in This Study

Name	**Sequence**
Cy3 Template	5’ TTG TAT AGA GTA ATT GAT TTT TT-Cy3 3’
Cy5 Template (18 Bp)	5’ Cy5- ATC AAT TAC TCT ATA CAA 3’
Cy3 Template (14 Bp)	5’ Cy5- AT TAC TCT ATA CAA 3’
Dicarboxylate Template	5’ TTG TAT AGA GTA ATT GAT 3’

T = NHS carboxy dT

AI.5.2.1 Preparation of Dicarboxylate DNA Template

The DMT ON DNA synthesis protocol was followed and Glen Research reagents, standard nucleotide phosphoramidite, and NHS carboxy dT phosphoramidite (cat. 10-1535-95) were used. The DNA was kept on the bead and vacuum dried. Aspartic dimethyl chloride was dissolved in 1 mL of DMF, and the solution was added to the bead in a vial. Few drops of triethyl amine were added to the solution, and the solution was left overnight. The solution was

removed from the vial, another batch of aspartic dimethyl chloride solution (1 mL) was added to the bead on the vial, and the mixture was left over two days. The solution was removed, and the DNA was cleaved from the bead using 1 mL of ammonium hydroxide at room temperature overnight. Then, it was purified using the standard DMT on Glen-Pak protocol and lyophilized.

AI.5.3 FRET Experiment

1.3 nmol of each DNA template (Cy5 and Cy3 template) were combined in 1 ml of 0.2M MOPS buffer. The solution was transferred to a cuvette with a stirrer bar and was placed inside a fluorometer. The FRET signal was measured with an excitation of 570 nm and an emission range between 660—720 with a constant heating at 37 °C. Next, 0.25 mM $MgCl_2$ were added and a FRET signal was measured, then 0.33 mM of EDTA were added, and a FRET signal was measured.

AI.5.4 Mass Analysis of the DNA Strands

Synthesised DNA strands were analyzed by MALDI-TOF. First, a matrix solution of 2,4,6-trihydroxylacetophenone (THAP) in 1:1 acetonitrile:water was prepared (25 mg/mL) as well as an ammonium citrate solution in water (25 mg/mL). These two solutions were mixed in a 9:1 ratio to yield the final matrix mixture. The synthesized DNA (5 nmol) was desalted using ZipTip (ZTC18S096) purchased from Millipore Sigma and was mixed in a 1:1 ratio with the matrix mixture. The measurements were carried out on a Voyager Elite (Applied BioSystems, Foster City, CA, USA) time of flight-mass spectrometer in linear positive mode.

AI.5.5 Denaturing Polyacrylamide Gel Electrophoresis

A denaturing 15% polyacrylamide gel was prepared by dissolving urea (4.8 g) in 40% Acrylamide/Bis Solution 19:1 (3.75 mL) (Bio-Rad Cat.161-0144) and 5 x TBE buffer (1 mL),

then diluted to 10 mL with MQ water. Tetramethylethylenediamine (10.7 μL, TEMED) and aqueous ammonium persulfate (80 μL) were added after urea was dissolved to induce polymerization. A portion of the aliquot and running dye mixture (3 μL) was loaded into a denaturing 15% polyacrylamide gel (8 M urea in 0.5 X TBE, 37.5 vol% of 40% acrylamide/bisacrylamide solution, 0.75 mm thick, 10 wells). PAGE was run at 150 V for 80 min. A fluorescent image was taken of the gel using a fluorescent imager with trans-UV illumination using an ImageQuant RT ECL instrument from GE Healthcare Life Science. Quantification of the fluorescence emitted by each band was analysed by using ImageQuant TL analysis software. The %con was determined based on the ratio of the fluorescence intensity of the product band over the sum of the fluorescence intensity of the product and reactant bands multiplied by 100%.

The equation is as follow:

$$\%\ Yield = \frac{I_{\text{Product Band}}}{I_{\text{Product Band}} + I_{\text{Reactant Band}}} \times 100\%$$

AI.5.6 Testing the Purity of the Synthesized DNA Probes by Stains-all

The DNA strands were loaded into 15% denaturing PAGE then stained with Stains-All (Aldrich cat # E9379). The Stains-All solution was prepared by dissolving Stains-All (25 mg) in 50 mL mixture of 1:1 (MilliQ H2O: Formamide). The PAGE was placed in a container with the Stains-All solution, covered with foil, and placed in a shaker for 15 min. The presence of one band only for each strand is an indication of the purity of the DNA strand.

AI.6 References

1. Chen, J.; Seeman, N. C., Synthesis from DNA of a molecule with the connectivity of a cube. *Nature* **1991,** *350*, 631.

2. Mirkin, C. A.; Letsinger, R. L.; Mucic, R. C.; Storhoff, J. J., A DNA-based method for rationally assembling nanoparticles into macroscopic materials. *Nature* **1996,** *382*, 607.

3. Nadrian, C. S.; Philip, S. L., Nucleic acid nanostructures: bottom-up control of geometry on the nanoscale. *Reports on Progress in Physics* **2005,** *68* (1), 237.

4. Lin, C.; Ke, Y.; Liu, Y.; Mertig, M.; Gu, J.; Yan, H., Functional DNA Nanotube Arrays: Bottom-Up Meets Top-Down. *Angewandte Chemie International Edition* **2007,** *46* (32), 6089-6092.

5. Mao, C.; Sun, W.; Shen, Z.; Seeman, N. C., A nanomechanical device based on the B-Z transition of DNA. *Nature* **1999,** *397* (6715), 144-6.

6. Yurke, B.; Turberfield, A. J.; Mills, A. P., Jr.; Simmel, F. C.; Neumann, J. L., A DNA-fuelled molecular machine made of DNA. *Nature* **2000,** *406* (6796), 605-8.

7. Alberti, P.; Mergny, J.-L., DNA duplex–quadruplex exchange as the basis for a nanomolecular machine. *Proceedings of the National Academy of Sciences* **2003,** *100* (4), 1569-1573.

8. Tian, Y.; Mao, C., Molecular Gears: A Pair of DNA Circles Continuously Rolls against Each Other. *Journal of the American Chemical Society* **2004,** *126* (37), 11410-11411.

9. Beissenhirtz, M. K.; Willner, I., DNA-based machines. *Organic & Biomolecular Chemistry* **2006,** *4* (18), 3392-3401.

10. Liedl, T.; Sobey, T. L.; Simmel, F. C., DNA-based nanodevices. *Nano Today* **2007,** *2* (2), 36-41.

11. Ferris, D. P.; Zhao, Y.-L.; Khashab, N. M.; Khatib, H. A.; Stoddart, J. F.; Zink, J. I., Light-Operated Mechanized Nanoparticles. *Journal of the American Chemical Society* **2009,** *131* (5), 1686-1688.

12. Vizer, S. A.; Sycheva, E. S.; Al Quntar, A. A. A.; Kurmankulov, N. B.; Yerzhanov, K. B.; Dembitsky, V. M., Propargylic Sulfides: Synthesis, Properties, and Application. *Chemical Reviews* **2015,** *115* (3), 1475-1502.

13. Lewis, F. D.; Liu, X., Phototriggered DNA Hairpin Formation in a Stilbenediether-Linked Bis(oligonucleotide) Conjugate. *Journal of the American Chemical Society* **1999,** *121* (50), 11928-11929.

14. Irie, M., Diarylethenes for Memories and Switches. *Chemical Reviews* **2000,** *100* (5), 1685-1716.

15. Brieke, C.; Rohrbach, F.; Gottschalk, A.; Mayer, G.; Heckel, A., Light-controlled tools. *Angewandte Chemie International Edition Engl* **2012,** *51* (34), 8446-76.

16. Dohno, C.; Uno, S.-n.; Nakatani, K., Photoswitchable Molecular Glue for DNA. *Journal of the American Chemical Society* **2007,** *129* (39), 11898-11899.

17. Liang, X.; Nishioka, H.; Takenaka, N.; Asanuma, H., A DNA nanomachine powered by light irradiation. *Chembiochem* **2008,** *9* (5), 702-5.

18. Mengguang, Z.; Xingguo, L.; Toshio, M.; Hiroyuki, A., A Light-Driven DNA Nanomachine for the Efficient Photoswitching of RNA Digestion. *Angewandte Chemie* **2010,** *122* (12), 2213-2216.

19. Liang, X.; Zhou, M.; Kato, K.; Asanuma, H., Photoswitch nucleic acid catalytic activity by regulating topological structure with a universal supraphotoswitch. *ACS synthetic biology* **2013,** *2* (4), 194-202.

20. Kamiya, Y.; Asanuma, H., Light-Driven DNA Nanomachine with a Photoresponsive Molecular Engine. *Accounts of Chemical Research* **2014,** *47* (6), 1663-1672.

21. Wang, W.; Yang, Y.; Cheng, E.; Zhao, M.; Meng, H.; Liu, D.; Zhou, D., A pH-driven, reconfigurable DNA nanotriangle. *Chemical Communications* **2009,** (7), 824-826.

22. Gueron, M.; Leroy, J. L., The i-motif in nucleic acids. *Current opinion in structural biology* **2000,** *10* (3), 326-31.

23. Gehring, K.; Leroy, J. L.; Gueron, M., A tetrameric DNA structure with protonated cytosine.cytosine base pairs. *Nature* **1993,** *363* (6429), 561-5.

24. Chen, L.; Di, J.; Cao, C.; Zhao, Y.; Ma, Y.; Luo, J.; Wen, Y.; Song, W.; Song, Y.; Jiang, L., A pH-driven DNA nanoswitch for responsive controlled release. *Chemical Communications* **2011,** *47* (10), 2850-2852.

25. Trewyn, B. G.; Slowing, I. I.; Giri, S.; Chen, H.-T.; Lin, V. S. Y., Synthesis and Functionalization of a Mesoporous Silica Nanoparticle Based on the Sol–Gel Process and Applications in Controlled Release. *Accounts of Chemical Research* **2007,** *40* (9), 846-853.

26. Tena-Solsona, M.; Rieß, B.; Grötsch, R. K.; Löhrer, F. C.; Wanzke, C.; Käsdorf, B.; Bausch, A. R.; Müller-Buschbaum, P.; Lieleg, O.; Boekhoven, J., Non-equilibrium dissipative supramolecular materials with a tunable lifetime. *Nature Communications* **2017,** *8*, 15895.

27. Sissoëff, I.; Grisvard, J.; Guillé, E., Studies on metal ions-DNA interactions: Specific behaviour of reiterative DNA sequences. *Progress in Biophysics and Molecular Biology* **1978,** *31*, 165-199.

28. Wilhelm, F. X.; Daune, M., Interactions des ions métalliques avec le DNA. III. Stabilité et configuration des complexes Ag–DNA. *Biopolymers* **1969,** *8* (1), 121-137.

29. Mathieson, A. R.; Olayemi, J. Y., The interaction of calcium and magnesium ions with deoxyribonucleic acid. *Arch Biochem Biophys* **1975,** *169* (1), 237-43.

30. Schildkraut, C., Dependence of the melting temperature of DNA on salt concentration. *Biopolymers* **1965,** *3* (2), 195-208.

31. Davidson, N.; Widholm, J.; Nandi, U. S.; Jensen, R.; Olivera, B. M.; Wang, J. C., PREPARATION AND PROPERTIES OF NATIVE CRAB dAT. *Proceedings of the National Academy of Sciences of the United States of America* **1965,** *53* (1), 111-118.

32. Daune, M.; Dekker, C. A.; Schachman, H. K., Complexes of silver ion with natural and synthetic polynucleotides. *Biopolymers* **1966,** *4* (1), 51-76.

33. Fiskin, A. M.; Beer, M., Determination of Base Sequence in Nucleic Acids with the Electron Microscope. IV. Nucleoside Complexes with Certain Metal Ions*. *Biochemistry* **1965,** *4* (7), 1289-1294.

34. Dove, W. F.; Davidson, N., Cation effects on the denaturation of DNA. *Journal of Molecular Biology* **1962,** *5* (5), 467-478.

35. Eichhorn, G. L.; Shin, Y. A., Interaction of metal ions with polynucleotides and related compounds. XII. The relative effect of various metal ions on DNA helicity. *Journal of the American Chemical Society* **1968,** *90* (26), 7323-7328.

36. Khosravinia, H.; P. Ramesha, K., *Influence of EDTA and magnesium on DNA extraction from blood samples and specificity of polymerase chain reaction*. 2007; Vol. 6.

37. Wu, P.; Brand, L., Resonance energy transfer: methods and applications. *Anal Biochem* **1994,** *218* (1), 1-13.

38. Clegg, R. M., Fluorescence resonance energy transfer. *Current Opinion in Biotechnology* **1995,** *6* (1), 103-110.

Appendix II

Supporting Information for Chapter Two

AII.1 PAGE Image of CuAAC Using Ligand: Cu Ratio (7:1)

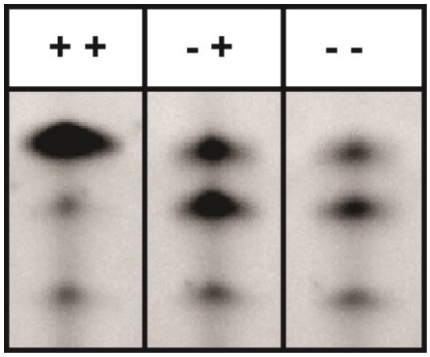

Figure AII.1 PAGE images of matched and mismatched CuAAC templated chemical ligation. (+ +): both template and azide probe present. (- +): no template but azide probe present, (- -) neither template nor azide probe present. *Experimental conditions:* 1 µM template, 1 µM 5' azide probe and 3' alkyne- 5' fluorescein probe, 700 µM THPTA, 100 µM $CuSO_4$, 1 mM Na ascorbate, 0.2 M NaCl, 27 °C.

AII.2 Melting Temperature Profiles of Nicked Duplex of Chemical Ligation System

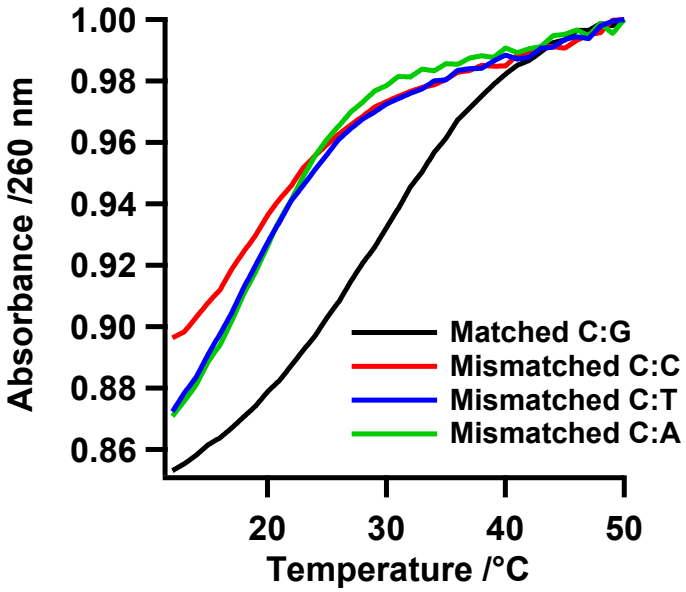

Figure AII.2 Melting temperature of matched and mismatched template with CuAAC, 1.3 nmol of each DNA (template, 5' azide probe and 3' alkyne- 5' fluorescein probe), 10 mM $MgCl_2$, 0.2 M NaCl.

AII.3 PAGE Images of Chemical Ligation System at 23 ºC

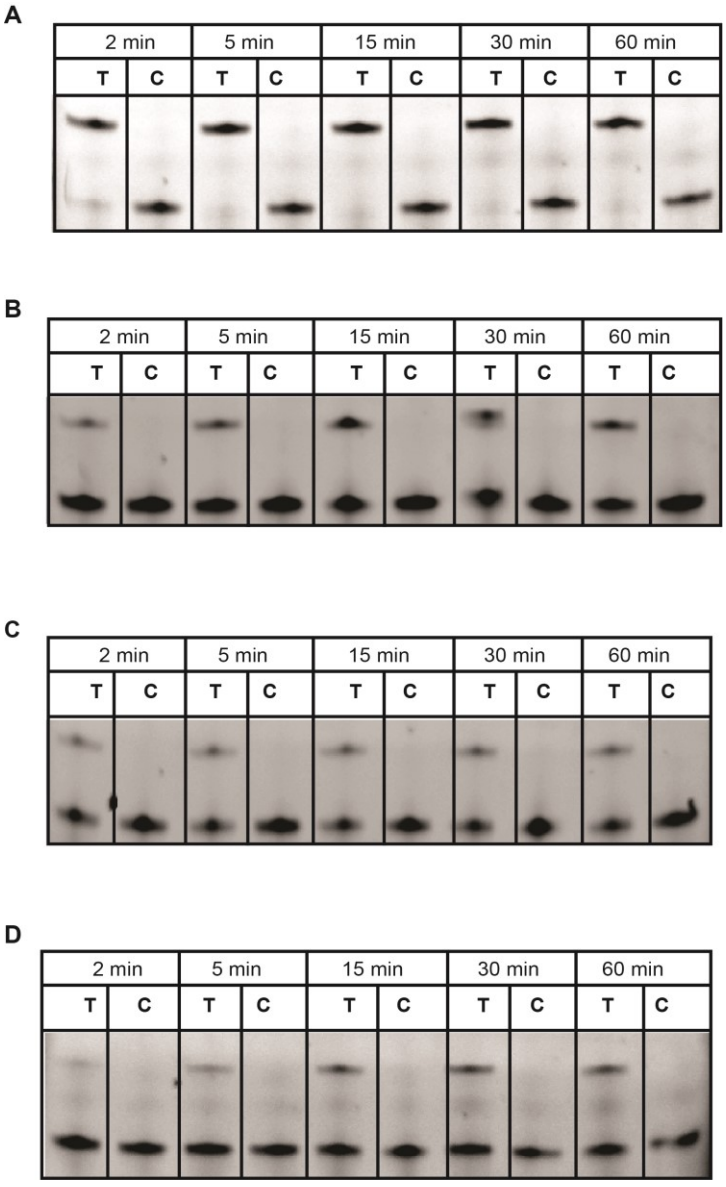

Figure AII.3 Gel images of matched and mismatched templated chemical ligation. 1 µM template, 2 µM 5' azide probe and 3' alkyne- 5' fluorescein probe, 900 µM $(BimC_4A)_3$, 600 µM $CuSO_4$, 11 mM Na ascorbate, 0.2 M NaCl, 0.010 M $MgCl_2$, 23 ºC. A) Matched G template B) Mismatched T template C) Mismatched A template D) Mismatched C template. T: in presence of template, C: in the absence of template**.**

AII.4 PAGE Images of Enzymatic Ligation System 23 ºC

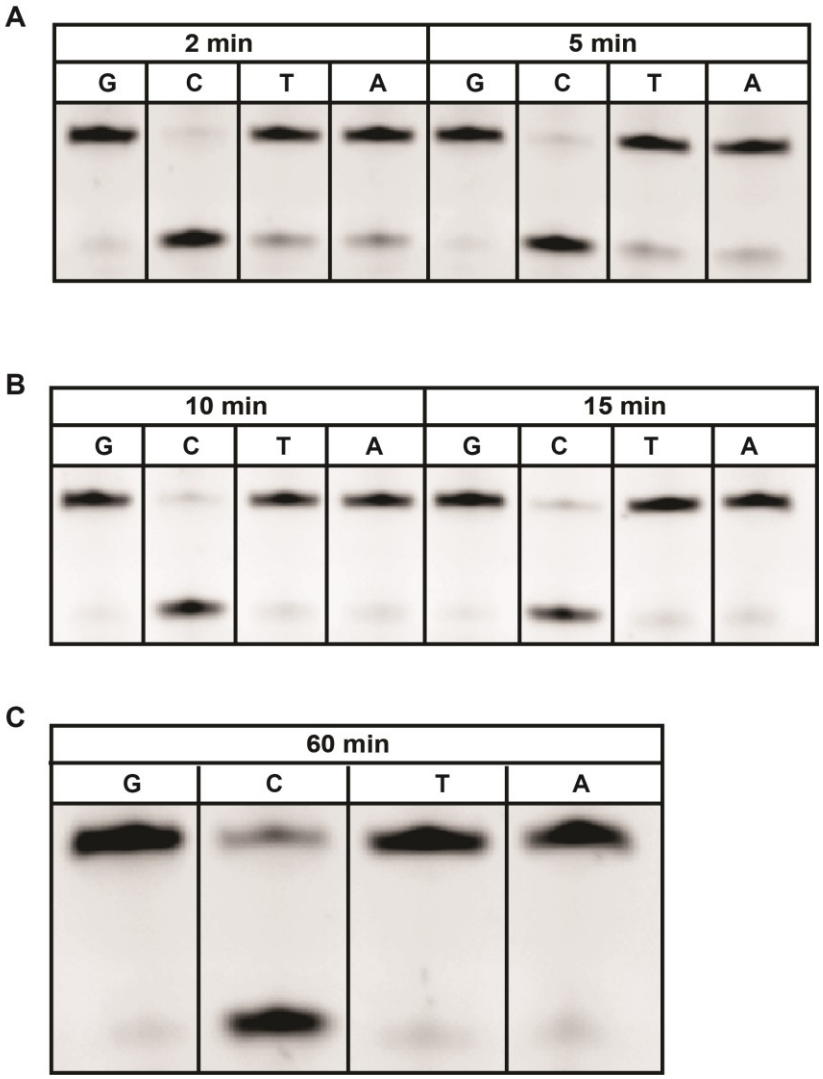

Figure AII.4 Gel images of the match and mismatched templated enzymatic ligation system, 1.4 µM template, 2.8 µM 5' phosphate probe and 1.4 µM 3' hydroxyl- 5' fluorescein probe, 2000 CEU T4 DNA ligase, 10 mM $MgCl_2$, 23 ºC.

Table AII.1 MALDI Characterization

DNA sequence name	Calculated mass	Observed mass
G matched template	5567.7	5568.1
C mismatched template	5527.7	5530.4
T mismatched template	5542.7	5544.34
A mismatched template	5551.7	5553.5
5’ azide probe	2706.8	2707.7
3’ propargyl-5’ fluorescein probe	3549.67	3551.5
5’ phosphate probe	2761.78	2761.9
3’ hydroxyl-5’ fluorescein probe	3549.67	3550.6
the triazole product	6256.47	6256.87

AII.5 Isolation of the Triazole Product and MALDI Analysis

The template (10 nmol), 5’-azide ODN (20 nmol), and 3’-alkyne -5’ fluorescein ODN (10 nmol), were combined in a vial that contained a salt solution of 0.2 M NaCl and 0.01 M $MgCl_2$ (a total volume of 4420 μL). This mixture was flushed with argon for 1 min and allowed to incubate in a covered thermal incubator at 23 °C for 15 min. During this time copper sulphate (18 mM, 167 μL) and $(BimC_4A)_3$ (18 mM, 250 μL) were mixed together, flushed with argon for 1 min and left to stand for 4 min, then sodium ascorbate (33 mM, 163 μL) was added to this pre-

mix and the mixture left to stand for 5 min. Next, the Cu (I) complex pre-mix (580 µL) was added to the incubated ODNs and timing started. The total volume was 5 mL and the final concentrations were: 2 µM template, 4 µM 5'-azide ODN, 2 µM 3'-alkyne -5' fluorescein-ODN, 600 µM $CuSO_4$, 900 µM $(BimC_4A)_3$ and 11 mM sodium ascorbate. After one hour, EDTA (aq) (0.5 M, 40 µL) was added to the mixture and the mixture was lyophilized. Triethylammonium acetate (0.1 M, 1 mL) was added to the lyophilized sample and the solution was desalted using Glen-Pak cartridge desalting procedure by Glen Research. The product was eluted with 1 mL of 50% ACN/H_2O and lyophilized. MilliQ H_2O (~ 70 µL) was added to the lyophilized sample and mixed well. The solution (30 µL) was taken and aqueous sucrose (1 M, 30 µL) was added. A portion of this mixture (5 µL) was loaded into each well and 15% denaturing PAGE was run following the standard procedure described previously. The product band was identified by fluorescent imaging, cut out of the gel, put in an eppendorf tube and the gel was crushed. MilliQ H_2O (500 µL) was added and the gel was left overnight. The gel was filtered using a spin-X centrifuge filter (CLS8160) purchased from Sigma-Aldrich, and the filtrate was lyophilized. MilliQ H_2O (30 µL) was added to the lyophilized sample and desalted using ZipTip (ZTC18S096). The sample was measured with MALDI following the MALD-TOF characterization procedure described earlier.

We also performed a scaled-up reaction using the 3'-propargyl with the fluorescein-modified thymidine DNA probe to determine the identity of the middle band on the gel following the previous method described above for the triazole product except for no template or azide DNA probe were used, and the ligand used was THPTA. The final concentrations in the reaction were: 2 µM of 3'-alkyne -5' fluorescein-ODN, 200 µM $CuSO_4$, 1000 µM THPTA and 11 mM sodium ascorbate. The chemical identity of the middle band was not clear from this

MALDI experiment as no mass was observed, which we attribute to the isolation of too little material. The bottom band was confirmed to be the 3'-propargyl- 5' fluorescein DNA probe.